Biochimica et Biophysica Acta 1827 (2013) 1048–1085

Contents lists available at SciVerse ScienceDirect

Biochimica et Biophysica Acta

journal homepage: www.elsevier.com/locate/bbabio

Review

The prokaryotic Mo/W-*bis*PGD enzymes family: A catalytic workhorse in bioenergetic☆

Stéphane Grimaldi [a], Barbara Schoepp-Cothenet [a], Pierre Ceccaldi [a,b], Bruno Guigliarelli [a,*], Axel Magalon [b,**]

[a] CNRS, Aix Marseille Université, IMM FR3479, Unité de Bioénergétique et Ingénierie des Protéines (BIP) UMR 7281, F-13402 Marseille Cedex 20, France
[b] CNRS, Aix Marseille Université, IMM FR3479, Laboratoire de Chimie Bactérienne (LCB) UMR 7283, F-13402 Marseille Cedex 20, France

ARTICLE INFO

Article history:
Received 23 November 2012
Received in revised form 21 January 2013
Accepted 23 January 2013
Available online 31 January 2013

Keywords:
Molybdenum
Prokaryote
Bioenergetic
Iron–sulfur
Quinone
Electron transfer

ABSTRACT

Over the past two decades, prominent importance of molybdenum-containing enzymes in prokaryotes has been put forward by studies originating from different fields. Proteomic or bioinformatic studies underpinned that the list of molybdenum-containing enzymes is far from being complete with to date, more than fifty different enzymes involved in the biogeochemical nitrogen, carbon and sulfur cycles. In particular, the vast majority of prokaryotic molybdenum-containing enzymes belong to the so-called dimethylsulfoxide reductase family. Despite its extraordinary diversity, this family is characterized by the presence of a Mo/W-*bis*(pyranopterin guanosine dinucleotide) cofactor at the active site. This review highlights what has been learned about the properties of the catalytic site, the modular variation of the structural organization of these enzymes, and their interplay with the isoprenoid quinones. In the last part, this review provides an integrated view of how these enzymes contribute to the bioenergetics of prokaryotes. This article is part of a Special Issue entitled: Metals in Bioenergetics and Biomimetics Systems.

1. Introduction

Approximately one-third of all proteins contain metal ions or metal-containing cofactors [1]. Molybdenum (Mo) and tungsten (W) are the only known second- and third-row transition metals to occur in biomolecules. Mo/W are found in nearly all organisms (*Saccharomyces* is a prominent exception [2]), in all kingdoms of life. More than 50 different Mo/W enzymes have been described in nature so far (see [2] for the most exhaustive census). This list is far to be complete since the strict anaerobic bacterium isolated from contaminated soil with tetrachloroethene in Japan, *Desulfitobacterium hafniense* Y51 [3], for example, encodes more than 50 identified members of the Mo/W-enzyme family [4]. The molybdoproteome moreover might be even more diverse than previously recognized in prokaryotes as suggested by the proteomic approach conducted by Cvetkovic et al. [5] revealing the existence of several Mo-binding proteins with unrelated sequence homology to any known molybdoenzymes. Although present only at 1 ppm in the Earth's crust, Mo is broadly distributed in biological systems due to the high solubility, and therefore bioavailability, of the molybdate anion (MoO_4^{2-}). Despite the high similarity between the chemical properties of Mo and W, W-containing enzymes are rare compared to Mo-containing enzymes. In particular, thermophilic prokaryotes are known to contain W-enzymes [6,7]. This fact has often been connected to the observed higher thermostability of the W-enzymes compared to the Mo-enzymes [8]. Differential bioavailability in anoxic environment [9] let some authors to propose that W prior to Mo has been used as early as in the Archaean.

With the exceptions of the multinuclear $MoFe_7$ cluster found in nitrogenase [10] and the binuclear MoCu center found in CO dehydrogenase [11], Mo/W is found in active sites in a mononuclear form coordinated by the organic cofactor pyranopterin (referred in the literature as Moco/Wco; see for example the review of Hille [12]). This pterin consists of a tricyclic pyranopterin moiety synthesized through a conserved multiple steps pathway [13]. In eukaryotes, the pyranopterin is found in the simple monophosphate form whereas in prokaryotes it is conjugated to nucleosides, usually either cytosine (pterin cytosine dinucleotide, PCD) or guanosine (pterin guanosine dinucleotide, PGD). A large proportion of Mo/W-enzymes encountered in prokaryotes and furthermore present in more than 90% of Mo/W-utilizing prokaryotic organisms [2,14] harbor in their active site a Mo/W atom coordinated by two molecules of PGD

☆ This article is part of a Special Issue entitled: Metals in Bioenergetics and Biomimetics Systems.

* Correspondence to: B. Guigliarelli, Unité de Bioénergétique et Ingénierie des Protéines UMR7281, CNRS/AMU, FR3479, F-13402 Marseille Cedex 20, France. Tel.: +33 491 164 567; fax: +33 491 164 097.
** Correspondence to: A. Magalon, Laboratoire de Chimie Bactérienne UMR7283, CNRS/AMU, FR3479, F-13402 Marseille Cedex 20, France. Tel.: +33 491 164 668; fax: +33 491 167 194.
E-mail addresses: guigliar@imm.cnrs.fr (B. Guigliarelli), magalon@imm.cnrs.fr (A. Magalon).

0005-2728/$ – see front matter © 2013 Elsevier B.V. All rights reserved.
http://dx.doi.org/10.1016/j.bbabio.2013.01.011

(Fig. 1). These latter enzymes are diverse in terms of structure and/or subunit composition (see below) but were named, referred to the first representative that has been crystallized [15], as members of the "DMSO reductase family". The latter enzyme represents an exception rather than the rule among this family (see Section 3.1) and this denomination furthermore referred to a precise enzymatic activity. The name Complex Iron–Sulfur Molybdoenzyme (CISM) superfamily has been recently introduced for molybdoenzymes harboring such a Mo- or W-*bis*PGD cofactor [16]. Rothery et al. in fact describe the members of this family, although with some exceptions, as heterotrimeric enzymes containing both a FeS subunit harboring four FeS clusters (denoted FCP) and a membrane anchor protein (denoted MAP). As it can be seen in Table 1, exceptions are today more frequent than the rule! We therefore preferred the denomination "Mo/W-*bis*PGD enzymes".

Many reviews have been published in the last decades even a recent special issue dedicated exclusively to Mo/W enzymes (Coordination Chemistry Reviews 2011, vol 255, issues 9–10). The Mo/W-enzyme superfamily is so large that it is indeed impossible to exhaustively address all together the structural, functional and biosynthetic aspects (see [17–19] for recent reviews on separate aspects). The biosynthesis of Moco and its assembly in Mo/W enzymes invokes a rather complex pathway. A dedicated overview article on this question is presented in this special issue. In the present review, we will focus on structural and functional aspects and highlight salient features of these enzymes. Since the Mo/W-*bis*PGD enzymes family illustrates in itself the extraordinary variety of Mo/W-enzyme superfamily (Table 1), analyzing their catalysis should allow us to set of principles common to Mo/W catalysis. In an ultimate step, applying them to the design of bio-mimetic constructs should contribute to improve the technology as practiced today. In particular, the Mo/W-*bis*PGD enzymes are involved in redox reactions, either with oxygen or sulfur atom transfer reactions or oxidative hydroxylations. In these reactions, the Mo or W undergoes two-electron oxidation/reduction between the states Mo(IV)/W(IV) and Mo(VI)/W(VI) (see for recent overview [20]). An exception to this rule is the tungsten–iron–sulfur enzyme acetylene hydratase (Ah) from *Pelobacter acetylenicus* catalyzing a non-redox reaction [21]. Although the pyrogallol:phloroglucinol hydroxyltransferase (Th) of *Pelobacter acidigallici* [22] catalyzes a net non-redox reaction as well, it involves a reductive dehydroxylation and an oxidative hydroxylation as separate but concomitant events. In contrast to the diversity (in term of chemical nature and redox potential; Table 2) of the substrates and the chemical reactions they support, the Mo/W-*bis*PGD enzymes could appear as relatively homogenous in term of catalytic site. The detailed examination of the Mo/W ion coordination mode reveals however that here is probably the determinant of the specific catalysis of each enzyme. Consequently, we will present, in a first part, a detailed description of the catalytic site relevant to its functioning (Section 2).

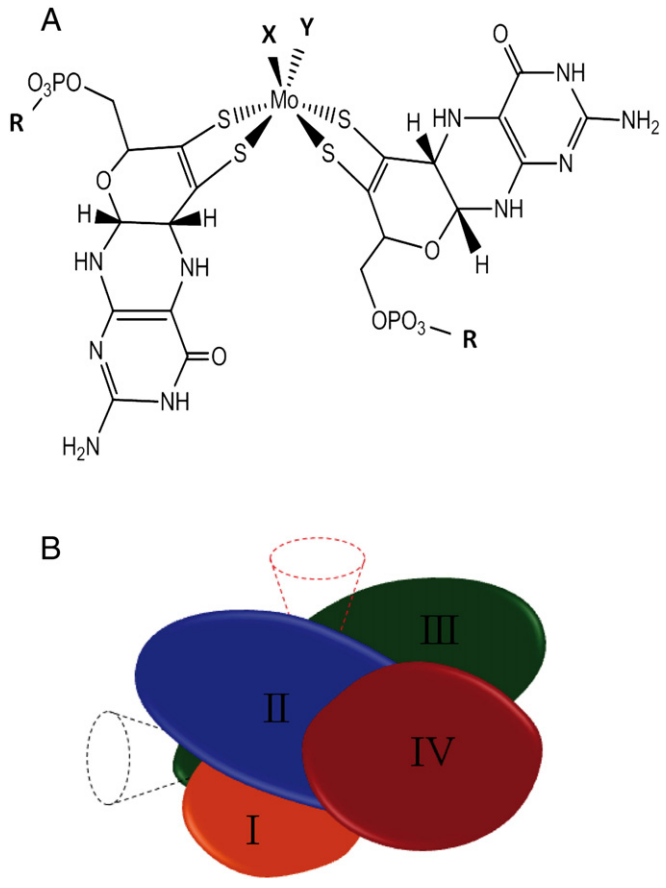

Fig. 1. Schematic description of the catalytic subunit of Mo/W-*bis*PGD enzymes family. A. Structure of the molybdenum cofactor showing the *bis*-pyranopterindithiolene coordination. The group R is guanosine (PGD) or cytosine (PCD). The Mo ligands X and Y can be: X = O or S; Y = Ser, Cys, SeCys, Asp. B. Schematic representation of the four-domain organization found in Mo/W-*bis*PGD enzymes. It is to note that these four domains do not correspond to consecutives sequences in the protein. All members of this family, except Ah, have an active site funnel along the red cone situated between domains II and III. Ah is the only currently known case where the funnel is situated at the intersection of domains I, II and III.

The Mo/W-*bis*PGD enzymes catalyze redox reactions that are key steps in carbon, nitrogen and sulfur cycles. The Mo/W-*bis*PGD structural module thus appears to have served multiple purposes for life, especially in energy harvesting. To this aim, the large catalytic Mo/W containing-subunit, present in all members of the family, is supplemented by a variable number of additional subunits to generate the multitude of individual subfamilies. This family is therefore a textbook example of the construction kit model introduced by Baymann et al. [23] and actualized by Schoepp-Cothenet et al. [24]. Recently, a detailed phylogenetic study revealed that several members of the Mo/W-*bis*PGD enzymes family have been present in LUCA [25]. The high solubility of MoS_4^{2-} salts supplied by alkaline hydrothermal vents [26,27] and their abundance in the oceans likely contributed to the early adoption in evolution of Mo as a redox cofactor [28]. The Mo/W-*bis*PGD enzyme structural module thus seems to have been recruited right from the life origins. Whereas the Mo/W coordination modulation likely represents the catalytic specificity determinant of the enzyme, the variation in subunit and cofactor composition together with the sub-cellular localization of the enzyme rationalizes its bioenergetic integration. The Mo/W-*bis*PGD enzymes have indeed been shown to contribute to the generation of chemiosmotic potential by coupling electron transfers they support to proton translocation. The published reviews focusing on this latter aspect are mainly focusing on nitrogen cycle (see for example [29,30]). The bioenergetic impact of the Mo/W-*bis*PGD enzymes are however of great importance for life in all major geochemical cycles, letting one of the author involved in the present review call the Mo/W-*bis*PGD enzyme catalytic subunit "the catalytic workhorse of bioenergetics" [24]. Consequently, we will have, in a second part, a description of the enzymes in terms of subunit composition and sub-cellular localization finally addressing the question of chemiosmotic potential generation by the enzymes (Section 3). We will especially discuss the connection of the involved enzymes with the liposoluble hydrogen carriers, i.e. isoprenoid quinones. Because the bioenergetic balance of a specific enzyme cannot be dissociated from the chain in which this enzyme is integrated, we will present, in a final part, an exhaustive overview of metabolic chains where the Mo/W-*bis*PGD enzymes are known to be involved (Section 4).

2. Structure and reactivity of the molybdenum/tungsten cofactor in Mo/W-*bis*PGD enzymes

Molybdenum is a well known metal having a high affinity for oxygen and sulfur, and its oxides and sulfides compounds are largely

Table 1
Actualized members of the Mo/W-*bis*PGD family. Catalytic subunits are denoted α, with α containing both Mo/W-*bis*PGD cofactor and [4Fe–4S] cluster, α′ containing Mo/W-*bis*PGD cofactor but no [4Fe–4S] cluster, and α″ containing Mo/W-*bis*PGD cofactor and [4Fe–4S] and [2Fe–2S] clusters. Electron transfer subunits are denoted β, with β folded as two ferredoxins containing three to four [Fe–S] clusters, β′ folded as globular di-heme *c* cytochrome, β″ folded as a Rieske protein with a [2Fe–2S] cluster, and β‴ containing FAD cofactor and zero or two [2Fe–2S] clusters. Electron entry/exit subunits are denoted γ, with γ the 4 TM dihemic cytb^{I}, γ′ the 5 TM dihemic cytb^{II}, γ″ the monohemic hydrophilic cytb^{III}, and γ‴ the membranous NrfD-type unit devoid of any cofactor. In addition to these subunits associated with multiple complexes, three units have been proposed to be part of specific complexes such as the tetrahemic cytochromes c_3 of Fdh in *Desulfovibrio desulfuricans* or c_{554} of Pcr in *Dechloromonas* species and, dihemic cytochrome cNarC of cNar in *Thermus thermophilus*. These elements are denoted δ. Formylmethanofuran dehydrogenases have been barely characterized and will be no further structurally described in this review. "nd" in the fourth column denotes undetermined in isolated protein.

Enzymes	Abb.	Example organism	Metal in active site	Subunit composition
Nitrogen metabolism				
Periplasmic nitrate reductase	Nap	*Rhodobacter sphaeroides*	Mo	αβ′
		Desulfovibrio desulfuricans	Mo	α
Respiratory nitrate reductase	nNar	*Escherichia coli*	Mo	αβγ′
	cNar	*Thermus thermophilus*	Mo	αβγ′δ
	pNar	*Haloferax mediterranei*	Mo	αβγ″
	pNar	*Pyrobaculum aerophilum*	Mo/W	αβγ″
Nitrite oxidoreductase	nNxr	*Nitrobacter hamburgensis*	Mo	αβγ′
	pNxr	*Candidatus Nitrospira defluvii*	nd	αβ
Assimilatory nitrate reductase	NarB	*Synechococcus*	Mo	α
	NasA	*Klebsiella pneumonia*	Mo	α″β
	NasC	*Bacillus subtillis*	Mo	αβ‴
TMAO reductase	Tor	*Shewanella massilia*	Mo	α′
Sulfur metabolism				
Polysulfide reductase	Psr	*Thermus thermophilus*	Mo	αβγ‴
		Wolinella succinogenes	Mo	αβγ‴
Sulfur reductase	Sre	*Aquifex aeolicus*	Mo	αβγ‴
Tetrathionate reductase	Ttr	*Salmonella typhimurium*	nd	αβγ‴
Thiosulfate reductase	Phs	*Salmonella typhimurium*	nd	αβγ
DMSO reductase	Dms	*Escherichia coli*	Mo	αβγ‴
	Dms	*Halobacterium* sp. NRC-1	Mo	αβγ‴
DMSO reductase	Dor	*Rhodobacter sphaeroides*	Mo	α′
Dimethylsulfide dehydrogenase	Ddh	*Rhodovulum sulfidophilum*	Mo	αβγ″
Carbon metabolism				
Formate dehydrogenase	Fdn	*Escherichia coli*	Mo	αβγ
	W-Fdh	*Desulfovibrio gigas*	W	αβ
	Fdh	*Desulfovibrio desulfuricans*	Mo	αβδ
Formate dehydrogenase	FdhF	*Escherichia coli*	Mo	α
Formylmethanofuran dehydrogenase	Fmd	*Methanobacterium thermoautotrophicum*	Mo	αβ
	Fwd	*Methanobacterium thermoautotrophicum*	W	αβεγ
Diverse metabolisms				
Biotin-*d*-sulfoxide reductase	BisC	*Escherichia coli*	Mo	α′
Selenate reductase	Ser	Thauera selenatis	Mo	αβγ″
	Srd	Bacillus selenatarsenatis	nd	αβγ‴
Perchlorate reductase	Pcr	*Dechloromonas aromatica*	Mo	αβδ
Chlorate reductase	Clr	*Ideonella dechloratans*	Mo	αβγ″
Arsenite oxidase	Aio	*Alcaligenes faecalis*	Mo	αβ″
Arsenate reductase	Arr	*Shewanella ANA-3*	Mo	αβ
		Wolinella succinogenes	nd	αβγ‴
Alternative arsenite oxidase	Arx	*Alkalilimnicola ehrlichii*	nd	αβ
		Halorhodospira halophila	nd	αβγ‴
Ethylbenzene dehydrogenase	Ebdh	*Azoarcus* str. EbN1	Mo	αβγ″
Acetylene hydratase	Ah	*Pelobacter acetylenicus*	W	α
Pyrogallol–phloroglucinol transhydroxylase	Th	*Pelobacter acidigallici*	Mo	αβ
Resorcinol hydroxylase	Rh	Azoarcus anaerobius	nd	αβ
C25dehydrogenase	C25dh	*Sterolibacterium denitrificans*	Mo	αβγ″

used as heterogeneous catalysts in important industrial processes like oxidative production of formaldehyde from methanol or methane, hydrodesulfurization of petroleum fractions, and olefin metathesis [31]. When metal oxides are deposited on porous support like silica, molybdenum is progressively dispersed [32] and it has been shown that the active sites where oxidative formaldehyde formation occurs are monomeric species with pentahedral $Mo(O)(OSi)_4$ or tetrahedral $Mo(O)_2(OSi)_2$ structure. The Mo═O sites located in the lateral plane are the most active and selective [33], in a way that is reminiscent of the situation encountered for the Mo cofactor of enzymes of sulfite oxidase family [12]. The redox states of Mo-oxides that are stable in aqueous solutions are Mo(III), Mo(IV) and Mo(VI), but at pH>3 Mo(III) disproportionate and only Mo(IV) and Mo(VI) are thermodynamically stable [34]. In contrast, when the metal is coordinated by the dithiolene moiety of the pyranopterin within a protein matrix, the Mo(V) state can be stabilized and the Moco is usually considered to cycle between Mo(IV), (V) and (VI) redox states during enzyme turnover [12]. It is worth noting that the chemical environment provided by the pterin cofactor and by the polypeptide chain strongly modulates the redox properties of the Mo ion and then appears as a key factor to finely tune the catalytic properties for a specific substrate. As a consequence, a salient property of Mo/W-*bis*PGD enzymes is their ability to ensure either two consecutive one electron transitions with a stable Mo(V) state (see below) or a direct two electrons transition between the Mo(IV) and Mo(VI) states. Such versatility of the redox processes at the active site has broadened up the range of redox reactions catalyzed by members of the Mo/W-*bis*PGD family as exemplified below with the one electron reduction of nitrite to nitric oxide or their ability to achieve uphill redox reactions.

Among the three main families of molybdoenzymes identified so far [12], the Mo/W-*bis*PGD enzymes family is the most diverse in terms of structural organization and used substrates. In this family,

Table 2
Principal redox couples considered in this review. Non-common substrates are indicated both with chemical formula and names.

Redox couples	Redox potential at pH 7 E_0' (mV)	References
Quinones		
MMK/$MMKH_2$	−220[a]	[227]
MK/MKH_2	−74[a]	[463]
DMK/$DMKH_2$	+36; −9[a]	[464,465]
UQ/UQH_2	+113[a]	[466]
Environmental compounds		
Methanofuran/formylmethanofuran $C_{34}H_{37}N_4O_{14}+CO_2/C_{35}H_{39}N_4O_{16}$	−497; −530	[12,427]
Carbon dioxide/formate CO_2/HCOOH	−430	[466]
$2H^+/H_2$	−410	[466]
Thiosulfate/sulfide + sulfite $S_2O_3^{2-}/HS^- + HSO_3^-$	−400	[466]
Sulfur/sulfide S^0/HS^-	−270	[466]
Pyrogallol/1,2,3,5-tetrahydroxybenzene	−84	[431]
Resorcinol/hydroxyhydroquinone	−33	[437]
Tetrathionate/thiosulfate $S_4O_6^{2-}/S_2O_3^{2-}$	+24; +170	[466,467]
1-Phenylethanol/ethylbenzene	+30	[440]
C25-hydroxycholesterol/cholesterol	+30	[167]
Arsenate/arsenite $HAsO_4^{2-}/H_3AsO_3$	+60; +139	[466,468]
TMAO/TMA	+130	[65]
DMSO/DMS	+160	[466]
Uranium trioxide/uranium dioxide UO_3/UO_2	+260; +410	[301]
Nitrate/nitrite NO_3^-/NO_2^-	+433	[466]
Selenate/selenite $SeO_4^{2-}/HSeO_3^-$	+475	[466]
Chlorate/chlorite ClO_3^-/ClO_2^-	+708	[469]
Fe(III)-citrate/Fe(II)-citrate	+385	[307]
Perchlorate/chlorate ClO_4^-/ClO_3^-	+788	[469]
O_2/H_2O	+820	[466]

[a] For quinones given redox potentials are E_m', rather than E_0', at pH 7. These values represent average values between those of the Q/SQ and SQ/QH_2 transitions.

the metal ion bound to the *bis*(pyranopterin guanosine dinucleotide) cofactor is coordinated by the four sulfur atoms of two dithiolene groups (Fig. 1A). Depending on the enzyme and its redox state, the coordination sphere of the Mo atom is completed by other ligands: an amino acid side chain in fifth position, and oxygen from an oxo group or a solvent molecule, or sulfur from a sulfido in sixth position. The nature of the coordinating amino acid can be used to subdivide this enzyme family in three groups: a first one where Mo is coordinated by Cys or SeCys, a second one where Mo is coordinated by Asp, a third one where Mo is coordinated by Ser. It is to note that no amino acid side chain coordinates the Mo ion in arsenite oxidase (Aio). This subdivision corresponds, with several exceptions, to the I, II and III classes introduced by Weiner and co-workers [35] based on coordination of FS0 iron–sulfur center (see below Section 3.1). Although Mo and W share similar chemical characteristics, due to their different bioavailability in oxic and mesophilic environments, Mo-enzymes are largely distributed while W-enzymes are found in a limited range of mainly anaerobic and thermophilic microorganisms. Also, the differences between their redox properties make the reactions catalyzed by W-enzymes generally having lower redox potentials than those catalyzed by Mo-enzymes [36].

Members of the Mo/W-*bis*PGD enzymes family are exclusively found in prokaryotes and use a broad diversity of substrates including oxides of nitrogen, sulfur, carbon, halogens, and metalloids in redox reactions which can be considered for most of them as simple oxygen atom transfer (OAT) between the substrate and the solvent. This is the case for DMSO reductase (Dor, Dms), DMS dehydrogenase (Ddh), biotin-*d*-sulfoxide reductase (BisC), nitrate reductases (Nars, Nap, Nas), nitrite oxidoreductases (Nxrs), TMAO reductase (Tor), alternative arsenite oxidase (Arx), selenate reductases (Ser and Srd), perchlorate reductase (Pcr), chlorate reductase (Clr), arsenate reductase (Arr), and formylmethanofuran dehydrogenase (Fmd, Fwd) which obey the general scheme: $R-O+2e^-+2H^+=R+H_2O$. In these reactions, the electrons are transferred by other redox cofactors in the enzyme. Similarly, sulfur atom transfer (SAT) reactions are catalyzed by polysulfide reductase (Psr), sulfur reductase (Sre), thiosulfate reductase (Phs), and tetrathionate reductase (Ttr) leading to the formation of H_2S, except for Ttr. Other important catalyzed reactions are the conversion of formate into CO_2 by formate dehydrogenases (Fdh), and the hydroxylation processes identified with substrates such as ethylbenzene for ethylbenzene dehydrogenase (Ebdh), resorcinol for resorcinol hydroxylase (Rh) and very recently with cholesterol side chain for C25dehydrogenase (C25dh), according to the scheme: $R-H+H_2O=R-OH+2e^-+2H^+$. In a less common way, some members of the Mo/W-*bis*PGD enzymes family are able to catalyze overall non-redox reactions such as the hydration of acetylene by acetylene hydratase (Ah) and the transfer of OH group between phenols by pyrogallol–phloroglucinol transhydroxylase (Th).

Thus, in spite of a limited range of coordination structure, members of the Mo/W-*bis*PGD enzymes family catalyze a very wide diversity of reactions. Additionally, no correlation appears between the nature of the Mo coordination and the catalyzed reactions (Table 3). This emphasizes the crucial role played by the surrounding protein to modulate the Moco reactivity and to date the structural factors that trigger substrate specificity, enzyme directionality and catalytic efficiency remain to decipher. This question was largely addressed during the last three decades and a huge amount of spectroscopic data, mainly based on EPR and EXAFS, was gained on various Mo-enzymes to investigate their catalytic mechanisms (see for instance [37]). Moreover, the increasing number of X-ray structure determinations for about 15 years brought invaluable

Table 3
Metal coordination of crystallized members of the Mo/W-*bis*PGD enzymes family. "dth" in the first column denotes the dithiolene moiety of the PGD molecules.

Metal coordination	Metal in active site	Function	Abb.	Organism	Structure	Ref.
$M(dth)_2(O)(OSer)$	Mo	DMSO reductase	Dor	*Rhodobacter sphaeroides*	1EU1	[42]
		DMSO reductase	Dor	*Rhodobacter capsulatus*	3DMR	[40]
		TMAO reductase	Tor	*Shewanella massilia*	1TMO	[41]
		Pyrogallol–phloroglucinol transhydroxylase	Th	*Pelobacter acidigallici*	1TI2	[22]
$M(dth)_2(S)(SCys)$	Mo	Nitrate reductase	Nap	*Rhodobacter sphaeroides*	1OGY	[68]
			Nap	*Desulfovibrio desulfuricans*	2JIP	[70]
			Nap	*Escherichia coli*	2NYA	[69]
			Nap	*Cupriavidus necator*	3ML1	[71]
	Mo	Polysulfide reductase	Psr	*Thermus thermophilus*	2VPZ	[88]
$M(dth)_2(S)(SeCys)$	Mo	Formate dehydrogenase	FdhF	*Escherichia coli*	1FDO	[91]
			FdhF	*Escherichia coli*	2IV2	[94]
			Fdn	*Escherichia coli*	1KQG	[92]
	W	Formate dehydrogenase	W-Fdh	*Desulfovibrio gigas*	1H0H	[93]
	W	Acetylene hydratase	Ah	*Pelobacter acetylenicus*	2E7Z	[104]
$M(dth)_2(O_2CAsp)$	Mo	Nitrate reductase	nNar	*Escherichia coli*	1Q16	[114]
$M(dth)_2(O)(OAsp)$	Mo	Nitrate reductase	nNar	*Escherichia coli*	1R27	[115]
	Mo	Ethylbenzene dehydrogenase	Ebdh	*Aromateum aromaticum*	2IVF	[131]
$M(dth)_2(O)$	Mo	Arsenite oxidase	Aio	*Alcaligenes faecalis*	1G8K	[169]

information on the Moco environment (see for instance [17]) which is now currently used in combination with theoretical studies to model Mo-enzyme reactivity (see for instance [38]). A conspicuous intrinsic property of the Mo ion is however, the great versatility of its coordination sphere and its affinity to various anions that made very complicated the analysis of this wealth of data. In many cases, spectroscopy has revealed that the Moco is present as a mixture of several species in a given enzyme preparation, the relevance of these species for the catalytic process being still largely debated. Moreover, such heterogeneities were also observed in the three-dimensional structures of the enzymes and due to the limitation of resolution, they led to controversial analysis of the Mo ion environment in a number of cases (see below).

In this section, we attempt to give an overview of the current knowledge on relationships between structural properties of the Mo/W cofactor environment and its reactivity. We focus on systems for which available experimental data and theoretical studies are sufficient to provide a rational understanding of this challenging question. For sake of clarity, enzyme systems are classified according to the amino acid ligand present in the first coordination sphere of the metal ion.

2.1. Mo/W-bisPGD enzymes with serine ligand

2.1.1. The first coordination sphere of the Mo ion

The difficulties related to the heterogeneity of the Moco are well exemplified by crystallographic studies of DMSO reductases (Dor) from *Rhodobacter* species. Crystal structure determinations of Dor from *Rhodobacter* species indicated an overall identical polypeptide fold of the catalytic subunit core arranged in four domains (I–IV) surrounding the Mo-*bis*PGD cofactor, with a substrate access funnel defined by the two domain II, III interface (Fig. 1). However, significant variations in the Moco coordination were observed in these studies. In the oxidized Mo(VI) enzyme, a pentacoordinate Mo-ion was initially observed in *R. sphaeroides* [39] with three sulfur atoms from the two dithiolenes, one Mo═O and the Oγ of the serine ligand (Ser147). Conversely, the crystallographic studies of the *R. capsulatus* enzyme reported a pentacoordination of the Mo(VI) ion with two oxo-ligands, two sulfur atoms from one dithiolene and the Ser147 Oγ ligand [15]. Subsequently, a seven-coordinate Mo-ion was proposed in this latter enzyme by including two additional sulfur atoms from the second dithiolene group [40] and a similar structure was determined in the closely related TMAO reductase (Tor) enzyme from *Shewanella massilia* [41]. These crystallographic structures were largely debated together with EXAFS data (see for details [37]), and the situation was clarified when a high resolution structure of the *R. sphaeroides* Dor demonstrated that the enzyme is present as a mixture of variable amounts of pentacoordinate and hexacoordinate Mo-ion in crystals [42]. The hexacoordinate structure of the Mo(VI) ion with four sulfur atoms from the two dithiolenes, a single Mo═O group and the Ser Oγ ligand was in agreement with EXAFS [43,44] and resonance Raman [45] data and is now considered to correspond to the active oxidized enzyme (Table 3). In contrast, the pentacoordinate one likely results from an enzyme inactivation with the dissociation of one PGD from the Mo and its replacement by a second oxo group, a phenomenon that seems to be common among members of the Mo/W-*bis*PGD enzymes family [46,47]. As the first crystal structures of reduced Dor have indicated the de-coordination of one dithiolene sulfur atom with respect to the oxidized enzyme [39,40], a catalytic mechanism was initially suggested in which the oxo transfer would be assisted by the dissociation and re-association of one PGD cofactor between the different redox states of the Mo-ion [39]. However, a detailed analysis combining crystallography and biochemical assays [48] clearly revealed that upon exposure of the enzyme to Hepes buffer, a pair of thiolates dissociates leading to enzyme inactivation, and that sulfur dissociation from the Mo-ion observed in crystals was an artifact. Interestingly, the enzyme structure obtained with the DMSO substrate bound to the active site showed that the DMSO molecule is directly coordinated to the Mo-ion through its oxygen atom which is hydrogen bound to the indole ring of Trp116 [49].

All these data led to a commonly accepted two-step mechanism in which the Mo ion remains coordinated to the four sulfur atoms of the two dithiolenes and to the Ser Oγ ligand during the whole catalytic cycle (Scheme 1).

This leads to a pentacoordinated *des*-oxo Mo(IV) ion in the reduced enzyme enabling the binding of DMSO via its oxygen atom to the Mo through a first transition state. The intermediate Mo(VI) state with bound DMSO then evolves through a second transition state and the S – O bond cleavage to an hexacoordinate Mo(VI) with Mo═O group, this second step being rate-limiting. This mechanism was supported first by DFT calculations [50] and later by ab initio and DFT methods [51,52] but the precise values of energy barriers (ranging from 14.6 to 19.2 kcal/mol) are still subject to discussion [38]. After DMS release, the hexacoordinated Mo(VI) species return to the *des*-oxo Mo(IV) species through the transfer of two electrons and two protons and the departure of a H_2O molecule.

In this mechanism, the reduction of the Mo(VI) species proceeds through two successive one-electron reduction steps resulting in an intermediate Mo(V) state which can be detected by spectroscopic techniques. Detailed redox titrations of the enzyme monitored by UV–visible spectroscopy indicate that the Moco is reduced by only two reducing equivalents and that the two pyranopterin ligands are not redox active [53]. A catalytic Mo(V) intermediate can be quantitatively isolated in the course of this reductive process, reaching 100% of the Dor enzyme when TMAO is used as an alternative substrate [53]. This Mo(V) species is characterized by a rhombic "high *g* split" EPR signal [54,55] showing an hyperfine coupling with a single exchangeable proton. This coupling was attributed to an hydroxyl ligand bound to the Mo(V) ion on the basis of ESEEM and HYSCORE studies of deuterium hyperfine coupling in a D_2O exchanged sample [56]. Similar Mo(V) EPR signals were observed in various Mo-enzymes with Ser coordination, their *g*-values showing a clear correlation when plotted as a function of the *g*-tensor anisotropy (Fig. 2). This indicates that in these enzymes, the Mo(V) ion displays the same coordination sphere, the *g*-tensor variations being due to small structural modifications (angle or distance bonds) induced by changes of the second coordination sphere of the metal or of its close environment [57,58].

More recently, the *g*-tensor and the ^{95,98}Mo hyperfine coupling analysis of the *high g split* signal, combined with computational study, confirmed this Mo(V)–OH structure [59]. This study revealed a relaxed geometry for this intermediate that lies between idealized octahedral and trigonal prismatic and was used to model electronic and MCD spectra. This energetically stabilized geometry explains why the Mo(V)–OH

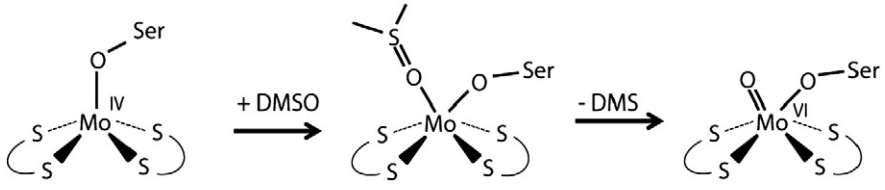

Scheme 1. Reaction mechanism of DMSO reductase.

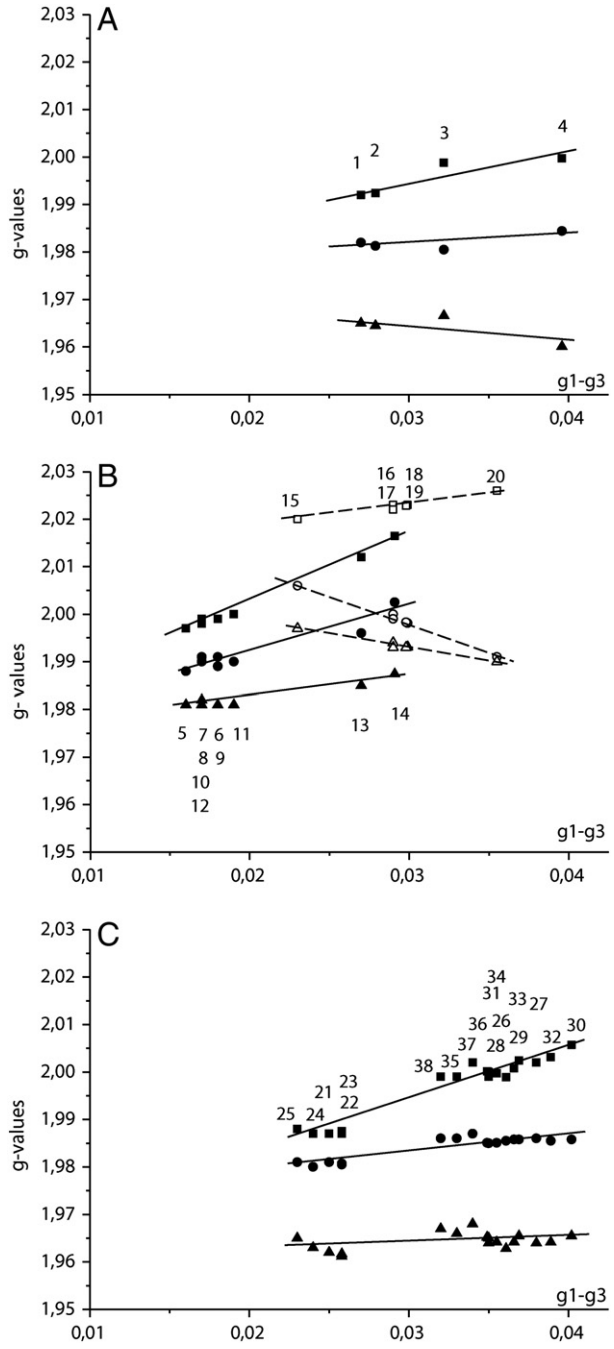

Fig. 2. Plots of the *g*-values of Mo(V) species against anisotropy for members of the Mo/W-*bis*PGD enzymes family. A. Moco with Ser ligand. *High g split* signals from *R. sphaeroides* Dor (1, 2) [44,56], BisC (3) [63], *S. massilia* Tor (4) [453]. B. Moco with Cys or SeCys ligand. Close symbols, *high g* type signals: *E. coli* NapA *high g resting* (5) [69], *R. sphaeroides* NapAB *high g resting* (6) [68] and NapA *high g resting* (7) [84], *P. pantotropha* NapAB *high g resting* (8) [55], and *high g nitrate* (9) [75], *S. gelidimarina* NapAB *high g resting* (10) [454], *D. desulfuricans* NapA *high g nitrate* (11) [74] and *high g turnover* (12) [70], *D. desulfuricans* Fdh (13) [98], and *W. succinogenes* Psr treated with polysulfide (14) [89]. Open symbols, *very high g* type signals: *Methanobacterium formicicum* Fdh (15) [455], *R. sphaeroides* NapAB (16) [68], *P. pantotrophus* NapAB (17) [75], *Synechococcus* sp. NarB (18) [87], *A. vinelandii* Nas (19) [456], and *very high g split* from *W. succinogenes* Psr (20) [89]. C. Moco with Asp ligand. High-pH signals from *E. coli* NarGHI (21) [122], (22) [120], (23) [119], high-pH (24) and high-pD (25) from *M. hydrocarbonoclasticus* NarGH [127]. low-pH signals (26), nitrate (27), nitrite (28) [119], nitrate 1 (29), nitrate 2 (30), nitrite 1 (31), nitrite 2 (32), chloride (33), fluoride (34) from *E. coli* NarGHI [120]. low-pH signal (35), low-pD (36), nitrate (37), and nitrite (38) from *M. hydrocarbonoclasticus* NarGH [127]. Linear correlations between the available data sets within each family can be extrapolated and are schematically indicated by straight or dotted lines to help the reader.

to Mo(IV) + H_2O reduction step is rate limiting when TMAO is used as substrate. Indeed, the calculations indicate that, with this substrate, the OAT event is activationless.

2.1.2. Role of the environment on the Moco reactivity

This oxygen atom transfer mechanism appears to be common within Ser coordinated Mo/W-*bis*PGD enzymes, which generally have a fairly open substrate binding funnel and exhibit broad substrate specificity towards S- and N-oxides [16]. Several mutagenesis studies were undertaken to address the structural factors influencing this specificity. Several residues (Thr148, Ala178, Arg217, Gly167, Gln179) predicted to form the wall of the funnel leading to the Mo active-site in *E. coli* Dms were mutated and found to affect substrate binding and/or specificity, while not spatially clustered [60]. Two highly conserved aromatic residues Tyr114 and Trp116 arranged around the Mo ion have attracted much attention as potential candidates involved in catalysis and/or in substrate specificity. In the structures of Dor from *R. capsulatus*, Trp116 hydrogen-bonds to the labile oxo group of oxidized enzyme [15,40] and to the oxygen of the DMSO in the structure with substrate bound at the reduced active site [49]. Trp116 is conserved in Tor and in BisC. Whereas substitution of this residue to phenylalanine in Dor caused a significant reduction in k_{cat} towards DMSO and TMAO, the K_m for DMSO is not markedly affected and the K_m for TMAO is slightly reduced [61]. This suggests that Trp116 does not greatly influence substrate binding while having an important role in the catalytic cycle. Spectroscopic studies of the as-isolated Trp116Phe mutant indicate that it harbors a pentacoordinate dioxo Mo center in which one dithiolene group is outside the Mo coordination sphere and replaced by a second Mo═O group [61,62], similarly to the "Hepes-modified" inactive form of the enzyme [42,48]. As such, Trp116 would prevent movement of the Mo-oxo unit away from the coordinating dithiolene in the resting Mo(VI) enzyme. Redox cycling the Trp116Phe mutant, however, regenerates transiently a wild-type like enzyme DMSO reducing activity [62]. Similar mutations of the equivalent residue (Trp90) in BisC exhibited also markedly decreased catalytic activities and drastic changes on the Mo(V) EPR spectral properties, with no significant alterations in either substrate affinity or specificity [63]. Thus, in agreement with mechanistic scheme presented above, by stabilizing the mono-oxo Mo(VI) species by hydrogen bond, this Trp residue could have a direct influence on the rate-limiting step of the catalysis and would play an important role in controlling the catalytic efficiency in Dor and BisC.

Tyr114 was found hydrogen-bound to the oxo ligand of the mono-oxo Mo(VI) in the first structure of Dor from *R. sphaeroides* [39]. The presence of this oxo-group as Mo ligand was however reassessed and it was proposed to be an artifact following an erroneous interpretation of the electron density maps caused by discrete heterogeneity of the Mo position in the crystals [42,48]. On the other hand, the tyrosine OH oxygen is located at 3.3 Å from the sulfur of the DMSO in the structure of Dor from *R. capsulatus* complexed with its substrate [49]. Interestingly, this residue is conserved in BisC [63,64]. The unique but striking difference in the arrangement of the residues directly surrounding the active center at the Mo ion in the Dor and Tor structures is the absence of Tyr114 in the latter [41]. While it is replaced by a threonine (Thr116) or a serine depending on the organism, no other residue occupies the space left empty by the missing aromatic side chain. This led to the hypothesis that Tyr114 is critical for the control of substrate specificity in the S-oxide/N-oxide reductases [41,65]. Substitution of this residue for a phenylalanine (Tyr114Phe) in recombinant Dor from *R. sphaeroides* expressed in *E. coli* [64], or in *R. capsulatus* [62,66] leads to a significant alteration of the catalytic properties toward DMSO and TMAO, resulting in an ~10 fold decreased efficiency of the enzyme toward DMSO and a slightly less efficiency with TMAO. Noteworthy, the substitution does not affect the Mo(V) EPR spectrum, indicating no interaction of the residue with the Mo center in this redox state [62]. In addition, protein film voltammetry measurements indicated that this residue is critical for protonation steps at the active site [66]. Insertion of a Tyr into Tor

in an equivalent position results in a decreased preference for TMAO relative to DMSO [64]. Altogether, these studies indicate that Tyr114 would function in substrate recognition: it would be important for correct positioning of the substrate in the Dor active site, most likely by providing a hydrogen bond with DMSO.

2.2. Mo/W-bisPGD enzymes with cysteine or selenocysteine ligand

Investigations of the structure and mechanism of Mo/W-*bis*PGD enzymes with Cys or Se-Cys coordination were subjected to long controversy due to uncertainties in the determination of the Mo ion ligands by X-ray crystallography and to the plasticity of this coordination sphere as shown by spectroscopy experiments. Moreover, by comparison with several enzymes carrying a Ser coordinated Moco (Dor, Tor, BisC), all those harboring a Cys or SeCys coordinated Moco contain at least one additional FeS cluster in the catalytic subunit (see Section 3.1). This makes spectroscopic approaches more complicated to address their catalytic mechanism. In this section, the structure and mechanism of several representative enzymes of this group, Nap, Psr, Fdh, Ah, which catalyze a large diversity of reactions, are reported.

2.2.1. Periplasmic nitrate reductases

2.2.1.1. The first coordination sphere of the Mo ion. In the case of periplasmic dissimilatory nitrate reductases (Nap), the first structure obtained for the oxidized enzyme NapA from *Desulfovibrio desulfuricans* has shown a Mo ion coordinated by the four sulfur atoms of the two PGD dithiolenes and by a fifth sulfur from a Cys residue [67]. An additional sixth ligand being OH or OH_2 was determined, and the same coordination was proposed from crystallographic studies at lower resolution of the enzymes NapAB from *R. sphaeroides* [68] and NapA from *E. coli* [69]. Detailed investigations of subsequent crystallographic data obtained with *D. desulfuricans* NapA, together with *B* factor analysis, assigned however this sixth ligand to a sulfur atom partially bond with the thiolate of the Cys ligand in the "as prepared" state of the enzyme [70]. This six sulfur coordination of the Mo ion was also confirmed by the recent high resolution structure (1.5 Å) of the NapAB enzyme from *Cupriavidus necator* (formerly *Ralstonia eutropha*) [71].

According to the initial NapA structure, the first theoretical investigations of enzyme reaction proposed a mechanism closely related to that of Dor, the serinate ligand being replaced by a cysteinate one. In the first step of this mechanism, nitrate binds through one oxygen atom to the Mo(IV) ion. This is followed by the N – O bond breaking step, leading to the release of nitrite and to the formation of a Mo(VI)–O intermediate [72,73]. However, by contrast with Ser coordinated Mo/W-*bis*PGD enzymes, EPR studies of Naps revealed a number of substoichiometric distinct Mo(V) species whose catalytic relevance was strongly discussed. These species were classified in three main groups according to their *g* values as *high g*, *very high g*, and *low g* species (Fig. 2B) [55,68,69,74]. Depending on enzyme preparations and treatments, the proportions of these species vary greatly, the *high g* species being usually the most abundant while the two others are considered as resulting from partial degradation of the Moco [75]. Mo(V) *high g*-type signals show characteristic hyperfine splittings attributed to the β-CH_2 protons of the cysteine ligand [76]. Depending on the enzyme, this signal can be observed in different conditions: in "as prepared" enzymes (*high g resting*), in enzyme under turnover with nitrate (*high g nitrate* or *high g turnover*), or in reduced enzyme. Moreover, kinetic studies of Nap by protein film voltammetry revealed that the enzyme activity decreases at very low potential suggesting that nitrate can bind more efficiently to Mo(V) than to Mo(IV) state [77,78]. The potential role of the Mo(V) state in nitrate binding was also emphasized in the catalytic cycle model proposed in line with the *E. coli* NapA structure determination [69]. Based on the redox potential of Mo(V) *high g* species deduced from EPR study of *R. sphaeroides* NapAB, a quantitative kinetic model was developed taking into account nitrate binding to both Mo(IV) and Mo(V) redox states [79]. This model was further improved by considering the kinetics of substrate binding and release, and protonation steps [80]. It enabled the interpretation of catalytic voltammograms obtained with *R. sphaeroides* NapAB in a broad range of substrate concentrations and pH. This led to the conclusion that in this enzyme, substrate binding is irreversible on the time scale of turnover, and that combined with protonation, it raises the redox potential of the Mo(V/VI) couple, triggering the energetics of intramolecular electron transfer with FeS within NapA [80].

The discovery of the sixth sulfur atom in the coordination sphere of the Mo ion in Nap [70] has strongly stimulated the reinterpretation of the structural models of the spectroscopically detected Mo species and enzyme mechanisms. Thus, a recent DFT investigation of the magnetic parameters (*g* and $A(^1H)$ tensors) of possible models for Mo(V) EPR detected species concluded that the *high g* Mo(V) species corresponds to a six sulfur coordination sphere in a pseudotrigonal prismatic geometry, with a partial disulfide bond between the sulfur ligand and the thiolate of the Cys ligand [58]. The *very high g* Mo(V) species would result from the two electrons reduction of this disulfide bond, leading to separated sulfido and thiolato ligands, but maintaining the six sulfur coordination of the Mo(V) ion. Moreover, the attribution of the *low g* species to a Moco with only one coordinated pterin moiety was confirmed in this study [58]. Interestingly, it is clear that independently of the bacterial species or of the conditions used to produced the Mo(V) *high g* species, all reported *g* values exhibit a strong correlation (Fig. 2B). This shows that in these species the Mo ion has the same coordination sphere, the *g*-tensor variations being due to more distant structural modifications. The same trend is also observed for the *very high g* species (Fig. 2B). In particular, this indicates that in the so-called *high g nitrate* or *high g turnover* species, nitrate or nitrite ions if present are not directly bound to Mo ion. These results emphasize the heterogeneity of the Moco in the "as prepared" enzyme. The structure proposed for *high g* Mo(V) from DFT calculations [58] is then very similar to that found in the more recent crystallographic studies of oxidized *D. desulfuricans* NapA [70] and *C. necator* NapAB [71]. However, the physiological relevance of this species was recently questioned. By combining EPR spectroscopy and protein film voltammetry of *R. sphaeroides* NapAB, it was shown that the *high g* Mo(V) species detected in "as prepared" enzyme corresponds to an inactivated form which needs to be reduced for reactivation. Thus, the disappearance of the *high g* Mo(V) EPR signal upon reduction is not a simple redox process but is accompanied by a still unknown chemical transformation making this reduction not reversible [47]. As such, this observation questions the significance of the Moco redox potentials determined by EPR and their use in catalytic models.

Taking into account the six sulfur coordination of the Moco, several theoretical and computational investigations of the Nap mechanism were performed [81–83]. As the disulfide bond between the sulfido and Cys-thiolato ligands blocks the direct access of nitrate to the Mo atom, various kinds of inner and outer coordination sphere mechanisms were investigated, the Mo ion being in the Mo(VI) or Mo(V) state (Scheme 2).

In outer sphere mechanisms, nitrate is guided through a narrow funnel to the active site and interacts with the sulfido Moco ligand leading to a O_2NO-S bond [81,83]. After release of nitrite, the remaining O═S− ligand of Mo must be reduced to restore the initial state of the enzyme. In inner sphere mechanisms, the direct binding of nitrate to the Mo ion requires a rearrangement of the active site in which the Cys-thiolato disconnects from Mo but remains attached to Mo by the terminal sulfur atom giving a Cys-S−S− ligand. This rearrangement would be stabilized by conserved methionines, Met141 adjacent to the Cys140 ligand and Met308, and seems consistent with Moco structural changes observed in the crystal structure of dithionite reduced *C. necator* NapAB [71]. In addition to the redox chemistry of the Mo ion, both kinds of mechanisms involve also a sulfur-based redox chemistry. Although the high energy barrier of the O_2NO-S bond formation likely excludes outer sphere mechanisms, the redox states of the Mo ion in

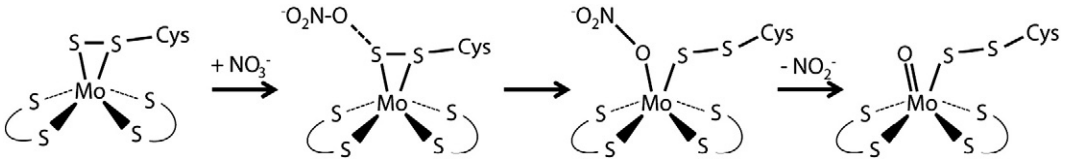

Scheme 2. One of the inner sphere reaction mechanisms proposed for Nap. The valence states of the Mo ion were not indicated since it was suggested that redox chemistry involves sulfur ligands. Adapted from [81,83].

the mechanism and the subsequent reduction steps of the formed oxo ligand into water molecule remains discussed [38].

2.2.1.2. Role of the environment on the Moco reactivity. The analysis of the *D. desulfuricans* NapA structure suggests that several conserved and charged residues (Asp155, Glu156, Asp355, and Arg354) enable to guide the nitrate ion from the solvent to the Moco [81]. In *R. sphaeroides* NapAB, the role of Arg392 (homologous to Arg354 of *D. desulfuricans* NapA) and of Met153, adjacent to the coordinating Cys152, have been addressed by site-directed mutagenesis. These conserved residues which lie at ~9 and 6 Å from the Mo ion, respectively, were substituted by Ala, and the purified mutants where characterized in detail [84,85]. For both mutants, Met153Ala and Arg392Ala, the substitution affected only the K_m for nitrate (increased by 10 and 200-fold, respectively), but not the k_{cat}, indicating that these residues are not involved in the catalytic reduction of nitrate but promote substrate binding [84]. These results substantiate a previous study of mutants of the equivalent residues (Arg421 and Met182) in NapAB from *C. necator* that revealed a drastic (Arg421Lys) or a complete (Arg421Glu, Met182His) loss of enzymatic activity monitored on periplasmic extracts [86]. In addition, a zinc inhibitory effect that seems specific to Nap was revealed [84]. Zn^{2+} binding inside the substrate channel in the presence of nitrate was found to be facilitated by the absence of the guanidium group of Arg392 and requires the Met153 side chain that likely coordinates this metal ion. It was then proposed that Arg392 act as a filter in protecting the active site against inhibition and direct reduction by small molecules [84].

Clearly, in spite of the numerous works done on the Nap enzymes, further investigations are required to rationalize the data gained by crystallography, spectroscopy, kinetics, and theoretical calculations. Noteworthy, the relationships between the various Mo(V) species identified by spectroscopy [58], those involved in the catalytic scheme deduced from kinetic studies [80], the crystallographic structure of the Moco [71], the potential catalytic intermediates [38] and inhibited forms [47] are still to establish. Such investigations would be also relevant for prokaryotic assimilatory nitrate reductases (Nas), which have a coordinating Cys residue of Moco and exhibit Mo(V) EPR signals similar to those given by Nap [87] but remain poorly characterized.

2.2.2. Polysulfide reductase

Polysulfide reductase (Psr) is another enzyme with Cys coordinated Moco, but instead of the common OAT, it catalyzes a sulfur atom transfer (SAT) reaction, giving HS^- as reaction product according to the equation: $S_n^{2-} + H^+ + 2e^- = S_{n-1}^{2-} + HS^-$ above pH 7. The structure of the oxidized *Thermus thermophilus* enzyme has been determined at 2.4 Å resolution and shows that, in addition to the four sulfur atoms from the *bis*-PGD cofactor, the Mo ion is coordinated by the thiolate group of Cys173 [88]. Moreover, a sixth ligand interpreted as an oxo group was proposed. This coordination was considered to be consistent with the first EPR analysis of Psr from *Wolinella succinogenes* which revealed Mo(V) signals resembling the *very high g* signal of Nap [89]. However, it is worth noting that the Mo(V) Psr signals obtained upon dithionite reduction or with polysulfide substrate are rather related to *high g* signals, while that produced after borohydride reduction correlates with *very high g* signatures (Fig. 2). According to the structural interpretation of these signals in Nap [58], they should correspond in both cases to Moco species with six sulfur coordination, indicating that very likely, the sixth ligand is sulfur as in Nap. These spectroscopic results have also suggested that polysulfide substrate binds directly to Mo [89] which was supported by a recent HYSCORE study of ^{33}S isotope-labeled polysulfide treated enzyme strongly indicating that the ^{33}S is indeed the sixth ligand of the Mo(V) center [90]. However, these spectroscopic studies require further analysis for these structural conclusions to be confirmed.

According to the Psr crystal structure, substrate selectivity of Psr would be related to the narrow funnel connecting the active site to enzyme surface, with basic residues limiting its entrance. As for Nap, an Arg residue (Arg332) is located in close vicinity of Moco and is hydrogen bound to two water molecules. This residue was proposed to stabilize the polysulfide substrate [88], but at this time, details on the catalytic mechanism remain to decipher.

2.2.3. Formate dehydrogenase

Formate dehydrogenases (Fdh) possess a Moco which shares common structural properties with Nap but catalyze a very different reaction, namely the conversion of formate into CO_2 that can be considered as a formal hydrogen atom transfer: $HCOO^- = CO_2 + 2e^- + H^+$.

Three crystal structures of Fdh have been reported, the two Mo-enzymes FdhF [91] and FdnGHI [92] from *E. coli*, and the W-containing FdhAB enzyme from *Desulfovibrio gigas* [93]. In the oxidized enzyme, all of them show a metal ion coordinated by the four sulfur atoms of a *bis*-PGD cofactor, and by the selenium atom of a SeCys. As for Nap, the nature of a sixth ligand was largely debated. First modeled as a long Mo–O bond in *E. coli* FdhF [91], this sixth ligand was attributed to a sulfur atom in *D. gigas* FdhAB [93]. Moreover, the initial crystal structure determination of formate reduced *E. coli* FdhF has suggested that the sixth ligand was lost upon reduction, but the re-analysis of data indicated that SeCys is no longer bound to Mo which becomes pentacoordinated with a sulfur atom as axial ligand in the reduced state [94]. This refined structure is in agreement with previous EXAFS studies of the enzyme [95] and with recent biochemical results showing that the sulfuration of the *E. coli* FdhF enzyme is essential for its catalytic activity [96].

Surprisingly, EPR studies of formate reduced *E. coli* FdhF revealed a nearly axial highly anisotropic Mo(V) signal (g= 2.094, 2.001, 1.990), which exhibits a strong hyperfine coupling with ^{77}Se in ^{77}Se-enriched enzyme [97]. This coupling reflects a direct coordination of SeCys to the Mo ion in the EPR active species, in contradiction with crystal structure of formate reduced enzyme, suggesting that the Mo(V) species has no relation with the crystallographically detected state, or that the enzyme was altered by X-ray in crystallographic studies [37]. Alternatively, EPR studies performed on *D. desulfuricans* Fdh suggest that these variations could be due to the influence of some enzyme inhibitors (azide, cyanide) [98]. In the absence of these inhibitors, the Mo(V) EPR signal obtained becomes much less anisotropic. Its *g*-values are then reminiscent of the *high g* Mo(V) signal found in Nap enzymes (Fig. 2), but with a stronger anisotropy which is consistent with replacement of a sulfur ligand from Cys by a selenium as observed for other enzymes such as NiFe hydrogenases [99] and can be explained by the increased covalence effects of selenium.

Based on structural homology between Fdhs, the conserved SeCys140 ligand of Mo and the proximal His141 and Arg333 (numbering of *E. coli* FdhF) are considered as essential residues for catalysis. The replacement of SeCys140 for Cys by site-directed mutagenesis in *E. coli* FdhF decreases

the enzyme activity by two orders of magnitude [100]. Moreover, Arg333 is homologous of Arg392 of *R. sphaeroides* NapA which was shown to be involved in nitrate binding [84]. In the X-ray structure of the oxidized *E. coli* FdhF, the side chain of Arg333 points towards the active site in a position to interact and orient the formate molecule, whereas in the formate-reduced enzyme, Arg333 is in contact with the free selenol from Se-Cys [94].

According to the initial *E. coli* FdhF structure, the first proposed mechanism resembles that of DMSO reductase with the replacement of the OH ligand by a formate ion coordinated through an oxygen atom to the Mo(VI) ion. In a second step, the formate C–H bond is cleaved with concomitant binding of hydrogen to Se, transfer of two electrons to the Mo, and release of CO_2 [97]. This leads to a pentacoordinated Mo(IV) ion with a protonated SeCys ligand which is subsequently oxidized to Mo(V) with the transfer of the proton from SeCys to the proximal His141. The catalytic cycle is then completed with the oxidation of Mo(V) to Mo(VI), the transfer of the proton to the solvent and the binding of a hydroxide to the Mo(VI) ion. After the finding of a sulfur ligand in the coordination sphere of the reduced *E. coli* FdhF Moco, this mechanism was adapted by replacing the OH ligand by SH and was addressed by theoretical calculations [101]. An alternative mechanism was also proposed in which the SH ligand remains bound to Mo in the whole catalytic cycle, while the Mo(VI) SeCys ligand is released to enable formate binding [94]. In this mechanism, the unbound SeCys is stabilized by interaction with proximal Arg333, and enables hydrogen atom abstraction from bound formate. Calculations of activation energy for C–H bond cleavage showed that the proton abstraction is much more favored with unbound SeCys (19 kcal/mol compared to 36 kcal/mol) [101]. This study did not consider, however, the role of the proximal His141 and Arg333 residues, and in a more recent DFT study, Mota et al. [102] have investigated the entire catalytic cycle by taking into account the influence of these residues. Their proposed mechanism is reminiscent of the inner sphere mechanism determined by Cerqueira et al. [81] for Nap (Scheme 3).

Starting from a hexacoordinated Mo(VI) structure with SeCys and sulfido ligands partly bound by a seleno-sulfide bond, the catalytic mechanism involves decoordination of SeCys with the transient formation of a Cys-Se–S Mo ligand to enable formate binding. The Se–S bond is then broken, allowing the formed selenide to abstract the hydrogen atom from formate. This leads to a cyclic intermediate with the CO_2 molecule bound to Mo(IV) ion by one oxygen and to the sulfur ligand by its carbon atom. After CO_2 release, Mo(IV) oxidation and proton transfer, the catalytic site is restored. As no Mo(V) state is involved in this mechanism, this questions the relevance of the EPR-detected Mo(V) species as for Nap. These DFT calculations indicate that Arg333 has indeed a key role in driving the formate ion toward the sulfur ligand through two strong hydrogen bonds, and promoting its binding to the metal ion by a single bond. A role of the positively charged side chain of Arg333 in driving the product release was also proposed. In addition, it was found that His141 lowers the activation energy for the dissociation of SeCys from the molybdenum by forming a hydrogen bond with the selenide anion, then allowing proton abstraction from the substrate to the SeCys. In this model, His141 is not directly involved in the removal of the formate α-proton. However, the role of His141 in catalysis, together with that of possible H acceptors in the active site, has been questioned by recent theoretical calculations [103]. The results favor a mechanism in which the metal center mediates H transfer from substrate to the SeCys by forming a transient Mo–H intermediate. Considering the existence of thiolate-coordinated Mo hydride compounds, these authors then conclude that a hydride transfer could be operating in FdhF catalysis. Thus, the exact role of His141 in the peculiar hydrogen atom transfer that is specific of FdhF still needs to be established.

2.2.4. Acetylene hydratase

By contrast with other enzymes with Cys or Secys Mo ligand, acetylene hydratase (Ah) catalyzes a non-redox reaction, the hydration of acetylene to acetaldehyde. This tungsto-enzyme from *P. acetylenicus* was crystallized in anaerobic conditions in the reduced most active state. The high resolution structure (1.26 Å) revealed that the W atom is coordinated by a Cys residue and by a water molecule hydrogen-bound to a close aspartate residue (Asp13) [104]. One striking difference with other Mo/W-*bis*PGD enzymes is a major rearrangement of the region between domain II and III leading to a completely different funnel accessing the active site in AH. This substrate access funnel is located at the intersection of domains I, II and III, giving access to a new face of the protein surface (Fig. 1). It leads to a different portion of the metal coordination sphere and was considered as a key factor for substrate specificity and reactivity. In the proposed mechanism, the W(IV)-bound water molecule would be activated by the Asp13 residue thanks to a pK_a shift induced by the proximal FeS cluster [104]. Although acetylene hydration reaction is not a redox process, it is striking that the lysine residue that is considered as essential for electron transfer between the FeS cluster and the Moco in Mo/W-*bis*PGD enzymes is also conserved in Ah (Lys48). It

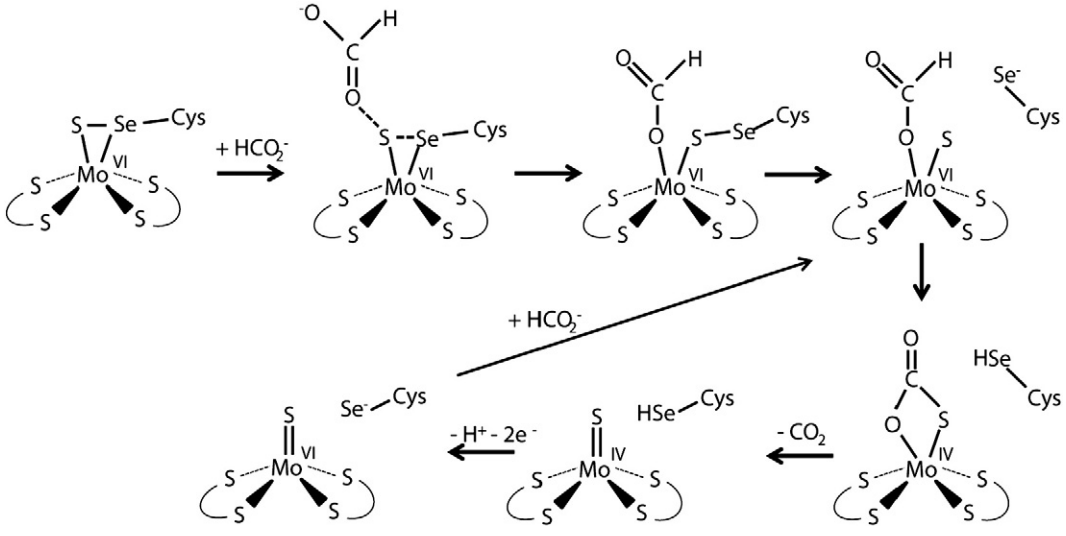

Scheme 3. Reaction mechanism proposed for FdhF with the activation step based on sulfur-shift process. Adapted from [102].

is proposed that in Ah, the rearrangement of a loop region between the two metal cofactors in Ah might be responsible for a strong increase in Asp13 pK_a induced by the proximal FeS cluster [104]. In the following step, the activated water would attack the triple bond of acetylene through an electrophilic addition mechanism. The critical role played by the carboxylic group of Asp13 was confirmed by site-directed mutagenesis experiments: enzyme activity is almost suppressed by Asp13Ala mutation while it is nearly unchanged in Asp13Glu variant [105]. Moreover, the presence of a hydrophobic cavity enabling substrate accommodation at the active site is supported by the strong decrease of activity when Ile142, which belongs to this cavity, is mutated into Ala.

Alternative mechanism involving a nucleophilic attack of water on a W-bound acetylene was also suggested [106], but DFT calculations indicated that these two mechanisms have very high energy barriers (~40 kcal/mol) and proposed that reaction proceeds through a $W{=}C{=}CH_2$ vinylidene intermediate [107]. Several other mechanistic schemes have been investigated by DFT methods on large active site models [108]. These authors concluded that the most energetically favorable mechanism involves the η^2 binding of acetylene on the W(IV) ion with the displacement of the water molecule ligand. This molecule is subsequently deprotonated by the carboxylate group of Asp13 and performs a nucleophilic attack on the bound acetylene, giving a vinyl anion stabilized by binding to W ion. Shuttled by Asp13, a proton is then transferred to this anion leading to a vinyl alcohol intermediate, which gives acetaldehyde after tautomerization. This first shell mechanism was recently supported by theoretical calculations performed on a biomimetic $W(IV)O(S_4)$ tungsten complex but with the participation of the W(IV)–OH ligand to deprotonate the water molecule [109].

2.3. Mo/W-bisPGD enzymes with Aspartate ligand

Enzymes where Moco is coordinated by Asp generally present a trimeric organization (Table 1) and contain several other redox cofactors, FeS clusters and hemes, giving a large diversity of spectroscopic signatures. The coordination of the Moco by Asp was demonstrated by crystallography in only two enzymes, nNar and Ebdh whose properties are described in this section.

2.3.1. Respiratory nitrate reductase

The most representative enzyme of this class is the membrane-bound respiratory nitrate reductase from *E. coli* NarGHI (i.e. nNar) that was spectroscopically investigated by Bray and coworkers more than thirty five years ago [110]. The ability to produce the enzyme either in a membrane-bound form NarGHI or in a soluble form NarGH was a great advantage to address the thermodynamic and structural properties of the various metal centers [111–113]. This was also used to determine the crystal structure of the oxidized enzyme in the two forms NarGHI [114] and NarGH [115] and to demonstrate the presence of an aspartate ligand to the Mo ion (Asp222). By comparison with Ser coordinated Moco enzymes, the catalytic subunit NarG has important sequence insertions that define an additional fifth domain in the structure. This domain V delineates a much narrow substrate binding funnel in NarG, and could play a role in modulating its substrate specificity towards nitrate and the small number of oxyanions identified as substrates [116,117]. In both structures, the Mo ion is coordinated by the four sulfur atoms of the two PGD cofactors, but surprisingly, the aspartate coordination is different in the two systems. In NarGHI, the Asp ligand is bidentate with the two oxygen atoms from the carboxylate group bound to Mo. In addition, one PGD cofactor was shown to be bicyclic with an open pyran ring [114]. In contrast, in NarGH structure, the two PGD cofactors are in the usual tricyclic pyranopterin state, and the aspartate ligand is monodentate, the sixth coordination position of the Mo being occupied by an oxo group at 1.8 Å [115]. However, these structures show highly distorted Mo coordinations with short distances between the oxo ligand, one of the dithiolene sulfur and the coordinating aspartate oxygen which could results from averaged structural heterogeneities arising from X-ray photoreduction [37]. These structural variations between enzymes led to suggest that the flexibility of the aspartate coordination and the pyran ring opening and closing could play a role in catalysis, especially for the proton transfer [115,118].

Early spectroscopic studies performed on *E. coli* nNar have reported two characteristic pH-dependent Mo(V) EPR signals, the low-pH and high-pH signals [119], both signals showing hyperfine coupling with a solvent exchangeable proton. This coupling is stronger for the low-pH signal which was shown to be sensitive to the presence of anions like nitrate, nitrite, chloride and fluoride [120]. The hyperfine coupling observed with ^{19}F showed that this anion was located close to the Mo(V) ion, but no such coupling was found with ^{17}O enriched nitrate indicating that these anions were not directly bound to the metal [121]. By comparing the pK_a of interconversion between high and low pH species (pK_a~8.3) with enzyme activity profile, it was proposed that only the low pH species is catalytically active [119]. However, this pK_a value was determined in the presence of chloride and it was subsequently shown that anion binding modifies the high pH/low pH signal transition pK_a [120,121]. Later, a pH dependence study of Mo(V) species redox potentials performed in absence of contaminating anions has suggested that both species could be involved in the catalytic cycle [122]. Moreover, this study showed that the replacement of the His49 ligand of the proximal FS0 cluster by Cys also affects the pK_a of the transition, while the structural organization of the Moco and the FS0 centers is not modified [123], indicating that this pK_a value is dependent on the H-bond network around the Moco. These Mo(V) EPR signals were detected in several other respiratory nNars from *Paracoccus denitrificans* [124] and *Marinobacter hydrocarbonoclasticus* [125]. In all cases these Mo(V) EPR active species were substoichiometric, revealing structural heterogeneities of the Moco in enzyme preparations and questioning their relationships with the structure determined by crystallography or EXAFS [121]. Interestingly, the binding of nitrate, nitrite or other anions changes only weakly the Mo(V) EPR signatures which remain correlated to the low- and high-pH signals (Fig. 2). This shows that the binding of these anions does not occur in the first coordination sphere of Mo(V) ion which remains likely unchanged in these different species. The more realistic interpretation of this Mo(V) coordination is that the aspartate ligand is monodentate and that the sixth position is occupied by an OH group. In the NarGH crystal structure, the monodendate molybdenum ligand Asp222 is hydrogen-bound to the Nε of the conserved His546 residue [115], whereas this H-bond is lost in the bidendate NarGHI structure [114]. This led to the hypothesis that this His may be the ionisable residue with pK_a~8 that defines the transition between the high and the low-pH Mo(V) forms evidenced by EPR. The interconversion between high- and low-pH species could be due to the protonation of this nearby residue, leading to a reorientation of the Mo(V)–OH ligand and to a change of the proton hyperfine coupling [125,126].

In spite of the long standing studies on nNar, it is striking that its reaction mechanism and the catalytic relevance of the Mo(V) species is still a matter of controversy. Notably, the ability of these enzymes to reduce various oxides of nitrogen, halogens [127] and metalloids [117], and to be a potential NO production enzyme [128–130] will be required to understand more deeply the interactions between the Moco, its surroundings and these substrates.

2.3.2. Ethylbenzene dehydrogenase

A monodentate aspartate ligand of Moco, Asp223, was also observed in the crystal structure of the ethylbenzene dehydrogenase (Ebdh) from *Aromateum aromaticum* [131], an enzyme closely related to Nar. In this case, one of the PGD has an open pyran ring. The sixth ligand of Mo is an oxygen atom from an acetate ion, the metal ion being considered to be in the reduced Mo(IV) state due to crystallization conditions. Interestingly, the second oxygen from the Asp223 carboxylate side chain is hydrogen bound to a Lys450-Nζ, and the same Asp–Lys pair is conserved in other Mo-enzymes of this group, selenate reductase (Ser) and chlorate reductase (Clr) [131].

By contrast with most enzymes with Mo/W-*bis*PGD cofactor which perform an OAT, Ebdh catalyzes the oxygen-independent hydroxylation of hydrocarbons, a process known to require the activation of C–H bond. Because of the high diversity of this enzyme in hydroxylating various alkylaromatic and heterocyclic compounds [132], the determination of its catalytic mechanism has attracted much attention. Different mechanisms considering that the C–H activation proceeds through homolytic or heterolytic cleavage were investigated by DFT computations [133]. In these calculations, the Mo(VI) ion of the oxidized enzyme was considered to be coordinated by a monodentate Asp223 ligand and by an oxo group, and the role of His192 lying near the Moco in protonation processes was also investigated. In this model, one of the pyran rings is taken open but the influence of the ring closure on the catalysis was not addressed. The results of calculations indicate that the lower energy barrier mechanism involves a radical formation with two one electron transfer steps: i) the homolytic activation of the C–H bond leading to a radical intermediate and the formation of Mo(V)–OH; and ii) a second electron transfer coupled to OH-rebound on the carbon atom. Models with His192 protonated or not give plausible reaction pathways and this mechanism led to calculated kinetic isotope effect in qualitative agreement with those measured experimentally [133]. More recently, this two step mechanism involving a substrate-derived radical and carbocation intermediates was shown to be consistent with kinetic properties of a broad range of substrate analogs [132].

2.4. Conclusion

At the present time, it is clear that it is not possible to reveal a unique principle which triggers the reactivity of Mo/W-*bis*PGD enzymes. Examination of the wealth of structural, spectroscopic, kinetic and computational data emphasizes the extraordinary high catalytic plasticity of these enzymes that is responsible for their evolutionary success and spreading in prokaryotes. Theoretical calculations have shown that catalytic pathways are extremely sensitive to proton and electron transfer processes. H-bond networks around the Moco and their variations in the catalytic cycle are strongly involved in the fine tuning of the cofactor reactivity and substrate selectivity. In spite of the spectacular progresses made by crystallographic approaches, the knowledge on these networks remains hardly accessible. Going further in this understanding will need to establish relationships between the Moco structures identified by crystallography and the spectroscopically detected species, and to decipher the structural basis of Moco heterogeneities. Going beyond the very close vicinity of Moco in these analyses will be also required as illustrated by inhibition processes of Nap which likely occur in a more distant surroundings [47,84]. In this respect, using Mo(V) species as magnetic probe to monitor long range structural changes of the enzyme or intercenter medium variations will be a powerful approach as shown in other Mo-enzyme families [134–136]. Moreover, it will also be essential to progress in trapping and characterizing catalytic intermediates and to make assignments to hypothetic species involved in kinetics models. This is specially required for enzymes with Cys (SeCys) or Asp Moco ligand that catalyze the most diverse reactions and for which mechanisms at play are still uncertain. Finally, beyond the Mo ion, the role of pyranopterins of Moco remains poorly addressed. Although it is well established that pterins can have a redox activity [118], as demonstrated for tetrahydrobiopterin cofactor in NO synthases [137,138], no evidence for the involvement of pyranopterins as redox cofactors was given. Instead, a recent extensive structural analysis of pyranopterins in Mo-enzymes suggests that changing the redox state of these cofactors could be a way to modify their conformation and to modulate the tuning of the Moco redox chemistry [139].

3. Molecular variation of the Mo/W-*bis*PGD enzymes

The Mo/W-*bis*PGD enzymes family shows an extraordinary variety of molecular organization and the unique common subunit is the catalytic one. The enzymes of this family can be monomeric, dimeric (with an additional subunit playing the role of electron transfer module, containing hemes, or FeS clusters and/or FAD cofactor), and trimeric (with an additional subunit playing — often but not always — the role of connection to the membranous quinone pool) (Fig. 3). We will briefly present all types of element with the aim of highlighting structural variability but first of all common functional features. An important pitfall when giving a Mo/W-*bis*PGD enzyme denomination from the first description is that it takes into account, in most cases, the enzymatic activity and not the phylogenetic affiliation. Actual view of the diversity and relationships within the Mo/W-*bis*PGD enzymes family should lead to reconsider earlier enzyme denomination thus facilitating a better description of their function. Readers are encouraged to read the review from Rothery et al. for an evolutionary point of view [16].

3.1. The catalytic subunit α

In the vast majority of enzymes from the Mo/W-*bis*PGD enzymes family the catalytic subunit, denoted α in Table 1, is named A referring to the genes' order in the operons where the gene encoding the catalytic subunit is located, in the vast majority, before all other genes encoding for structural proteins. In the case of the *aio* (formerly *aox*) operon, homogenization to the global Mo/W-*bis*PGD enzymes nomenclature has been recently obtained [140] and the gene coding for the catalytic subunit (formerly *aoxB* [141]) is now denoted *aioA*, whereas the gene encoding for the electron transfer subunit (formerly *aoxA*) is now denoted *aioB*. Some recalcitrant cases to the homogenization do still exist since in the *nar* operons (there are two Nar complexes in *E. coli*), the genes encoding for the catalytic subunits are denoted *narG* and *narZ* [142] and the genes encoding for the catalytic subunits of assimilatory nitrate reductase are denoted *narB* in *Cyanobacteria* or *nasC* in *Bacillus subtilis* (see [143] for recent review).

Although of highly variable size (from 710 residues for NasC to 1200 residues for NarG), all the available structures show a similar scaffold defining four different conserved domains (I–IV) in the catalytic subunit (Fig. 1B). The remarkable feature is the non-contiguous location of these domains within the primary protein sequence. This is the result of a long evolutionary history from the origins of life that provided a great divergence of sequences despite a high folding conservation. Whereas the catalytic subunit shows great divergence in term of amino acid sequences (less than 8% identity between catalytic subunits from Aio and Nar for the most divergent representatives of the family) structures can be easily superimposed (see the work of Schoepp-Cothenet et al. [25]). The four domains (I–IV) (related by an internal pseudo-two-fold axis; see Fig. 1B) bury the cofactors deep inside the protein. Access to this site is consequently provided via a funnel-like entrance whose position (but not the detailed architecture, that defines the enzymatic specificity), between Domains II and III, is almost conserved in the family. The Ah (ID: 2E7Z) [104] is the only presently known exception in the family showing a completely different access, at the intersection of Domains I, II, and III (see Fig. 1B). Much of the sequence that does not align structurally in between all the catalytic subunits is located within a fifth domain denoted Domain V. This domain, variable in size (eventually even absent) is proposed to play an essential role in defining the substrate binding cavity [116,117,144].

In a large majority, Mo/W-*bis*PGD enzymes catalytic subunit contains not only the Mo/W cofactor but also a [4Fe–4S] cluster known as FS0. In these Mo/W-*bis*PGD enzymes, with the exception of Ah, this FS0 represents the electron transfer relay between the catalytic site and the electron transfer subunit. Referring to this FS0, Trieber et al. have introduced a classification among the Mo/W-*bis*PGD enzymes family [35]. Dor (ID: 1EU1) [15,39], Tor (ID: 1TMO) [41,145], BisC [146] and Th (ID: 1TI2) [22] being the only currently known Mo/W-*bis*PGD enzymes not containing any FeS cluster in the catalytic subunit are grouped in a Class III of this classification. Sequence homologies suggest the Resorcinol hydroxylase (Rh) to belong to this group. Phylogenetic analyses

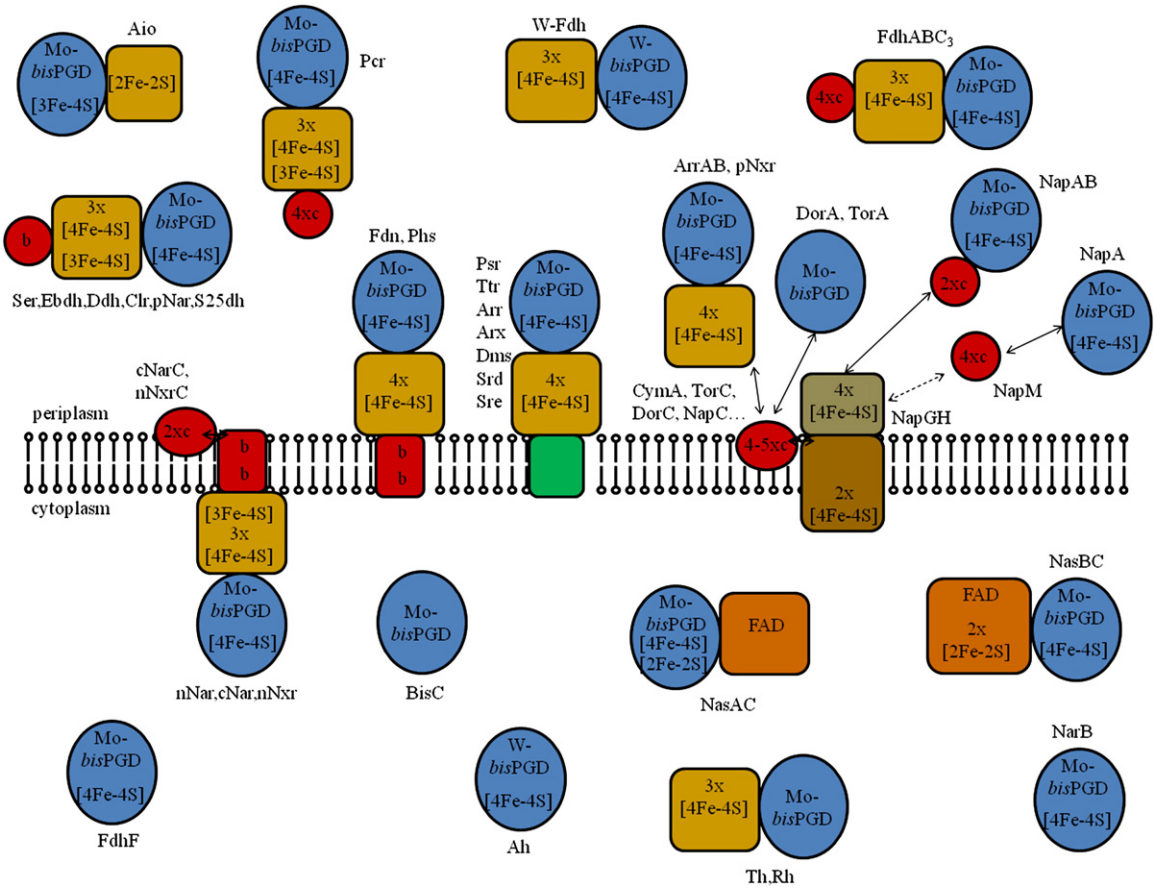

Fig. 3. Composition and localization diversity of Mo/W-*bis*PGD enzymes. As detailed in the text, the Mo/W-*bis*PGD enzymes are text book examples of the "redox construction kit" principle described by Nitschke and co-workers [23,24]. The Mo/W-*bis*PGD catalytic module is the single conserved α unit of all the members. It can contain Mo/W-*bis*PGD only or Mo/W-*bis*PGD and FeS clusters. This catalytic unit can be complemented by variable β units and even more diverse γ units. These additional subunits vary not only in terms of protein folding (see Fig. 3) but also in terms of cofactor composition. The β subunit can be FAD/FeS, FeS only or hemes containing proteins whereas γ subunit contains hemes or is devoid of any cofactor. In addition to composition diversity, these enzymes present all possible localization in the cell: soluble or membrane-bound; periplasmic or cytoplasmic.

suggest that the loss of the FS0 and the related binding domain is a relatively late event and that the common ancestor of the whole Mo/W-*bis*PGD enzymes family almost certainly contained the FeS cluster [16,25]. In enzymes belonging to this Class III, Ser serves as a common protein ligand to the Mo ion. However there is no strict correlation between absence of FS0 and Ser as ligand since DMSO reductase DmsABC from *E. coli* does present a Ser as Mo ligand and also harbor FS0.

The two other groups of this classification, Class I and Class II, were denoted referring to the FS0 ligands motif. Domain I of the catalytic subunit holds the N-terminal Cys group that provides coordination to this [4Fe–4S] cluster. Four Cys are found in the Class I enzymes. It is to note that this FS0 binding motif is observed in all the enzymes presenting a Seleno-Cys/Cys coordination of the Mo/W that are, in large majority, enzymes harboring a β subunit with four [4Fe–4S] clusters (see Section 3.2.1): Nap (ID: 1OGY, 3ML1, 2NYA and 2NAP) [67–69,71], Fdh, Fdn (ID: 1KQG, 1H0H and 1FDO) [91–93], Psr (ID: 2VPZ) [88] and Ah (ID: 2E7Z) [104]. Due to their close sequence homologies with Psr and Nap, arsenate reductase (Arr) [147], tetrathionate reductase (Ttr) [148], sulfur reductase (Sre) [149], thiosulfate reductase (Phs) [150] and assimilatory nitrate reductases NasA and NarB are supposed to belong to this Class I group. The assimilatory nitrate reductases are however highly variable in structure [151] and the catalytic subunit, as the archetypal Class I NarB from *Cyanobacteria* or NasA from *B. subtillis*, can contain a Mo-*bis*PGD cofactor and one [4Fe–4S] center [87,152]. But the enzyme, as in the case of NasA from *K. pneumoniae* [153] or NasC from *P. denitrificans* [154], can also contain an additional C-terminal region that may bind a [2Fe–2S] cluster through Cys-rich motifs.

In NarG (ID: 1Q16 and 1R27) [114], the first residue ligating FS0 has been revealed to be a His (moreover spaced by three residues from the second Cys rather than two) giving rise to very special properties (high spin ground state in the reduced form) of the FS0 cluster [155,156]. This FS0 binding motif has subsequently been established in Ebdh (ID: 2IVF) [131], and proposed in Ser [157], dimethyl sulfide dehydrogenase (Ddh) [158], and Clr [159]. Whereas precise properties of FS0 have only been established for Nar, unusual properties of the FS0 cluster in Ser, Ddh [160–162] could also be related to the same FS0 binding motif. In the trimeric Dms from *E. coli*, again unusual properties of FS0 have been revealed linked again to the spacing, between the two first Cys residues, by three residues rather than two [163]. Such a FS0 binding motif (H/CX_3C) spaced by three residues) was originally proposed as being characteristic of the Class II group [35]. Based on their sequence, Ddh [160], *E. coli* and *Halobacterium salinarum* NRC-1 Dms [163,164], Ser [161], proteobacterial nitrite oxidoreductases (nNxr), Clr, or Pcr [165], archaeal nitrate reductases (pNar) [166] have also been proposed to belong to this Class II group. Recently however new binding motifs of "Class II" enzymes have been revealed in C25dehydrogenase (C25dh) and nitrite oxidoreductases (pNxr) [165,167]. Today the FS0 binding motif of "Class II" enzymes is considered to be $H/CX_{3-4}C/D$. The crystallized enzymes carrying such a FS0 binding motif, Nar [114] and Ebdh [131], have revealed an Asp as Mo ligand and a [3Fe–4S] cluster instead of [4Fe–4S] cluster in place of the FS4 cluster in β subunit (see Section 3.2). Based on primary sequences, other members of the Class II have been proposed to share these properties.

McDevitt et al. [158] have proposed that the "Class I/II/III" subdivision does also correspond to phylogenic relationships since the members of

these different classes group together into separate monophyletic clades in the phylogenetic tree of the Mo/W-*bis*PGD enzymes family. Recent publications are however against this idea [25,165,168]. The "Class III" enzymes all cluster together in a branch but with Dms enzymes, considered to be "Class II" enzymes. "Class II" enzymes also cluster together with the exception of the latter enzyme. The "Class I" enzymes represent today the vast majority of known Mo/W-*bis*PGD enzymes and clearly do not cluster together on a single branch. It appears to us more rigorous to classify the enzymes based on the Mo/W ligand: Ser-group, Asp-group and Cys-group, replacing III, II and I classes, respectively. This is probably more functionally relevant. The Aio [169] is atypical in the Mo/W-*bis*PGD enzymes family and does not belong to any of these Classes or ligand-group: its FS0 is a high redox potential [3Fe–4S] cluster coordinated by only three Cys and Mo does not have any protein ligand. The new classification would therefore allow to create a new group: None-group.

One important feature of the catalytic subunit is the relationship between the presence of a twin arginine translocation peptide signal (tat leader sequence) at the N-terminus of the immature protein and the final sub-cellular location of the mature complex. This sequence can be the archetypal RRXFLK but more often is slightly modified to RRXFIK, RRXFLR, RRXLLK, RRXWLK, RRXFLQ, RRXFLS, or RRXLMQ. When present in the catalytic subunit of αβγ enzymes, the tat leader sequence targets the heterodimer αβ to the periplasmic compartment where it associates with its eventual γ subunit. The Ttr is a special case since both the catalytic and the electron transfer subunits can, in some organisms, harbor a tat leader sequence [170,171]. In the case of dimeric NapAB enzymes, the tat leader sequence targets the α subunit to the periplasmic compartment where it associates with the cytochrome β subunit exported via the sec system [172]. In the case of Nars, whereas bacterial enzymes are found attached to the cytoplasmic membrane facing the cytoplasm, archaeal enzymes have been shown to be facing the periplasm. This localization seems to well correlate with the presence of a predicted tat leader sequence at the N-terminus of the immature pNarG (see [166] for review). Fine examination of all the available bacterial *narG* genes revealed a vestigial leader sequence uncleaved in the mature NarG protein [173,174]. A similar vestigial non-functional and uncleaved leader sequence also exists in the mature cytoplasmic and soluble BisC enzyme [174]. Aio represents an exception in the Mo/W-*bis*PGD enzymes family since the tat leader sequence (Aio is indeed periplasmic) is harbored by the electron transfer subunit rather than the catalytic one [175,176].

3.2. The electron transfer subunit β

3.2.1. Archetypal β subunit

Most of the Mo/W-*bis*PGD enzymes contain a multiple FeS-harboring protein as β subunit (Fig. 4), from which several structures have been resolved (ID: 1TI2, 2IVF, 1H0H, 1KQG, 2VPZ, 1Q16 and 1R27). Despite this common feature, the size, ranging from 191 residues in the case of the *Wolinella succinogenes* Psr to 512 residues for nNar, is highly variable. The harbored FeS are four [4Fe–4S] clusters in the Fdn (ID: 1KQG) [92] or the Psr (ID: 2VPZ) [88]. The FS1–FS4 (with increasing distance from the FS0) clusters are coordinated by typical $C_AXXC_BX_{2-11}C_CX_3C_D$ motifs. From sequence analysis, the β subunits encountered in Ttr [148], Sre [149], Srd [177] and Arr [178] are supposed to harbor also four [4Fe–4S] clusters. Three [4Fe–4S] and one [3Fe–4S] can also be carried by the β subunit as in nNar (ID: 1Q16,1Y4Z) [114] and Ebdh (ID: 2IVF) [131], or only three [4Fe–4S] in Th (ID: 1TI2) [22] and the W-containing Fdh (ID: 1H0H) [93]. Ddh [160], Dms [163], Ser [161], Clr, or Pcr have also been proposed to carry three [4Fe–4S] and one [3Fe–4S]. Based on sequence analysis, Phs has been proposed to carry three [4Fe–4S] and one [3Fe–4S] on its β subunit [150]. The sequence of PhsB however carries the same four FeS binding motifs than PsrB demonstrated to harbor four [4Fe–4S]. This is in line with its closer phylogenetic relationship with Psr [147] than to Nar. Together

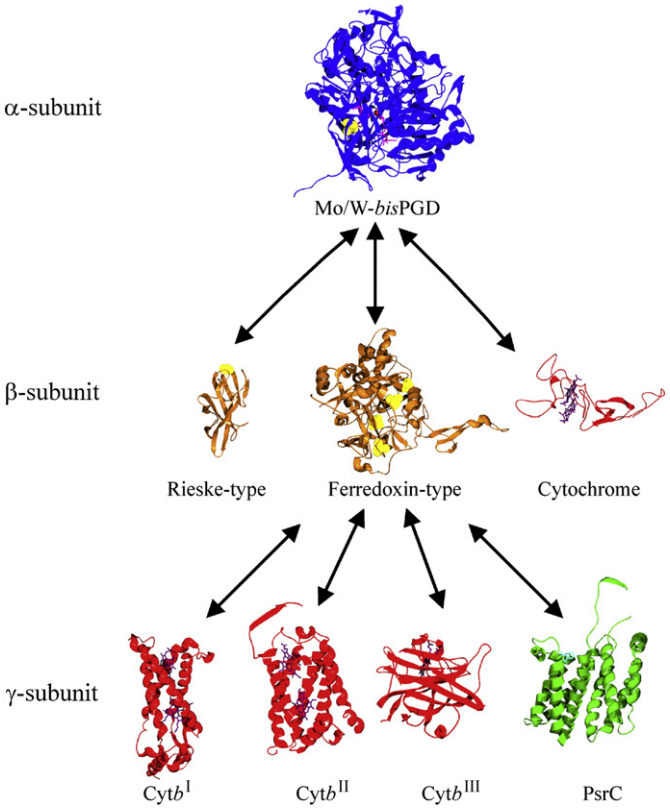

Fig. 4. Structural modularity cascade of the Mo/W-*bis*PGD enzymes. Several, but not all types of Mo/W-*bis*PGD enzymes have been crystallized (see Table 3). The available structures give a picture of a modularity in cascade among this family from the monomeric cases to the heterotrimeric cases. Indeed whereas several monomeric cases with only the α subunit have been resolved in structure, only three types of β subunits potentially associated with an α subunit are available in data bases: the Rieske-type from Aio, the ferredoxin-type from Nar and the cytochrome from NapAB. Among these β subunits, only one, i.e. the bacterial ferredoxin-type, have been observed associated with a γ subunit. This γ subunit is highly variable in structure as exemplied by the cyt*b*^{I} from Fdn, cyt*b*^{II} from Nar, the cyt*b*^{III} from Ebdh and the PsrC from Psr.

with the FS0 when exists, these FS1–FS4 clusters are arranged in a W shape. As in the case of the catalytic subunit, domains can be delimited in this type of β subunit. Domains I and II are ferredoxin-like domains harboring two FeS clusters each sandwiched between two helices on one side and a β-sheet on the other, with the exception of Th in which Domain II only holds one cluster [22]. Although not superimposable, structural Domains I and II are observed in nNar, Fdh, Ebdh, and also in Th where an additional third domain is folded in β-barrels [22]. In addition to these relatively well characterized systems, publications reported that the pNxr [165] and C25dh [167] would possess such FeS subunit.

3.2.2. "Exotic" β subunits

Mo/W-*bis*PGD enzymes carrying a β subunit distinct from the multiple-FeS protein are rare. We presently know four other types of β subunits present each in one specific system: a di-heme cytochrome (*c*-type) in the NapAB heterodimers [68,69], a Rieske type protein in the AioAB heterodimer [169], and two different FAD/[2Fe–2S] proteins in the dimeric Nas [152,179]. Only the first two proteins have been resolved in structure.

NapAB are all soluble and periplasmic enzymes. Whereas NapAB of α-proteobacteria, such as *R. sphaeroides* purifies as a tight heterodimeric complex [68], the γ-proteobacterial *E. coli* NapA and NapB proteins purify independently due to weaker interactions but form together the functional complex. In *R. sphaeroides* NapB (ID: 1OGY) two extended arms fold away from the core structure to embrace the NapA subunit [68]. In NapAB, heme II is located into the vicinity of FS0 whereas heme I is exposed to the solvent, arguing for this latter heme to be the electron

acceptor from the physiological partner NapC. This membranous partner is responsible for the connection of the enzyme to the membranous quinol pool (see below Section 3.3.3).

The AioB Rieske protein (ID: 1G8K), by its [2Fe–2S] cluster and its protein fold, is homologous to the well characterized subunit of the Rieske/cyt*b* complex (also known as complex III in mitochondria, bc_1 complex in proteobacteria and b_6f complex in plants and cyanobacteria) [169,180]. A characteristic Cys-X-His-X_n-Cys-X_2-His sequence motif, observed in other Rieske proteins, binds the [2Fe–2S] cluster. In the *A. faecalis* Aio structure, two loops containing each a Cys/His couple are held together by a disulfide bridge which is strictly conserved in the Rieske/cyt*b* complexes and considered to be crucial for properties of the cluster in this latter complex. This bridge is not fully conserved in the Aio, where the properties of the enzyme do not seem to depend on it [181,182]. The [2Fe–2S] cluster, exposed to the solvent, is the electron donor to the partner, which in proteobacterial systems (the only characterized) are soluble *c*-type cytochromes (see [183] for a review). All Aio are periplasmic but only some of them have been observed attached to the cytoplasmic membrane. It is not clear at present whether the tat signal peptide, harbored by AioB and which would then remain uncleaved, could be responsible for the membrane association in a same manner as observed in the Rieske/cyt*b* complex [183].

Data on the assimilatory nitrate reductases other than genetic are very scarce. Among them, the NasBC from *B. subtilis* [152] and the NasAC from *K. pneumonia* [179] or from *R. capsulatus* [184] are the only heterodimeric enzymes characterized in some extent. NasB in *B. subtilis* and NasC in *K. pneumonia* or *R. capsulatus* are both responsible for the electron transfer from NAD(P)H to the catalytic subunit in cytoplasm. The two proteins are however highly divergent, not only at a global sequence level, but also at a structural and cofactor composition levels. The NasB-type subunit is 771 residues long and therefore larger than the catalytic one whereas the NasC-type protein is 396 residues long. Sequence and biochemical analyses suggest that NasB and NasC both harbor a FAD cofactor but NasB presents in addition clear motifs for the coordination of two [2Fe–2S] clusters.

3.3. The electron entry/exit γ subunit

This component is the most variable element of the Mo/W-*bis*PGD enzymes but each type of γ subunit is encountered in several representatives of the Mo/W-*bis*PGD enzymes family. The cytc_3 characterized with *Desulfovibrio* species Fdh [185,186], the tetrahemic c_{554}-type cytochrome characterized in the *Dechloromonas* Pcr [187] and the dihemic cytochrome characterized in the *T. thermophilus* cNar [188–190], have been observed each in a single system. With or without cofactors, integrated or not into the membrane, this γ subunit is of primordial importance for the mode of enzyme connection to the whole bioenergetic chain in which it is involved. In the great majority of cases, this third subunit is responsible of the reaction with the membranous isoprenoid quinones (see Section 3.4).

3.3.1. Cytb^{I}, b^{II} and b^{III} γ subunits

Two types of transmembrane diheme cytochrome *b* and one type of hydrophilic monoheme cytochrome *b*, which have all been resolved in structure (Fig. 4), are present as γ subunit in members of the Mo/W-*bis*PGD enzymes family. All represent typical "redox kit units" as already discussed and form different enzymatic systems even out of the Mo/W-*bis*PGD enzymes family [23,24]. The first cytochrome cytb^{I} (ID: 1KQG) usually contains 4 trans-membrane helices (TM) and the two hemes are ligated by histidine residues on TM1 (1 His), TM2 (1 His) and TM4 (2 His). Cytb^{II} (ID: 1Q16) features 5 TM and the heme ligands are located on TM2 (2 His) and TM5 (2 His). Cytb^{I}, takes part to the FdhN [92]. Due to its global sequence homology (although containing a fifth TM) to the FdhN γ subunit, PhsC is proposed to be also a cytb^{I} cytochrome [16]. Cytb^{II} is exemplified by the γ subunit of the bacterial nNar enzyme [114] and has been proposed as third subunit in nNxr and cNar [29]. The function of such units is to connect the related enzymes to the membranous quinol pool. Why there are two structurally distinct membrane-integral *b*-type cytochromes for this purpose remains unknown. The idea that cytb^{I} could serve as quinone-reducing, and cytb^{II} as quinol-oxidizing element, does not match with the function of PhsC in oxidizing MK to reduce thiosulfate.

A third cytochrome *b* is a hydrophilic antiparallel β-sheet monohemic one: cytb^{III}. This subunit is encountered as γ subunit of Ebdh from which 3D-structure is available (ID: 2IVF) [131]. Based on sequence homologies and/or spectroscopy, archaeal pNar [166,191,192], Ser [157,161,193], Ddh [158,162], Clr [194] and C25dh [167] have furthermore been proposed to contain such a subunit. This unit doesn't connect the enzymes directly to the quinol pool but one of them (named Orf7 or NarM) could however bind its related complex, archaeal pNar, to the cytoplasmic membrane by two α helices in both N- and C-termini [166,192]. Although observed associated with the cytoplasmic membrane, the C25dh does not present a C25dhC unit predicted to harbor a TM. In this case the association could be mediated by a currently unknown protein [167]. All these cytochromes *b* have in common unusual Met and Lys residues as axial heme ligands. The wire function of this protein is achieved by exposing two distinct heme edges at the protein surface.

3.3.2. The NrfD-type γ subunit

The "NrfD-type" unit (named from the first representative of the group, characterized in periplasmic nitrite reductase [195]) is a membrane-integrated protein devoid of any cofactor but still responsible of injecting or extracting electrons to or from quinones/quinols. Sequence homologies indicate that this protein takes part in several diverse enzymes in the Mo/W-*bis*PGD enzymes family, such as Psr [196], Ttr [148], Sre [149] and Dms [197]. Arsenate reductase-type enzymes (Arr/Arx) are special cases where this subunit exists only in some of them [147]. Although clearly related together, these units have a variable number of TM: 8 in the case of PsrC, Arr and DmsC, and 9 in the case of TtrC. The crystal structure of *T. thermophilus* PsrC provided the single 3D picture of this element (Fig. 4). Crystal containing MK (ID: 2VPW) allowed to precisely visualize the quinone binding site in this complex (Fig. 7). Scarce if not no information does exist however on the other NrfD-containing systems of the Mo/W-*bis*PGD enzymes family, and it is too early to try listing conserved features on these sites (see Section 3.4).

3.3.3. c-Type cytochromes as additional subunits

In *D. vulgaris* [186] and *D. desulfuricans* [185], very special Fdh, $FdhABC_3$, have been purified and characterized which contain, in addition to the catalytic subunit and the ferredoxin β subunit, a 16 kDa cytochrome. This last subunit is homologous to the typical soluble cytochrome c_3 (Tplc_3) that plays the role of redox partner for periplasmic hydrogenases from which 3D-structure is available (ID: 2BQ4) [198]. Tplc_3 are small (13–15 kDa) globular cytochromes containing four covalently bound hemes all with *bis*-histidinyl axial coordination (see [199] for review) having negative redox potentials. The close proximity of the hemes results in redox cooperativity giving rise to special redox properties of these cytochromes. All these characteristics are also encountered in the C_3 subunit of the $FdhABC_3$ [185,186]. Similarly to the cytb^{III} of Ebdh this c_3 does not bind $FdhABC_3$ to the membrane.

The *pcr* operon of two *Dechloromonas* species [187], revealed a *pcrC* gene coding for a protein product similar to the soluble tetrahemic cytochrome c_{554} from *Nitrosomonas europaea* (ID: 1FT5) [200]. As its homolog, PcrC would not be membranous and therefore would not link the Pcr enzyme to the membrane and would play the role of additional electron wire for the enzyme, similar to the c_3 subunit depicted above. Recently, Nilsson et al. [194] proposed that this element could be a partner rather than a true subunit of the enzyme. Since no further characterization has been performed, this question remains open.

In addition to its ability to physically interact with cNarI, cNarC is required for correct assembly of an active NarGH complex [189,190]. This subunit, a dihemic *c*-type cytochrome, is therefore considered as true subunit of the Nar complex from *T. thermophilus* and would therefore constitute the fourth subunit of this complex. Sequence analysis revealed that the two *c*-type hemes are bound to the hydrophilic domain at the N-terminus part of the protein facing the periplasm and that a single TM at the C-terminus part of the protein anchors the cytochrome into the cytoplasmic membrane. Such a di-hemic cytochrome *c* has been proposed, based on genome sequencing, as a partner subunit in nNxr [201,202].

For these three *c*-type cytochromes and also for the cytb^{III} units, we can wonder what their role is in their respective system. When the catalysis is for sure to be attributed to the α subunit and the electron transfer function to the β subunit, cytb^{III}, c_3, PcrC and cNarC appear as functionally redundant. The first three units are additional electron transfer relays without linking the enzyme to the quinone pool whereas cNarC is an additional membrane anchor for a complex already bound to the membrane and linked to the quinone pool by cNarI. Further functional studies of these enzymes are required to answer to this question.

3.3.4. Extra-complex units connecting soluble enzymes to the quinone pool

Bioenergetic electron transfer chains involving soluble enzymes require connecting electron transfer in the soluble compartments to redox reactions of the liposoluble hydrogen carriers. This task is usually fulfilled by a Rieske/cyt*b* complex (or an Alternative Complex III as proposed recently [203]). But over the last 10 years, a family of membrane-anchored *c*-type cytochromes, the NrfH/NapC/NirT family, has been recognized as the major cytochrome Rieske/cyt*b* complex-independent pathway for electron transfer between the quinol pool and water-soluble periplasmic oxidoreductases. These cytochromes contain multiple hemes *c* that do not take strictly part in the complex but are the obligate partners. The structural archetype (the only one available) of this family is the tetrahemic *c*-type NrfH cytochrome involved in nitrite reduction to ammonium donating electron to the pentahemic NrfA [204]. NrfH-type cytochromes demonstrated to function with Mo/W-*bis*PGD enzymes are numerous. TorC is the partner of the TorA enzyme [205], DorC is the partner of DorA protein [206], NapC is the partner of the NapAB complex [207], whereas CymA in *Shewanella* species has been demonstrated to serve multiple enzymes among them, ArrAB [208]. Such a cytochrome has also been proposed to serve the Pcr and Clr enzymes [194]. Predicted structure derived from DNA sequences suggests that the common feature of the NrfH/NapC/NirT-type cytochromes is the presence of an N-terminal transmembrane α-helical anchor that binds a tetra-heme globular domain to the periplasmic face of the plasma membrane (as exemplified by the NrfH itself). Some members of the family such as TorC [209] and DorC [210] have an additional C-terminal extension that binds a fifth heme.

In addition to NapC described above, Nap system can contain additional proteins predicted to be FeS proteins, NapG and NapH, demonstrated together to form stable complexes and to be involved in quinol oxidation [211,212]. NapH is a membrane protein containing four TM but containing also a hydrophilic domain facing the cytoplasm and harboring two [4Fe–4S] clusters. The NapG element is a hydrophilic one, containing four [4Fe–4S] clusters and situated in the periplasm, bound to the membrane via its interaction with NapH. This sub-complex could appear, as already evoked for the c_3, PcrC, cNapC and cytb^{III}, as an additional redundant element of the Nap system. Several works thus have been conducted to elucidate the respective role of NapC and NapGH. Since the common function of these two elements is to get electrons from the quinol pool their possible respective role are discussed in Section 3.4.2.

Due to their great variation in composition, the Mo/W-*bis*PGD enzymes present highly variable cofactor content. We can consequently wonder in which extent the variable electron pathway thereby managed, correlates to the substrates' redox properties. Compared to biochemical and genetic data, redox data on Mo/W-*bis*PGD enzymes are rare. Fig. 5 illustrates the variations in redox potentials along the electron transport chain of enzymes for which data are available, with indication of related cofactor's situation in the global architecture of the enzyme. In all the resolved structures, distances between adjacent cofactors have all been revealed compatible with electron transfer suggesting that all the cofactors must be involved in electron transfer pathway. Redox potentials of initial electron donor and final electron acceptor, "subs" and "co-subs", are also indicated when available. The Mo/W-*bis*PGD enzymes family support conversions of substrates in a redox potential range approaching 1 V (Table 2). In the case of photosynthetic Reaction Centers and Rieske/cyt*b* complex, correlations between the redox potential of the substrate (isoprenoid quinones) and the one of all the cofactors in the enzymes have been observed (see for instance, [213,214]). Conversely, in the case of the herein considered Mo/W-*bis*PGD enzymes, there is no straightforward correlation between the redox potential of the substrate and those of the whole cofactor's chain. In the vast majority

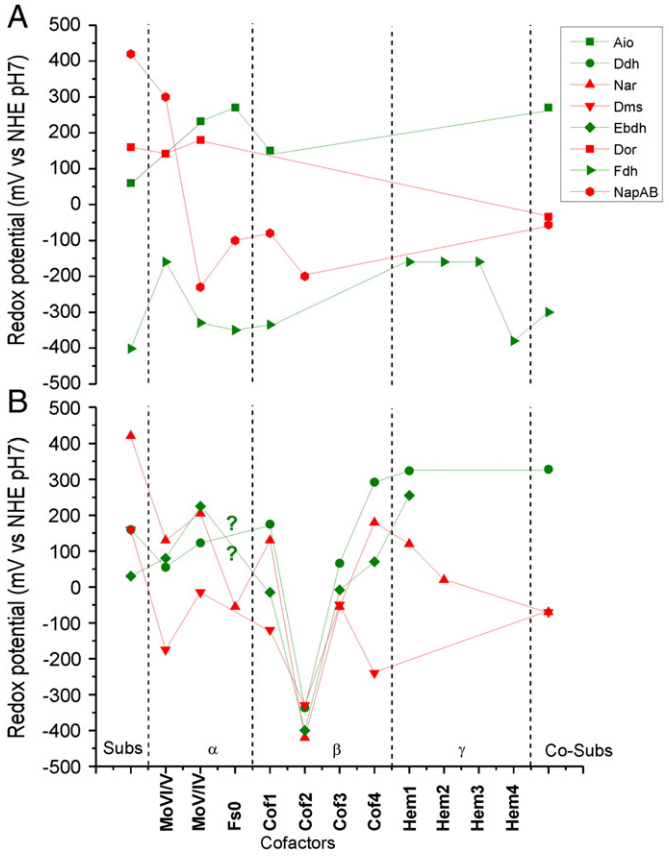

Fig. 5. Schematic illustration of internal electron transfer pathway in Mo/W-*bis*PGD enzymes. The redox potentials of the cofactors are presented in order of their spatial situation in the enzyme (α-subunit, β-subunit and γ-subunit). Note that, in physiological redox reaction, a reduction or an oxidation can take place in the Mo/W cofactor, changing thus the sense of global electron transfer in the enzyme. As such, reductases are red colored and oxidases or dehydrogenases are green colored. In the left column called "Subs", lie the natural organic or inorganic substrates listed in Table 2. In the right column called "co-Subs", lie co-substrates as diverse as proteins (cytochromes, azurin) or quinols/quinones. Panel A includes enzymes with small uphill step(s) while panel B includes enzymes with much larger uphill step(s). Data for *A. faecalis* Aio come from [181,457,458], with a redox potential of a two electrons Mo(VI/IV) transition. The data for *R. sulfidophilum* Ddh come from [160,459], data for *E. coli* nNar come from [155,156], data for *E. coli* Dms come from [460], data for *T. selenatis* Ebdh come from [461], data for *Rhodobacter* Dor come from [54,210], data for *R. sphaeroides* Nap come from [68,207], data for *Desulfovibrio* Fdh come from [185,462]. For DorC, the redox potential of the heme lying in the C-terminal part, thought to be the direct electron donor to DorA, is used. For soluble c_3, the heme receiving electrons from Fdh is unknown and the lower redox potential is used. The question marks denote "undetermined".

of cases, the thermodynamics of the overall enzyme reaction appears to only be driven by the physiological substrate's and redox partner's (co-substrate) redox potentials. Hence, in the cases of reductases, the redox potential of the co-substrate is lower than that of the substrate (e.g. Dms, with DMSO and MK) thermodynamically favoring the global reaction. The reciprocal is true with dehydrogenases and oxidases for which the redox potential of the co-substrate is higher than that of the substrate (e.g. Aio, with As(III) and cytochrome c_{552}). Noteworthy, one or several steps of the global exergonic reaction can be uphill defining two groups of enzymes. In the first group, shown in panel A and exemplified by Aio, Dor, Nap or Fdh, the uphill step(s) do(es) not exceed 200 mV. In the second group, shown in panel B and exemplified by Ddh, nNar, Dms and Ebdh, the uphill step(s) can largely exceed 300 mV such as the electron transfer steps to or from the FS2 cluster in the archetypal β subunits. However, this shared property does not necessarily have a functional signification since it does not represent any convergence. All the enzymes of this latter group are indeed of the Class II (see Section 3.1) and are phylogenetically related. Published data addressing the question of the necessity of such a step are scarce. For instance, shifting the low potential of the nNar's FS2 to higher redox potential by site-directed mutagenesis has no dramatic functional impact suggesting that this uphill step is not absolutely required [113].

3.4. Role of quinones in Mo/W-bisPGD enzymes bioenergetics

Numerous Mo/W-*bis*PGD enzymes are known to directly interact with isoprenoid quinones/quinols either through their membrane subunit that contains two *b*-type hemes (cytb^{I} and b^{II} subunits) or that do not bind any cofactor (NrfD-type γ subunit), or via extra-complex components that transiently bind to the enzyme and contain multiple *c*-type hemes or FeS clusters. Thus, understanding the reactivity of such quinone-utilizing molybdoenzymes towards these molecules constitutes an essential step for delineating their individual mechanism and elucidating their bioenergetic role. In this context, the work on respiratory Mo/W-*bis*PGD enzymes reviewed hereafter greatly contributed to the advancement of our knowledge on transverse questioning, namely (i) the determination at atomic resolution of quinone binding mode within protein complexes, (ii) the specificity of quinone utilization by a given complex in those organisms containing several types of quinones differing in their structure and properties, in line with energy conservation, catalytic directionality and defining the role of the protein environment, and finally (iii) the impact of the orientation (periplasmic or cytoplasmic) of a quinone binding site within the membrane subunit on its bioenergetic efficiency.

3.4.1. Structures and properties of relevant quinones

Isoprenoid quinones are amphiphilic molecules found in nearly all living organisms [24,215]. They are composed of a polar head group and a hydrophobic side chain. The apolar isoprenoid side chain gives the molecules a lipid-soluble character and allows them to freely diffuse in biological membranes. The quinone head group has a ring moiety with two oxygen atoms at positions 1 and 4 and is directly involved in redox reactions (Fig. 6). Indeed, quinones can oscillate between three different oxidation states. The oxidized quinone (Q) state has two keto groups. The addition of one electron results in the formation of an anionic semiquinone intermediate ($SQ^{\bullet -}$), and with the uptake of one proton, a neutral semiquinone intermediate (SQH•) is formed. The addition of a second electron and proton generates the fully reduced quinol (QH_2). Therefore, quinones couple electron transfer reactions to proton binding and release, a property that is crucial to transmembrane proton transport. In prokaryotic bioenergetic processes involving molybdoenzymes, quinones serve mainly as redox mediators between dehydrogenases and terminal reductases, donating or accepting two electrons to or from the Mo active site through a one-electron transfer chain containing FeS clusters and eventually hemes. Thus, quinones act as "gates" between one and two-electron processes. This involves the obligatory

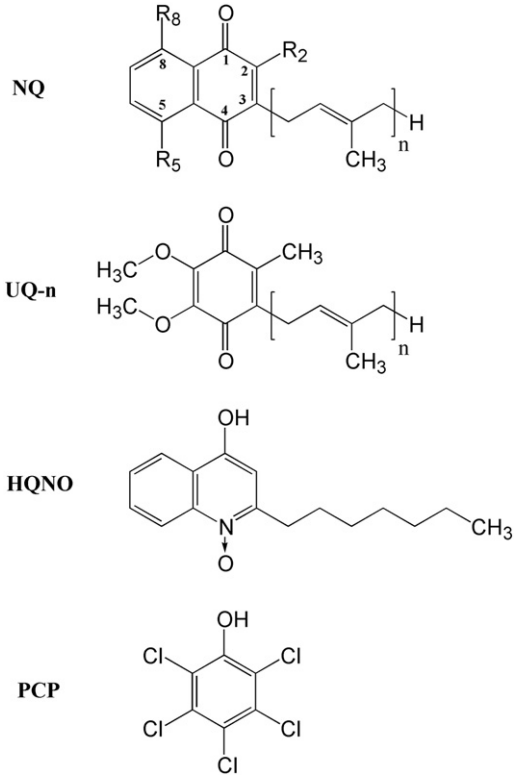

Fig. 6. Structure of isoprenoid quinones and of some quinone analogs discussed in this review. NQ, naphthoquinone; menaquinone (MK-n) corresponds to [$R_2 = CH_3$, $R_5 = R_8 = H$], demethylmenaquinone (DMK-n) to [$R_2 = R_5 = R_8 = H$], and methylmenaquinone (MMK-n) is found with [$R_2 = CH_3$, $R_5 = CH_3$, $R_8 = H$] or [$R_2 = CH_3$, $R_5 = H$, $R_8 = CH_3$]; UQ-n, ubiquinone (UQ-n); HQNO, 2-heptyl-4-hydroxyquinoline *N*-oxide; and PCP, pentachlorophenol. n is the number of isoprenoid units.

transient formation of highly reactive semiquinone catalytic intermediates during enzyme turnover. *E. coli* NarGHI is the sole molybdoenzyme in which such an intermediate has been specifically studied (see Section 3.4.3) [216–221].

Although quinones are considered to be highly mobile in the lipid bilayer of the membrane, reactivity of enzymatic complexes towards quinones occurs at specific well-structured protein sites named Q sites. Their accurate description is currently a major challenge for a detailed understanding of the function of Mo/W-*bis*PGD enzymes. For instance, previous studies on photosynthetic or alternative respiratory proteins to Mo/W-*bis*PGD enzymes demonstrated that the protein environment can dramatically modulate the quinone redox chemistry to an extent that a quinone can have very different functional properties when associated with different sites. Indeed, while the quinone redox potential in a bacterial membrane is expected to be close to that measured in organic solution [222], the midpoint redox potentials of the two one-electron processes Q/SQ and SQ/QH_2 can drastically change upon binding to a protein Q site, considering in particular the associated proton transfer chemistry. In addition, conformational flexibility during quinone turnover may take place.

The great majority of biological isoprenoid quinones belong to naphthoquinones (NQ) or benzoquinones. Their hydrophobic side chain can vary not only in the length but also in the degree of saturation, as well as in the presence of additional groups. Menaquinone (MK-n) is the most widespread microbial respiratory quinone (Fig. 6). It contains 2-methyl-1,4-naphthoquinone ring as a head group. Its side chain is most frequently composed of n = 6–10 prenyl units. In some prokaryotes, compounds with different modifications of the head group are found. Among them, demethylmenaquinones (DMK) and methylmenaquinones (MMK) are often used by proteobacteria and gram-positive bacteria [215,223–226]. In contrast, ubiquinones (UQ-n, also named coenzymes

Q) are found only in α-, β- and γ-proteobacteria and consequently in mitochondria. They are 2,3-dimethoxy-5-methyl-1,4-benzoquinone with an isoprenyl tail containing a variable number n of isoprenoid units, ranging mostly between n = 8–10 in bacteria.

Another important parameter distinguishing the different kinds of quinones is their midpoint redox potential E_m' (Q/QH_2) (Table 2). MK and DMK (and MMK as proposed in [227]) are low-potential electron carriers with negative redox potential values whereas the high-potential UQ has an E_m'-value of about +100 mV. The distribution of MK and UQ on the phylogenetic tree of species strongly indicates that MK are the most ancient type of isoprenoid quinones [24,213]. In addition, high-potential quinones such as UQ have only appeared in species permanently or periodically exposed to high concentration of oxygen, suggesting that high O_2 tensions and/or concomitant increase in ambient redox potential are evolutionary unfavorable for organisms using MK-based energy-converting systems. The reduced menaquinones (MKH_2, menaquinols) indeed becomes rapidly and non-catalytically oxidized in the presence of oxygen, therefore these compounds cannot efficiently operate in atmosphere containing oxygen [213].

3.4.2. Specificity of quinone utilization by Mo/W-bisPGD enzymes

Many prokaryotes can synthesize more than one type of quinones (see for reviews, [215,228]). Moreover, the quinone contents are regulated by a yet unknown mechanism in response to the type of electron acceptor present in the medium, the growth phase, and the available carbon source [229–232]. Altogether, this contributes to the high metabolic flexibility and complexity of these organisms that can rapidly adapt to environmental changes [233]. Thus, the question of the specificity of quinone utilization by Mo/W-*bis*PGD enzymes was raised. This is difficult to study in classical enzyme assays either due to the insolubility of the native substrates or due to the inability of native substrate to be removed from the enzyme without altering enzyme structure. Therefore, this issue has been addressed using mutant strains lacking genes involved at specific stages of the quinone biosynthetic pathways in which the quinone content has been chemically analyzed. This approach has been combined with growth assays using different electron donors or acceptors or with in vitro assays, both eventually complemented with the use of different quinones or analogs (for reviews, see [234–236]).

The facultatively anaerobic proteobacterium *E. coli* is the most studied organism in this context. UQ-8, MK-8 and DMK-8 are the major quinones but smaller amounts of UQ-1 to UQ-7, MK-6 to MK-9 and DMK-7 have also been reported [215]. Using *E. coli* strains deficient in the synthesis of UQ, (MK + DMK) or of (MK + UQ), it has been shown that not all molybdoenzymes are able to use all three types of quinones. Our current knowledge of the specificity of quinone utilization by molybdoenzymes in prokaryotes allows distinguishing two groups of enzymes:

(i) in group 1 enzymes, the specificity observed can be explained simply on the basis of the redox potentials of the quinones and of the acceptors. Typical examples include *E. coli* DmsABC and TorAC. In anaerobic respiration with DMSO (E_0' (DMSO/DMS) = +160 mV) and TMAO (E_0' (TMAO/TMA) = +130 mV), the naphthoquinones (MK + DMK) are required and cannot be replaced by UQ (Table 2) [235,237–240]. Further, whereas *E. coli* TorAC and DmsABC cannot use UQ, both are able to oxidize MK and DMK as well [239]. In contrast, mutants of *Shewanella oneidensis* (formerly S. *putrefaciens* MR-1 or *Alteromonas putrefaciens*) deficient in MK and MMK, but which have wild-type levels of UQ, retain the ability to use TMAO as an electron acceptor [241]. Whereas the specificity of Ttr has been much less investigated, available data suggest that UQ are not involved in electron transport to tetrathionate (E_0' ($S_4O_6^{2-}/S_2O_3^{2-}$) = +24 mV to +170 mV, Table 2) in *S. typhimurium* or in *Citrobacter freundii* [242,243].

Some Arr and Arx are predicted to contain a membrane integral subunit Arr/ArxC that might serve as anchor to the Arr/ArxAB complex and which is proposed to promote electron transfer between the quinone pool and the enzyme. The structural homology between PsrC and ArrC suggests a similar function for both enzymes. In the case of Arr, the electrons would be transferred from liposoluble MKH_2 to the catalytic molybdenum subunit and then onto As(V) [147]. This would be consistent with the substantial driving force provided by the low-potential MK given the midpoint potential of the arsenate/arsenite couple (E_0' ($HAsO_4^{2-}/H_3AsO_3$) ~ +60 to +139 mV, Table 2). In line with this reasoning, a recent genomic survey searching for quinone biosynthetic pathway genes indicates that only the group of Arr-containing bacteria presents species synthesizing MK alone whereas only the group of bacteria containing Arx presents a species synthesizing only UQ [182]. This led the authors to stipulate that all Arr-harboring strains oxidize MKH_2 via an As(V) reduction process whereas the Arx-harboring strains reduce UQ via an As(III) oxidation process. While this hypothesis still needs to be tested by detailed kinetic studies on both enzymes, it is similar to the behavior of quinol-fumarate reductase in *E. coli*, which uses MK for reduction of fumarate and UQ for oxidation of succinate [244]. Overall, this example illustrates the possible role of the electrochemical potential of the quinone in determining the enzymes' directionality.

Whereas the ε-proteobacterium *W. succinogenes* contains MK-6 and 2-,[5,8]-dimethyl-3-hexaprenyl-1,4-naphthoquinone (MMK-6) in its cytoplasmic membrane [224], activities of polysulfide respiration measured in nearly-inactive proteoliposomes containing purified Psr and either hydrogenase or formate as primary dehydrogenases was restored upon addition of MMK-6 but was maintained at a basal level upon addition of MK6 [196]. This indicates that MMK-6 is specifically involved in polysulfide respiration and cannot be substituted by MK-6. While the redox potential of the substrate is not known, it is assumed to be close to that of the S^0/HS^- couple i.e. ~−270 mV (Table 2). On the other hand, MMK-6 might have a much lower redox potential (~−220 mV) [227] than that initially predicted [196]. However, to our knowledge, no detailed study has been published yet that supports this value. If it is correct, the reduction of polysulfide by $MMKH_2$ is likely to be slightly endergonic and the specificity of *W. succinogenes* Psr towards MMK-6 is probably due to differences in the redox potential of the two naphthoquinone species.

A common feature of the above mentioned enzymes is that the substrate redox potential lies in the range of that covered by the different quinones, or at least close to it. This is not the case for *S. enterica* PhsABC that belongs to group 1 enzymes. Whereas this bacterium can synthesize UQ, MK and DMK, thiosulfate respiration in this organism is blocked in strains that cannot synthesize NQ [237,245]. Further, the very low rates of thiosulfate reduction exhibited in the *ubiE* mutant deficient in UQ and MK synthesis imply that $DMKH_2$ is a poor substrate for PhsABC and that consequently MKH_2 is virtually the sole electron donor to the enzyme [246]. A remarkable aspect of thiosulfate reduction in *S. enterica* is that under standard conditions, the overall reaction of thiosulfate reduction ($E_0'(S_2O_3^{2-}/HS^- + HSO_3^-) = -400$ mV) by MKH_2 is highly endergonic, unless less than with the other quinols [235]. This results in an unfavorable $\Delta E_0'$ of ~−330 mV for the reaction. Based on the sequence similarity between the FdnGHI subunits of *E. coli* formate dehydrogenase and the PhsABC subunits of *S. enterica* thiosulfate reductase, a structural model of PhsABC has been proposed, suggesting that this enzyme uses a reverse redox-loop mechanism that consumes the *pmf* (Fig. 8), in consistency with its strong inhibition by agents that degrade the *pmf* [246]. In addition, this would become thermodynamically

possible as the value $\Delta E_0'$ of ~ −330 mV would be attenuated by the more physiologically reasonable concentrations of thiosulfate, sulfite and sulfide in the cell, and possibly by the redox state of the MK pool. Interestingly, the reaction is reversible under physiological conditions, and is then *pmf*-independent. It can function with DMK as electron acceptor, while the physiological forward reaction cannot utilize it. It was thus suggested that the inability of $DMKH_2$ to support thiosulfate reduction is due to the unfavorable redox potential of $DMKH_2$ relative to MKH_2 rather than discrimination between the two types of naphthoquinols by the quinol oxidizing site of thiosulfate reductase [246]. Thus, the quinone specificity of the group 1 enzymes listed above does not appear to be based on quinone discrimination by the Q site, but rather to be related to the quinone redox potentials that drive enzyme reactivity.

(ii) in group 2 enzymes, the observed quinone specificity cannot be explained on the basis of the redox potentials of quinones and acceptors. Prominent examples are given by bacterial nitrate reductases. Considering the nitrate/nitrite redox potential of +420 mV, basically, low and high-redox potential quinones can serve as electron donors. Using *E. coli* mutants of quinone biosynthetic pathways, it has been shown that either MKH_2 or UQH_2 can transfer electrons to Nap in *E. coli*, but not $DMKH_2$ which is however intermediate in redox potential [247]. However, Nap couples more effectively to MKH_2 oxidation than to UQH_2 oxidation [248]. NapC was shown to be essential for electron transfer from both UQH_2 and MKH_2 to NapAB. In contrast, NapG and NapH were found to be essential for periplasmic nitrate respiration in cells that only contained UQH_2 [248,249]. Thus, it was concluded that NapG and NapH form a specialized UQH_2 dehydrogenase required to transfer electrons via NapC to the NapAB complex [211,248]. A working model for electron transfer within the NapABCGH complex was proposed, that mainly includes two, partially independent, electron transfer pathways to the Nap complex depending on the nature of the quinol used. 2-Methyl-1,4-naphthoquinone (Menadiol, E_0' (menadiol/menadione ~ −1 mV), a closer structural analog of MKH_2 than UQH_2, was used as exogenous electron donor and was shown to be able to support NapGH-dependent electron transfer via NapC to the NapAB complex, in contrast to the apparently poor electron donor UQ-0 (E_m' (UQH_2-0/UQ-0 ~ +162 mV) [211]. This illustrates the difficulty to extrapolate results obtained from experiments that rely on quinone analogs to the function of the system with its natural endogenous quinone substrates. Interestingly, in the ε-proteobacterium *W. succinogenes*, nitrate respiration is independent of a NapC-type protein [250]. Rather, the NapGH module mediates electron transport from MKH_2 to the periplasmic NapAB complex, thereby substituting the function conventionally carried out by NapC [251]. The quinone specificity of this enzyme towards the two endogenous redox carriers MK-6 and MMK-6, the role and the number of Q sites are still to be evaluated [212].

Synthesis of the membrane-bound nitrate reductase nNarGHI is optimally induced under anaerobic conditions and high nitrate concentrations. Under these conditions, whereas all three quinones are found in high concentrations with DMK as the major species, nNarGHI functions with UQ and MK, but for unknown reasons, not with DMK, similar to the Nap system [238,239,248,252,253]. In contrast to Nap, bacterial growth assays of mutant strains synthesizing only UQ or NQ using nitrate as electron acceptor indicate that NarGHI oxidizes UQH_2 and MKH_2 with similar efficiency [238].

The selectivity of group 2 enzymes is likely to be due to the structural properties of the quinones (Fig. 6). It should also be mentioned that the redox potential of the bound quinone may differ from that of the freely diffusing molecule. In both cases, the protein environment could drive this specificity by tuning the quinone binding and/or redox properties. Thus, describing the atomic details of the quinone binding mode to Mo-*bis*PGD enzymes is an essential step for understanding the reactivity and specificity of these systems.

3.4.3. Resolving quinone binding in Mo/W-bisPGD enzymes

Deep understanding of the reactivity of a quinol-utilizing enzyme requires detailed structural information on the quinone binding mode in different redox states of the enzyme. This is challenging given the location within the membrane and the high molecular weight of the complexes involved, the quinone lability, and the transient character of quinone/protein interactions.

To date, there is no evidence for the presence of quinones that function as tightly bound (i.e. non-exchangeable) cofactors in quinone processing Mo/W-*bis*PGD enzymes, as found in the Q_A site of the photosynthetic reaction center [254] or in the Q_H site of cytochrome bo_3 [255–257]. Therefore, whereas the presence of multiple Q sites has been discussed in the past for some cases, the more recent experimental evidence indicates that Mo/W-*bis*PGD enzymes harbor a single Q site. Using protein-film electrochemistry, it has been recently proposed that MK-7 may function not just as a substrate but also as a tightly bound cofactor in CymA from *Shewanella* [258,259]. Indeed, catalytic signals in cyclic voltammetry are observed when MK-0 or UQ-10 is supplied to CymA films for which the tightly bound MK-7 has not been removed whereas these signals are absent in *n*-dodecyl β-D-maltoside-washed CymA films devoid of MK-7 [259].

Only a limited number of high-resolution three dimensional structures of quinone-interacting Mo-*bis*PGD enzymes are available. A three-dimensional structure of PsrABC from *T. thermophilus*, an obligate aerobe thermophilic bacterium that contains MK-8 and MK-7 as its sole isoprenoid quinones [215], has been solved at 1.9 Å resolution in complex with MK-7 [88] (Fig. 7A). MK-7 binds in a mainly hydrophobic pocket situated in the heme-lacking PsrC subunit, on the periplasmic side of the membrane and in close proximity to the proximal [4Fe–4S] of the electron-transfer subunit PsrB. In addition, the resolution of the PsrABC crystal structures co-crystallized with either UQ-1 or with the inhibitor pentachlorophenol (PCP) (Fig. 7B) indicated that all three compounds bind in the same pocket, suggesting that this site is the physiological Q site. Slight variations with respect to the hydrogen-bonding of the substrate are resolved, that may be relevant for understanding enzyme reactivity and specificity towards quinols. The available structural data cannot be further discussed with regard to the specificity of quinone utilization by this enzyme. In particular, in vitro measurements of UQH_2 or MKH_2:polysulfide oxidoreductase activity of *T. thermophilus* PsrABC have never been reported. In contrast, no high-resolution structural information on the quinone binding mode in *W. succinogenes* PsrABC is available that could provide useful molecular details to understand its high specificity towards MMK-6.

High-resolution crystal structures of two other quinone processing molybdoenzymes have been obtained in the presence of bound inhibitors, namely *E. coli* FdnGHI in complex with 2-heptyl 4-hydroxyquinoline *N* oxide (HQNO) [92] and nitrate reductase NarGHI from the same organism with PCP bound to it [260], at 2.8 and 1.9 Å resolution, respectively. A histidine ligand (FdnI His169, NarI His66) of the heme (b_C in FdnI, b_D in NarI) that forms part of the inhibitor binding pocket is hydrogen bonded to the N-oxide group of HQNO or to the hydroxyl group of PCP. An additional hydrogen bond is formed between the PCP and one of the heme b_D propionate group. The ligand for the OH group of HQNO (equivalent to the MK O1) is less clear and the involvement of a water molecule (w1990) or of the Nε atom of Asn110 has been discussed. Moreover, it has been recently shown that the presence of an anionic cardiolipin tightly associated to NarGHI is required for quinol binding to the enzyme [218] and a similar situation has been proposed to occur in FdnGHI [261].

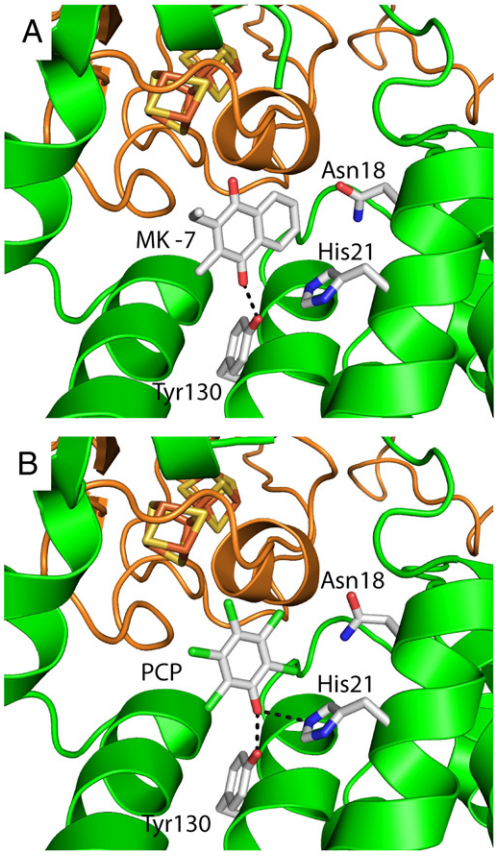

Fig. 7. Quinone binding site in *T. thermophilus* Psr. Binding mode of (A) MK-7 and (B) PCP in *T. thermophilus* PsrC as inferred from X-ray crystallographic studies [88]. Whereas the side-chain of Tyr130 is a direct ligand to the O1 MK-7 and to the equivalent hydroxyl group of PCP, the His21 Nε provides an additional hydrogen bond to the same oxygen of PCP. The MK-7 O4 carbonyl is uncoordinated. Only the two first carbon atoms of its isoprenoid side-chain could be modeled in the electron density map. The PsrB and PsrC subunits are orange and green, respectively.

A major progress in the determination of the quinone binding mode in NarI has been achieved by taking advantage of the ability of the enzyme to highly stabilize an endogenous menasemiquinone intermediate within its quinol oxidation site hereafter referred to as MSQ_D in reference to its close proximity to heme b_D [216,219]. Whereas the unusually high menasemiquinone stability Ks~70 (the highest measured so far for a quinone processing respiratory complex) allows this protein-associated quinone to function as an efficient converter between n = 1 and n = 2 electron transfer steps, it raises the question of its consequence for enzyme functioning. Taking advantage of the high stability of the paramagnetic menasemiquinone intermediate, intensive spectroscopic characterization of its binding mode by advanced EPR spectroscopy has been performed. Remarkably, EPR experiments on NarGHI have been carried out in its physiological membrane environment, without having to resort to detergent-solubilised purified protein, and using the natural endogenous semiquinones as spectroscopic targets. Using the unpaired electron delocalized over the MSQ_D ring as a magnetic probe of its nuclear environment, high resolution pulsed EPR methods provided direct evidence for nitrogen-ligation to this radical. A multifrequency ^{14}N and ^{15}N HYSCORE study allowed its assignment to a Nδ imidazole nitrogen of a hydrogen-bonded histidine residue [220]. The latter was attributed to the heme b_D axial ligand His66, the only His residue present in the NarGHI Q_D site, in consistency with the crystallographic studies. Further, the use of ^{1}H HYSCORE and ^{2}H ENDOR spectroscopies in combination with $^{1}H_2O/^{2}H_2O$ exchange experiments demonstrated a strongly asymmetric binding mode of MSQ_D via the formation of a single short in-plane hydrogen bond to the His66 residue [217]. This atypical binding mode is proposed to strongly contribute to the unusually high redox stability of MSQ_D.

Further EPR and HYSCORE experiments have revealed that an endogenous ubisemiquinone (USQ) radical can be formed in NarGHI and that it binds to the same residue as MSQ_D does, demonstrating unambiguously that a single Q site of NarGHI accommodates the two types of substrates [221]. These conclusions contrast with the interpretation of several biochemical studies relying on the use of quinol analogs and/or inhibitors [262–264] which have to be reevaluated. In addition, the relationship between NarGHI activity and phospholipids has been investigated by combining biochemical and biophysical methods [218]. It has been shown that an anionic cardiolipin is tightly associated to the enzyme and is essential for its functionality. The reinterpretation of X-ray diffraction data has enabled to identify a specific binding site of cardiolipin in close proximity of heme b_D. The results indicate that one of the cardiolipin acyl chain is responsible for structural adjustments of the heme b_D and of the adjacent quinol substrate binding site, allowing reactivity towards quinol. Overall, these studies provide the first molecular basis to understand the interplay of quinone, heme and phospholipid in the activation of a bacterial respiratory complex [218,261].

Attempts toward the identification of putative quinone reactive sites can often only be achieved on the basis of indirect biochemical studies combining site directed mutagenesis and the use of quinol analogs or inhibitors. A typical example is provided by the membrane subunit DmsC of *E. coli* DmsABC whose three-dimensional structure has not been solved yet. As previously mentioned DmsC does not contain any metal prosthetic groups but is essential for MKH_2 binding and oxidation. The use of fluorescence titration and stopped-flow methods revealed the presence of a single high-affinity HQNO binding site located in the DmsC subunit. In addition, mutation of His65 to Arg in DmsC blocks quinol activity and eliminates HQNO binding [265,266], suggesting that this residue could be important for quinol binding. Substitution of DmsC-Glu87 into Lys results in the inability of the enzyme to support anaerobic growth on glycerol/DMSO minimal media, to oxidize lapachol and to bind HQNO, indicating that this residue is probably important for MKH_2 binding and oxidation [267]. In addition, it could act as proton acceptor in the menaquinol binding site (see Section 2.4.4). Although the PsrC residues equivalent to DmsC-His65 and Glu87 are located within the same region as that of the crystallographically identified PsrC Q site, these residues are however located in different helices from those directly involved in substrate or analog binding (Fig. 7). This suggests a different substrate binding mode in DmsC and PsrC.

While no high resolution structural data of a member of the cytochrome *c* quinol dehydrogenases family that connect soluble molybdoenzymes to the quinone pool has been determined, a crystal structure of the archetype of this family (that includes NapC, CymA, TorC and DorC, see Section 3.3.3), namely the MKH_2-interacting *D. vulgaris* cytochrome *c* nitrite reductase NrfHA, has been solved in complex with HQNO [204,268]. This provides a structural model for MKH_2 binding to members of the family. The HQNO binding site is located at the membrane–periplasm interface. The polar head of HQNO forms H bonds to NrfH-Asp89, a residue that occupies the heme distal ligand position, via its hydroxyl group, and to NrfH-Lys82 and Asn67 via its N-oxide (equivalent to MKH_2 O4). Lys82 is strictly conserved among the family, whereas Asp89 may be replaced by a His or a Glu [204]. Mutation of Lys91 (equivalent to Lys82 of *D. vulgaris* NrfH or to Lys103 in *E. coli* NapC) into a Gln in the tetraheme *c*-type cytochrome CymA in *Shewanella* sp. ANA-3 reduces enzyme activity with the quinol analog 2,3-dimethoxy-1,4-naphthoquinol (MKH_2-0) as electron donor and nearly abolishes HQNO binding [269]. In vivo, in contrast with the wild-type, the mutated CymA is unable to support growth with arsenate as electron acceptor [208].

While histidines are involved in the coordination of the ubi- and menasemiquinones in NarGHI [219–221], HQNO in FdnGHI [92] and possibly MK-7 in PsrABC [88] or HQNO in DmsC [266], this is not a

general trend for quinone binding and no common pattern for quinone binding has yet emerged, in spite of a previous tentative [270].

3.4.4. Quinones as hydrogen carriers

In addition to their role in electron transfer processes, quinones have the ability to exchange protons by being either mono- or biprotonated. During catalytic turnover, two protons can thus be either released at quinol oxidation sites, or can be picked up at quinone reducing sites. Therefore, given that biological membranes are not permeable to protons, the orientation of a Q site on either the cytoplasmic or the periplasmic side of the membrane is an essential factor in determining the coupling efficiency of a given enzyme. This can be illustrated by the NarGHI complex. The overall topology of the complex ensures that the free energy in the QH_2/NO_3^- redox couple is conserved as *pmf* via an electrogenic redox half loop mechanism (Fig. 8). During quinol oxidation at the periplasmically oriented Q_D site within the *b*-cytochrome NarI, electrons are transferred one at a time to the hemes giving rise to the transient formation of a semiquinone intermediate [216,217,220,221]. Electrons are subsequently transferred through an ~9 nm electron wire of eight metal centers and ultimately reduce nitrate at the N side of the cytoplasmic membrane. The two protons issued from quinol oxidation are released on the P side of the membrane while nitrate reduction on the N side consumes two protons (Fig. 8). This charge separation makes the nNar enzyme electrogenic (or proton motive) in that a net of two positive charges is translocated across the cytoplasmic membrane during transfer of two electrons to nitrate ($H^+/e^- = 1$).

When no high resolution structural data are available, the Q-site orientation may be predicted from the knowledge of the ratio (H^+/e^-) of translocated protons per electron transferred to or from the substrate during enzyme functioning which can be experimentally measured, or from structural models based on sequence similarities with enzymes of known structures. Combining site-directed mutagenesis, enzymatic assays using quinol analogs and/or inhibitors, potentiometric redox titration monitored by EPR spectroscopy and HQNO fluorescence quench titrations, the Q site of DmsC was predicted to be located close to the periplasmic side of the cell membrane [265–267,271] (Fig. 8). This suggests that there is a direct transfer of electrons from the Q site to the proximal FeS cluster located in the DmsB subunit. DmsB Tyr104 was discovered to play a major role for communication between both sites [271].

The H^+/e^- ratio accounts for (i) proton translocation by quinone/quinol turnover, (ii) *pmf* generation by susbstrate turnover and (iii) possibly direct proton pumping. Prokaryotic Mo-*bis*PGD enzymes can be differentiated on the basis of (i) the location of the active sites for the electron donor or electron acceptor on the positive (P) or negative (N) sides of the membrane, (ii) the location of the quinone/quinol binding site on the P or the N sides and the direction of electron transfer (P to N or N to P), and (iii) the number of protons involved in substrate

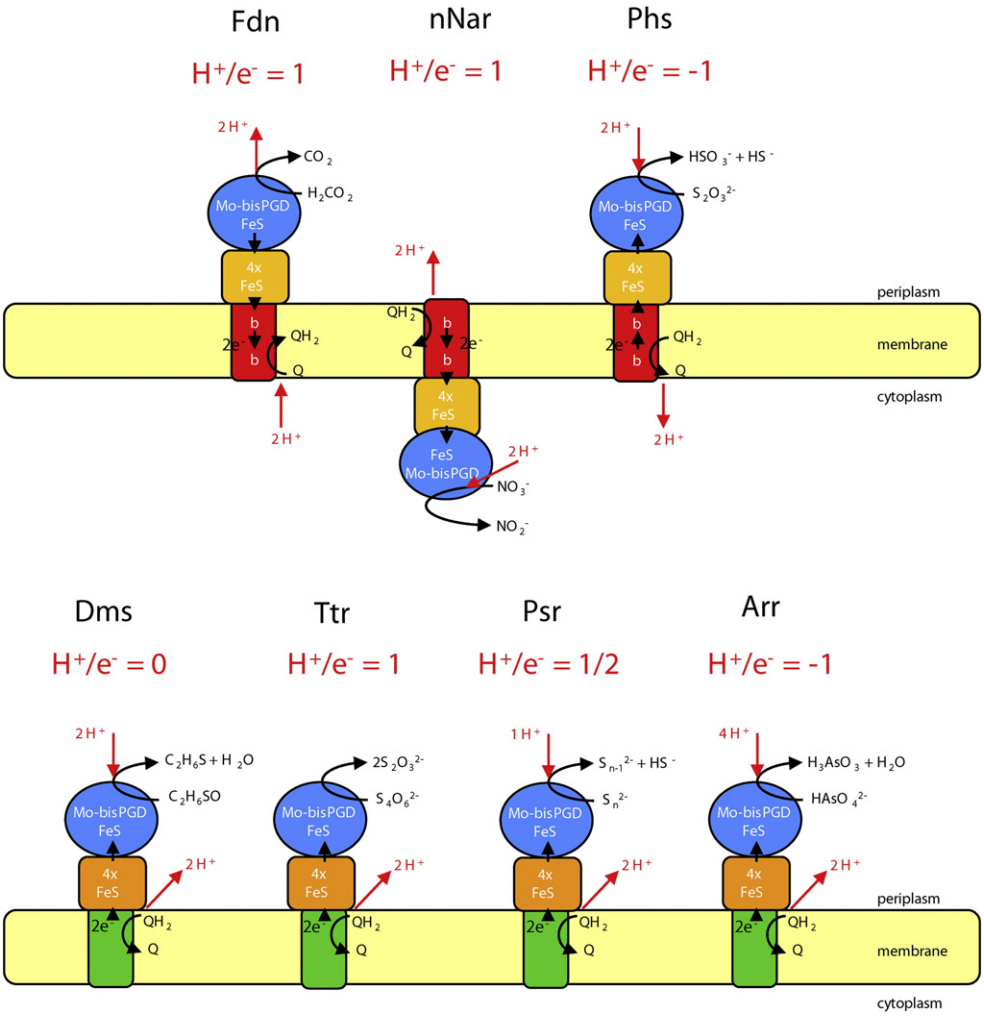

Fig. 8. Illustration of topological variations at the quinone reacting sites of selected Mo/W-*bis*PGD enzymes. Quinone-dependent substrate turnover results in either electrogenic ($H^+/e^- = 0.5$ or 1), electroneutral ($H^+/e^- = 0$) or *pmf*-dissipating ($H^+/e^- = -1$) overall reactions. For simplicity, only monomeric enzyme forms are shown.

conversion. The different localizations of the electron donor/acceptor and quinone/quinol centers allows for electrogenic i.e. proton motive (e.g. Fdn, nNar, Psr and Ttr), electroneutral i.e. non-proton motive (e.g. Dms) or even energy-dissipating reactions (e.g. Phs and Arr) (Fig. 8). Finally, it has been proposed that a protonmotive Q-cycle could operate in the NapGH complex of *W. succinogenes* or in some periplasmically-oriented "Archaeal" membrane-bound nitrate reductases [166,212].

The relative order of (de)protonation and electron transfer events is generally very speculative. Proton transfer from or to the Q site out of the membrane must be facilitated by a combination of either (de) protonable/polar residues, water molecules and eventually heme propionate groups that are present in the Q site. In the cytoplasmically-oriented HQNO binding site of FdnI, the water molecule (w1990) that seems to be a direct ligand of the inhibitor appears connected to the cytoplasm through a water chain maintained by hydrogen bonds to polar residues and a heme b_C propionate. This chain appears to be a proton pathway to the MK binding site allowing quinone protonation during enzyme turnover [92]. Quite similarly, a chain of water molecules located between the propionate of heme b_D and the bulk solvent has been resolved in the PCP binding site of *E. coli* nNarGHI. This "proton wire" could be involved in proton shuttling from the quinol toward the periplasm [260]. Molecular modeling of the physiological substrates UQH_2 and MKH_2 based on the PCP position suggested the involvement of the NarI-Lys86 residue, located at one end of the PCP binding pocket at the protein surface, in quinol binding and deprotonation. Interestingly, substitution of this residue into Ala drastically reduces or even abolishes quinol oxidase activity of the enzyme towards various quinol analogs and prevents semiquinone formation and HQNO binding [219,260]. In addition, HYSCORE experiments exclude a direct H-bond between the semiquinone and Lys86 [217,220]. Rather, a through-space interaction has been detected between MSQ_D and the Nξ of Lys86 using ^{15}N selective labeling [272]. A redox-dependent binding mode of the quinone at the Q_D site has been recently proposed that involves Lys86 as a direct hydrogen bond donor to the reduced quinol [217].

To conclude, more biochemical and structural information is required to draw a more conclusive picture of the structure and function of the quinone-reactive molybdoenzymes, including those discussed here. In those cases where the quinone/quinol-reactive modules do not tightly associate with the terminal oxidoreductase (Fig. 3), purification and characterization is often more difficult owing to lack of convenient assays. These systems represent particular challenges for the future.

4. Metabolic chains involving Mo/W-*bis*PGD enzymes

As outlined above, members of the Mo/W-*bis*PGD family are exclusively found in bacteria and archaea, and often sustain catalytic reactions which involve oscillation of the redox state of the Mo or W atom at the active site. Electrons are transferred to or from the active site by a number of various metal centers (FeS clusters, heme *b* or *c*) present in associated subunits or by interacting partners. These enzymes with a complex overall architecture are also diverse in terms of cellular localization (Fig. 3). Although this review focuses on bioenergetic contribution of the Mo/W-*bis*PGD family members, it appeared interesting to us to present those members which do not contribute to the *pmf* generation. These rare enzymes highlight by themselves the primordial role of this family for the cellular energy conservation in prokaryotes.

4.1. Nitrogen cycle

Molybdoenzymes of the Mo/W-*bis*PGD family are well-known to participate to the nitrogen cycle through the conversion of nitrate to nitrite by the so-called nitrate reductases (see for review [29]). In contrast to the eukaryotic nitrate reductase which contains a Mo-PPT cofactor, the prokaryotic ones share in common a Mo/W-*bis*PGD-containing catalytic subunit where the reduction of nitrate to nitrite occurs. Nitrate reductases have been classified by taking into consideration, (i) localization of the enzyme in the cell, (ii) molecular properties of the catalytic center, (iii) structural organization and (iv) function. Thereof, at least three different types of nitrate reductases, each of which providing a different physiological role, can be found in prokaryotes (Fig. 3). The three types are the soluble, assimilatory nitrate reductases (Nas) located in the cytoplasm; membrane-associated "respiratory" nitrate reductases (Nar); and the soluble, "respiratory" nitrate reductases (Nap) located in the periplasm. It has to be mentioned that Nar and Nas can be found in both archaea and bacteria whereas Nap are only found in a sub-group of bacteria. Basically, each nitrate reductase falls clearly into the assimilatory or respiratory class. On the basis of their cellular location and structural organization, the respiratory Nar enzymes again fall into three subgroups. The nNar and cNar enzymes are firmly attached to the cytoplasmic side of the inner membrane while it remains unclear whether periplasmic pNar enzymes are connected to the membrane (see Section 4.1.2). A fourth distinct category can be illustrated by Mo-*bis*PGD enzymes catalyzing the nitrate reduction in the reverse direction i.e. nitrite oxidation and named Nxr. A prominent participation of Nxr in nitrite oxidation can be taken with the nitrification process and the anammox process producing N_2 from nitrite and ammonium. All categories will be developed in the following with a specific emphasis on the participation of nNars to the bioenergetics of the cells (Fig. 9).

4.1.1. Nas and nitrogen assimilation

The first reduction step in nitrate assimilation, the two-electron reduction of nitrate to nitrite catalyzed by Nas, is followed by the six-electron reduction of nitrite to ammonium. The ammonium so formed is then predominantly incorporated into either glutamine or glutamate. The assimilatory reduction of nitrate to ammonium is an energetically expensive process since it requires eight electrons and complex prosthetic groups for the nitrate and nitrite reductase enzymes, in addition to the high affinity active nitrate transport system. As such, the nitrate assimilation pathway functions as an electron sink. In order to avoid this energetic cost under unnecessary environmental conditions, archaea and bacteria have evolved a similar strict control of the expression of the assimilatory pathway. Thus expression of the *nas* genes is subjected to dual control based on ammonium repression by a general nitrogen-regulatory system, and specific nitrate or nitrite induction [273–276].

Genetic and biochemical characterization of assimilatory nitrate-reducing systems has been focused mainly on cyanobacteria [277–281]. For instance, the overwhelming majority of *Synechococcus* sp. can utilize nitrate or nitrite as sole nitrogen sources in oceanic surface waters even in presence of ammonium which indicates that a different regulation is at play and exploited under those nitrogen-limited environments [282]. In comparison, only few physiological, genetic and biochemical studies have been conducted on heterotrophic bacteria such as *Klebsiella oxytoca* [179,283], *Azotobacter vinelandii* [284], *P. denitrificans* [154], the photoheterotroph *R. capsulatus* [285], the Gram-positive *B. subtilis* [152] or more recently on Actinomycetes [286,287]. Bioinformatic analyses have revealed that *nas* genes are present in many archaea [288] but, to date, physiological, genetic and biochemical characterization of nitrate assimilation have only been performed on *Haloferax mediterranei* [276,289–292].

Although nitrate assimilation pathways are dependent on cytoplasmic nitrate and nitrite reductases, a high degree of flexibility is observed regarding the nature of the physiological electron donor to these enzymes which has immediate consequences in terms of integration within the cell metabolism. In cyanobacteria, a [2Fe–2S] ferredoxin reduced by Photosystem I constitutes the electron donor to both the nitrate and nitrite reductases NarB and NirA, respectively, thus linking functionally nitrate assimilation to photosynthetic processes [275]. On the contrary, a Rieske-type [2Fe–2S] ferredoxin, NasG, was shown to be essential for

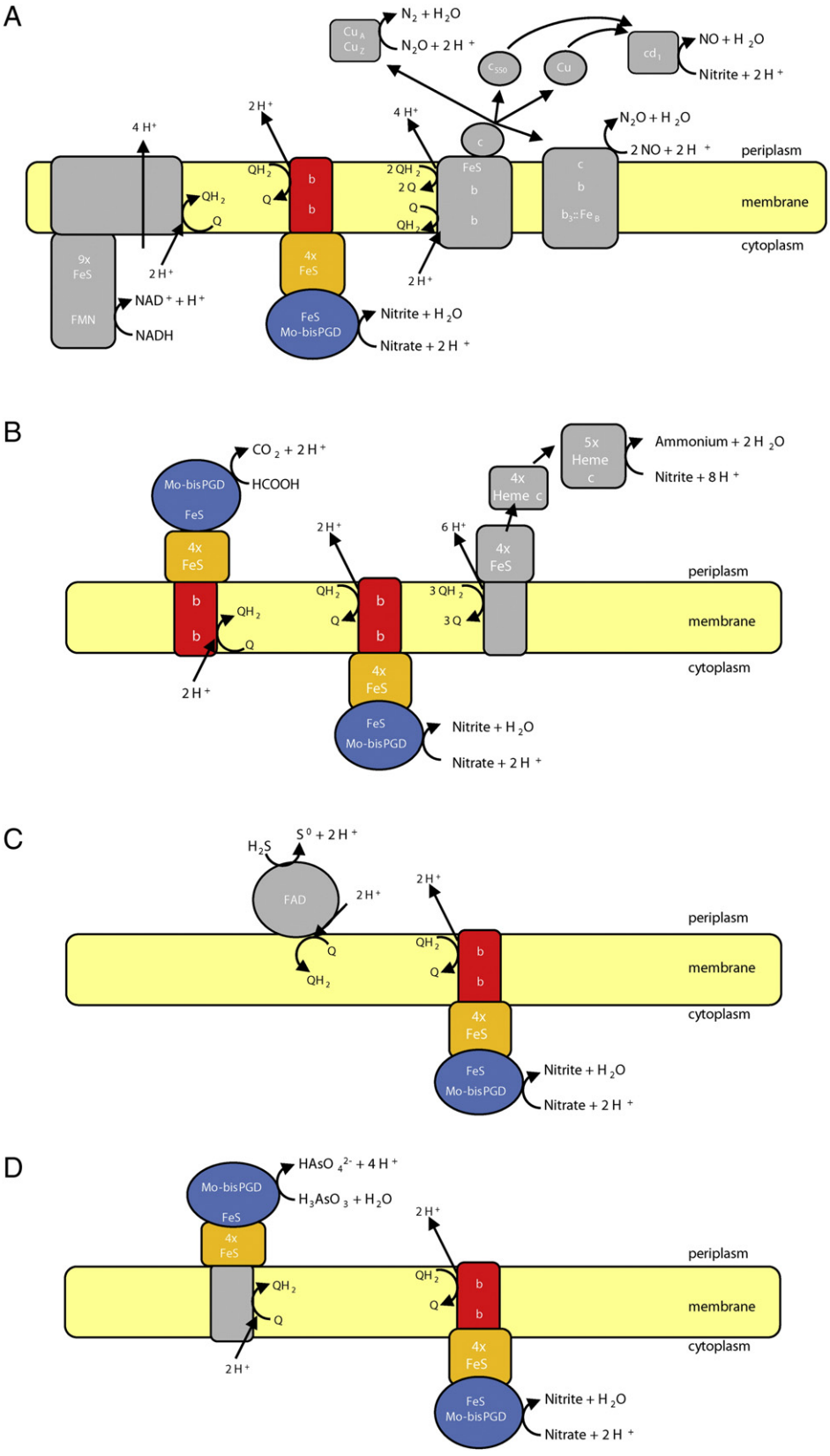

Fig. 9. Schematic representation of the bioenergetic chains involving nNar in prokaryotes. A. nNar linked to the denitrification pathway in *P. denitrificans* allowing sequential conversion of nitrate to dinitrogen. Electrons are provided by complex I (colored in gray) ensuring quinone reduction while both nNar and the bc_1 complex catalyze quinol oxidation. The Nir, Nor and Nos enzymes are reduced thanks to various soluble *c*-type cytochromes reduced by the bc_1 complex. B. Respiratory nitrate ammonification involving two Mo-*bis*PGD enzymes, formate dehydrogenase FdnGHI as quinone reductase and nitrate reductase NarGHI as quinol oxidase. The third complex colored in gray is the nitrite reductase NrfABCD (for example in *E. coli*). C. nNar linked to sulfur oxidation involving a periplasmic sulfide:quinone oxidoreductase (colored in gray) attached peripherically to the inner membrane and nNar (for example in *T. denitrificans*). D. nNar linked to arsenite oxidation involving two Mo-*bis*PGD enzymes, a periplasmic facing arsenite oxidase Arx ensuring quinone reduction at a yet undefined site within the membrane anchor subunit and the nNar (for example in *A. ehrlichii*). Owing to the various postulated mechanisms used by neutrophilic anaerobic nitrate-dependent iron-oxidizing bacteria, the reader has to refer to the following reference for their extensive description [310].

coupling of the physiological electron donor, NADH, to both the nitrate and nitrite reductases NasC and NasB, respectively in *P. denitrificans* [154]. NasG, encoded by the *nasG* gene (also named *nirD*, *nasD* or *nasE*), is conserved in several bacterial *nas* gene clusters. Nitrate assimilation is thus linked to the redox status of the NADH pool. In haloarchaea such as *H. volcanii* or *H. mediterranei*, the physiological electron donor to the assimilatory nitrate is proposed to be [2Fe–2S] ferredoxin and not NADH [289].

4.1.2. Nar and denitrification or nitrate respiration

A prominent example of the participation of molybdoenzymes of the Mo/W-*bis*PGD family to the nitrogen cycle can be taken with denitrification, a key process that contributes to the nitrogen cycle on Earth through the biological production of NO, N_2O and N_2 gasses from nitrate under anoxic conditions (Fig. 9A). The ability to use nitrate as a terminal electron acceptor in energy metabolism is found in most prokaryotes, many of them being able to perform the entire denitrification process. For instance, *Enterobacteriaceae* are not able to denitrify nitrate or nitrite to N_2. Instead, reduction of nitrate via nitrite to ammonia occurs during anaerobic growth. In recent years, the denitrification pathway has been implicated in the virulence of several bacterial species, including *Brucella*, *Pseudomonas* or the obligate human pathogens *Neisseria gonorrhoeae* and *Neisseria meningitidis* [293–295]. Conversely this process has only been partially described genetically or biochemically in some *Haloarchaea* species.

The first step of the bacterial denitrification pathway, catalyzed by the cytoplasmically-oriented membrane-bound NarGHI-type nitrate reductase (i.e. nNar), is directly coupled to the generation of a *pmf* to sustain cell growth. The nNar is largely conserved among all nitrate respiring bacteria. The enzyme has been extensively studied in mesophilic nitrate reducing bacteria such as the ammonifier *E. coli* and the denitrifiers *Paracoccus* and *Pseudomonas* species. The *E. coli* NarGHI enzyme has been crystallized and serves as the prototype in our understanding of the structure and function of respiratory nitrate reductases in other bacteria [114,115]. The overall topology of the NarGHI complex ensures that the free energy in the QH_2/NO_3^- redox couple is conserved as *pmf* via an electrogenic redox half loop mechanism. Considering the nitrate/nitrite redox potential of +420 mV, quinones of low and high-potential can serve as electron donors (see Section 3.4). Accordingly, the reduction of nitrate can be coupled to a wide range of electron donors, including NADH, formate, lactate, glycerol-3-phosphate, hydrogen or succinate yielding electron transfer chains with various H^+/e^- ratio. In *E. coli*, formate is the preferred electron donor to NarGHI thanks to a similar transcriptional pattern. By contrast to NarGHI, the formate dehydrogenase FdnGHI is inversely oriented with the Mo catalytic site in the periplasm [92]. These two membrane-bound enzyme complexes from *E. coli* form together the paradigmatic Fdn-Nar full redox loop [296] (Fig. 9B). Both enzymes contribute to the *pmf* and cycle quinone/quinol between them with an overall coupling stoichiometry of $4H^+/2e^-$ and a $\Delta E_0'$ approaching 0.8 V. In the denitrifier *Pseudomonas* species containing only UQ, NADH or formate can also serve as electron donor to nNar through either one of the three different NADH:quinone oxidoreductases or the typical FdnGHI, respectively [297]. In the chemolithoautotrophic facultative anaerobe proteobacterium *Thiobacillus denitrificans*, it has long been reported that sulfur oxidation to elemental sulfur can be performed using nitrate as terminal electron acceptor [298]. In addition to aerobic metabolism capability, *T. denitrificans* can perform the whole denitrification pathway but also sulfur-compound oxidation coupled with energy conservation. The recent availability of the complete genome sequence together with transcriptional analyses revealed that genes encoding the nNar complex are part of a transcriptional regulon up-regulated under denitrifying conditions which also includes genes encoding sulfide:quinone oxidoreductases (Sqr) [299,300]. Under anaerobic conditions, sulfur-compounds oxidation ensured by Sqr on the P side of the membrane may be electrogenically linked to the nNar, catalyzing the first denitrification step (Fig. 9C). More recently, anaerobic nitrate-dependent U(IV) oxidation, a novel and potentially counteracting metabolic process involving nNar has been described in *T. denitrificans*. Considering the redox potential of the UO_3/UO_2(s) couple of +410 mV or +260 mV for crystalline or amorphous UO_2, respectively [301] (Table 2), strong thermodynamic constraints are imposed for nitrate-dependent UO_2 oxidation. Such a situation would require participation of the whole denitrification process involving reactions with much higher E_0' than with nNar only. Beller et al. reported that two putatively membrane-associated *c*-type cytochromes play a major role in this metabolic process in *T. denitrificans* [302]. Such observation satisfies the condition that electron carriers with sufficiently high redox potentials are required to accept electrons from UO_2. However, the exact delineation of the electron transfer chain coupling UO_2 oxidation with nitrate reduction remains enigmatic. In *T. denitrificans*, nNar can also participate to anaerobic oxidation of a number of electron donors with high redox potentials such as Fe(II) [303] or pyrite (FeS_2) with dinitrogen being the final end product [304]. Another example of how nNar can be electronically linked with various electron donors in bacteria can be taken with the facultative chemoautotrophic γ-proteobacterium *Alkalilimnicola ehrlichii* which couples arsenite oxidation to nitrate reduction (Fig. 9D) [305]. Finally, it has long been reported that a phylogenetically diverse group of bacteria sustains anaerobic iron oxidation coupled with nitrate reduction by a nNar enzyme [303,306]. However, iron oxidation only proceeds in presence of an additional electron donor such as acetate. While in acidic environments, iron oxidation is systematically coupled with O_2 as terminal electron acceptor due to the high E_0' of the Fe(II)/Fe(III) couple at low pH as exemplified in the best-studied case *Acidithiobacillus ferrooxidans*, in neutrophilic environments, Fe(II) can be used as electron donor in anoxic environments to a wider range of substrates (O_2, nitrate, chlorate) owing to its lower redox couple (Table 2) [307,308]. Only recently, experimental proof of an energy benefit from this metabolism has been provided in the neutrophilic β-proteobacterium Strain 2002 [306] or in the bacterium *Acidovorax* sp. Strain 2AN [309]. To date, Fe(II) takes place likely outside the cell but the nature of the components connecting iron oxidation to quinol oxidation by nNar remains elusive. Accordingly, several alternative mechanisms have been proposed (refer to [310] for their extensive description) and remain to be experimentally tested.

While the nNar enzyme is associated with anaerobic metabolism, it appears that this enzyme is also present in a number of bacteria considered as obligate aerobes such as *B. subtilis* [311,312] or in the pathogen *Mycobacteria* sp. [313]. In fact, anaerobic nitrate reduction was shown to be coupled to energy generation in *B. subtilis* since cells grow anaerobically in minimal medium using glycerol as a nonfermentable carbon source only if nitrate is present [314]. Genomic analysis of *B. subtilis* strikingly revealed that this organism only possesses a limited set of primary electron-donating dehydrogenases among which several putative non-proton pumping NADH dehydrogenases (Ndh, YumB and YutJ), a glycerol-3-phosphate dehydrogenase (GlpD) and a succinate:quinone oxidoreductase (SdhABC) [315]. If the exact nature of the electron-donating enzyme to the MK pool remains unclear under anaerobic conditions, *B. subtilis* transfers the electrons exclusively to the nNar enzyme. Moreover, the corresponding electron transfer chains will only be energy-coupled at the nitrate reductase level which can explain the low growth yield attained under these conditions. If the significance of nitrate reduction in the physiology of the above-mentioned organisms is partly understood to date, expression of an active nNar complex in *Mycobacteria* is essential in protecting the hypoxic cells from environmental stresses [316] and in contributing to their virulence under hypoxic conditions by allowing cell proliferation [317,318]. Under hypoxic conditions, mild acidic conditions promote the dissipation of the *pmf*, rapid ATP depletion and cell death. It was shown that the presence of nitrate was associated

with ATP synthesis, maintenance of a membrane potential and thus was sufficient to restore cell survival under hypoxic acidic conditions [316]. On the other hand, produced nitrite is actively secreted to avoid toxicity.

Several archaeal denitrifiers possess a Nar complex which shows two main differences as compared to the cytoplasmic version found in most bacteria: a periplasmic location thanks to the presence of an intact Tat signal sequence in NarG (i.e. pNar) and the presence of a monohemic cytb^{III} subunit named Orf7. Such situation has been reported in several *Haloarchaea* such as *H. mediterranei*, *Haloferax denitrificans*, *H. volcanii* or *Haloarcula marismortui* [319–322]. As mentioned before, presence of two putative transmembrane helices at both N and C termini of the monohemic cytb^{III} subunit may serve as membrane anchor of the NarGH complex. At present, it is not known how electrons move from the Q-pool to pNar and whether energy conservation is ensured during nitrate reduction in archaea due to its periplasmic location. Analysis of the genes of the *pnar* cluster has allowed many authors to speculate on the overall structural organization of this enzyme [166,321,323]. Proteins encoded within the same operon as *narGH* genes include a transmembrane diheme cytochrome *b* (NarC) sharing similarities with the cytochrome *b* of cytochrome bc_1 complexes [323], a Rieske-type FeS subunit (NarB), two other potential membrane proteins and the dedicated chaperone NarJ. Interestingly enough, one may notice the absence within the operon of a gene encoding for a homolog of cytochromes *c* or *f* supporting at least the existence of a Rieske/cyt*b* complex [324]. Accordingly, a supercomplex made up of NarGH and Rieske/cyt*b* complex has been hypothesized which would display quinol:nitrate oxidoreductase activity coupled with an effective generation of *pmf* through an electrogenic Q-cycle-type mechanism [166], instead of the typical redox-loop mechanism. The absence of a *c*-type cytochrome ensuring electron transfer would be compensating by the hydrophilic monoheme cytb^{III} subunit. Apart the *Haloarchaea*, pNar with either Mo or W ion is also encountered in the hyperthermophilic denitrifier and facultative anaerobe crenarchaeon *Pyrobaculum aerophilum* able to perform dissimilatory nitrate reduction using H_2, thiosulfate or organic compounds as substrates [325]. Indeed, NarGH has been copurified with a monoheme cytb^{III} subunit (NarM) from the membrane fraction [191], that corresponds to the above-mentioned Orf7. In fact, pNar from all *Pyrobaculum* species contains a hydrophilic monoheme cytb^{III} [192]. Interestingly, a very different genetic context for the *pnar* cluster is observed in *Pyrobaculum* sp. as compared with *Haloarchaea* with the absence of additional genes encoding a Rieske/cyt*b* complex. However, anaerobically grown cells with nitrate produced two membranous *c*-type cytochromes proposed to be part of nitrite reductase and of a Rieske/cyt*b* complex retrieved elsewhere in the genome [326]. This chain, although with a pNar, would therefore resemble that of a *Paracoccus*-type denitrification chain, with complex I, Rieske/cyt*b* complex, cd_1-nitrite reductase and qNor (Fig. 9A). Recently, transcriptomic analysis of *P. aerophilum* revealed that the pNar enzyme is expressed independent of the terminal acceptor (oxygen, nitrate, arsenate or ferrous iron) [327]. At this stage, energy-coupling ensured by pNar in archaea remains an open question and only scarce information are available concerning how pNar are integrated in the cell metabolism.

Variations of the nNar organization have been observed in the hyperthermophilic bacterium *T. thermophilus* HB8 which encodes an atypical NarCGHI complex (i.e. cNar) and a NADH dehydrogenase (Nrc) by a self-transposable element allowing anaerobic growth with nitrate as terminal electron acceptor [328,329]. Both enzymes are considered to form a supercomplex ensuring electron transfer from NADH to nitrate using MK-8 as electron carrier based on the observed interaction between their respective transmembrane subunits NrcE and NarI [188]. The unique difference with nNar is the participation of a fourth subunit, NarC, a periplasmic di-heme *c*-type cytochrome. Furthermore, integrity of the NarCGHI complex is required for electron transport towards the Nir, the Nor or the Nos reductases in denitrifying *T. thermophilus* strains [330]. Together with the diheme cytochrome *b* NarI, NarC cytochrome *c* component of the cNar enzyme is used as a branching point to deviate electrons towards enzymes of the denitrification pathway. Finally, cNar from the obligatory anaerobic *Geobacter metallireducens* has recently been proposed to be involved in degradation of aromatic compounds [331]. When grown with benzoate, cells showed higher nitrate reductase activity and upregulation at the transcriptional level of the corresponding genes. Similar to the nNar from *T. denitrificans*, *G. metallireducens* was reported to perform anaerobic nitrate-dependent U(IV) oxidation [332]. However, clear understanding of the participation of cNar to both metabolic processes in *G. metallireducens* awaits further studies.

Aside from the nitrate reductase activity displayed by nNar enzymes, several studies have reported the ability of nNar from *E. coli* [128] or *S. typhimurium* [129] to catalyze nitrite reduction, a one-electron step ending to nitric oxide (NO), a highly reactive and toxic gas that can freely diffuse into cells and attack DNA molecules or the redox centers of proteins [333,334]. Recently, it has been reported that endogenous *S*-nitrosylation of proteins is a prominent feature of anaerobic respiration on nitrate in *E. coli*, thanks to the nitrite reductase activity of nNar [335]. While the importance of such activity in bioenergetic terms remains elusive, Rowley et al. reported that up to 20% of catabolized nitrate is converted into NO in *S. typhimurium* [130]. Such NO-producing activity has now to be reconciled with the participation of nNar to the virulence of a number of microbial pathogens or to the reported inflammation-induced nitrate respiration [336–338].

4.1.3. Nap and anaerobic respiration or dissipation of excess reductant

An alternative to the membrane-bound nitrate reductases are the periplasmic ones (also called Nap) found almost exclusively in Proteobacteria and which fulfill different physiological roles depending on the organisms [29,339–341]. As described above, membrane-bound nitrate reductases but also Nap enzymes catalyze the first step of the denitrification process which is regarded as an anoxic or micro-oxic process [342,343]. To date, no strictly aerobic denitrifier has ever been isolated which indicate that organisms have to choose between oxygen and nitrate if both are available. The most often oxygen preference is due to the fact that more energy is gained from oxygen respiration than from nitrate respiration. However, nitrate reduction by Nap enzymes can alternatively be used for other purposes than respiration, i.e. redox homeostasis under oxic conditions. This is typically the case during chemoheterotrophic or photoheterotrophic growth in the presence of highly-reduced carbon substrates [344–349]. The generated excess of reducing equivalents can then be dissipated by Nap enzymes which are directly uncoupled from energy conservation. Indeed, in bioenergetic terms, quinols which serve as electron donors for Nap are oxidized on the periplasmic side of the cytoplasmic membrane by two distinct membrane-bound quinol-oxidizing systems (NapC or NapGH) depending on the organism and the electrons flow towards the periplasm where they ultimately reduce nitrate to nitrite. Thus, as compared to nNar, the free energy of the QH_2/NO_3^- redox couple is not conserved as *pmf*. However, how Nap can contribute to the anaerobic respiration metabolism? Studies performed on *E. coli* cells have clearly shown that Nap can support anaerobic respiratory growth under nitrate-limiting conditions using glycerol as non-fermentable carbon source owing to a higher nitrate affinity as compared to nNar [350,351]. Based on such observation, it has been considered that Nap would be required to scavenge nitrate present in low levels in the micro-oxic environment of some pathogenic bacteria as *Haemophilus influenzae* [340] or *Campylobacter jejuni* [352,353]. Owing to the periplasmic location of the Nap enzyme, the non-utilization of the nitrate uptake system (NarK/NarU) which also functions as nitrate/H^+ symport [354–356] and as such being energetically disadvantageous may provide an explanation. Interestingly, during anaerobic growth by glucose fermentation, *E. coli* Nap fulfils a redox-balancing role rather than an energy-conservation role reinforcing the idea that Nap may serve different functions within the same organism depending on growth conditions [211]. In

ε-proteobacteria, respiratory nitrate reduction sustained by Nap exclusively results in the production of either ammonium (ammonification) or dinitrogen gas (denitrification) (see for review [353]). For instance, the ε-proteobacterium *W. succinogenes* grows by respiratory nitrate ammonification using formate or H_2 as electron donor, energy conservation being made at the electron input level only [357]. To date, there is some controversy whether the food-borne pathogen ε-proteobacterium *C. jejuni* is able to grow anaerobically on nitrate through a Nap enzyme despite the use of formate or H_2 as electron donors [358,359]. If respiratory nitrate ammonification sustained in *C. jejuni* by Nap and Nrf enzymes plays an important role in host invasion and colonization in micro-oxic environments such as the intestinal tract [352,359], the exact role of Nap either in redox-balancing or in anaerobic respiration remains to be defined. Respiratory nitrate ammonification was also demonstrated in *S. oneidensis* MR-1 using Nap instead of nNar in *Enterobacteriaceae* [360]. In this particular case, CymA, an analog of NapC, serves as electron donor to Nap. Noteworthy, CymA is also the electron donor to the soluble and periplasmic cytochrome *c* nitrite reductase Nrf catalyzing the subsequent step in the ammonification process [361]. An atypical situation is encountered in Nap of the δ-proteobacterium *D. desulfuricans* with two main differences: the absence of the NapB subunit and the additional presence of NapM, a soluble and periplasmic tetrahemic *c*-type cytochrome [362]. How electrons flow towards NapA thus remains unclear with several putative routes including quinol-dependent ones involving some of the NapC, G, and H proteins and quinol-independent one involving NapM (Fig. 3).

However, as mentioned above, Nap is also associated with other functions such as dissipating excess reductant, a process that is not systematically linked to anaerobic respiration metabolism [340,341]. A typical example can be taken with the denitrifier *Paracoccus pantotrophus* in which aerobic nitrate reduction by Nap only occurs using butyrate or caproate (highly reduced carbon sources) and not with succinate or malate (more oxidized substrates) [345,348]. Moreover, under anaerobic denitrifying conditions, Nap is not expressed in *P. pantotrophus* [348] thus confining Nap to aerobic growth conditions, a situation also encountered in *C. necator* [363]. Recently, it has been shown that magnetite biomineralization in *Magnetospirillum gryphiswaldense* MSR-1 is closely linked to nitrate reduction catalyzed by Nap [364]. As observed in other organisms, the authors postulate that Nap is involved in redox balancing using nitrate as oxidant to dissipate excess reductant thus facilitating magnetite formation. Finally, Nap enzymes can also function as electron sinks, e.g. during photosynthesis in *R. sphaeroides* [172,365].

4.1.4. Nxr and nitrification or anammox

Nitrification is the microbially catalyzed sequential oxidation of ammonia to nitrate via nitrite as reaction intermediate and constitutes per se a key process in the biogeochemical nitrogen cycle in both aquatic and terrestrial ecosystems. While the first step i.e. ammonia oxidation is performed by both aerobic ammonia-oxidizing bacteria (AOB) or archaea (AOA), the second step of the nitrification process is exclusively sustained by chemolithoautotrophic nitrite-oxidizing bacteria (NOB) which gain energy from the oxidation of nitrite to nitrate [366,367]. Under oxic conditions, nitrite oxidation by NOB is the principal source of nitrate, which constitutes the major fraction of the fixed nitrogen in the oceans but also the predominant inorganic nitrogen form in aerated soils. Nitrite oxidation is catalyzed by a Mo-*bis*PGD enzyme, nitrite oxidoreductase (nNxr), a membrane-bound enzyme found in *Nitrobacter* species which shows high sequence similarity with nNar [368] while showing a similar structural organization to cNar (Section 3.3.3). The enzyme can catalyze in vivo reaction in both directions, nitrate reduction being part of the dissimilatory nitrate reduction pathway using organic compounds as electron donors [369–371]. In this latter case, nNxr are supposed to have quinol oxidizing activity through the membrane anchor subunit nNxrI. Whether quinone reduction is associated with nitrite oxidation remains to be defined. Interestingly enough, the nNxr of *Nitrobacter* and *Nitrococcus* is oriented towards the cytoplasm while genomic analyses revealed that Nxr in *Nitrospira* is phylogenetically distant and oriented on the periplasmic side of the membrane (i.e. pNxr) [165,168]. As such, NOB are phylogenetically diverse (α, γ, β *proteobacteria*, *nitrospirae* or *chloroflexi*) and occur in a wide variety of aquatic and terrestrial environments [165,168,201,202,366,372]. Biochemical studies performed on nNxr from *Nitrobacter winogradskyi* have shown that electrons issued from the strongly endergonic nitrite oxidation reaction by cytoplasmically-oriented Nxr are transferred to a terminal cytochrome *c* oxidase via a cytochrome c_{550} [373]. Genomic analyses of the chloroflexi *Nitrolancetus hollandicus* let some authors to propose a similar electron transport chain [168]. However, physiological and biochemical information are scarce which limits our understanding of how nNxr are connected to the electron transfer chains.

An alternative pathway involving pNxr is the anammox process i.e. anaerobic ammonium oxidation that produces N_2 by reducing nitrite and oxidizing ammonium, a unique bacterial trait performed by autotrophic anoxic ammonia-oxidizing bacteria (AnAOB) (see for review [374]). During this anoxic process, nitrite can also be oxidized to nitrate with the released electrons being used for carbon dioxide reduction by the acetyl-coenzyme A pathway [375,376]. More interestingly, anammox bacteria such as *Kuenenia stuttgartiensis* and *Scalindua* sp. have been shown to perform dissimilatory nitrate reduction using organic electron donors such as formate, propionate or acetate [377,378]. As such, the reduction of nitrate to nitrite and to ammonia serves as a source of substrates for N_2 formation by the anammox process. Such metabolic connection may explain the presence of anammox bacteria in marine environment and their ability to out-compete other organisms in ammonium-limited conditions. Complete genome sequence of *Kuenenia stuttgartiensis* revealed the presence of a single operon encoding NarGH subunits of an Nxr-type [375]. In the exergonic nitrate reduction reaction, electrons are issued from oxidation of organic compounds using MK as electron carrier. However it has to be pointed out that, in the reverse strongly endergonic nitrite oxidation reaction, no biochemical information is available. The presence of a canonical Rieske/cyt*b* complex and of genes encoding cytochromes and clustered with *narGH* in *K. stuttgartiensis* constitute elements of a hitherto uncharacterized electron transport chain which may function in a similar manner to NOB [375,379]. Finally, the anammox pathway is spatially confined to a compartment named anammoxosome bound by a single bilayer membrane [374]. It is thus considered that Nxr in *K. stuttgartiensis* is oriented towards the anammoxosome thus participating in either nitrite oxidation or nitrate reduction [376]. The question of the exact location of the electron donor enzymes such as formate dehydrogenase in the dissimilatory nitrate reduction pathway is thus open.

4.1.5. Trimethylamine N-oxide, a source of organic nitrogen

Me_3NO (TMAO) is an abundant nitrogen storage compound in fish and other marine organisms but detectable levels of TMAO are also present in seawater. It constitutes an alternative substrate for the DMSO reductases (both Dms and Dor, see below) but also the specific substrate of the TMAO reductases TorA [205]. Closely homologous to DorA, TorA studied only in *E. coli* and *Shewanella* species, is a periplasmic soluble enzyme reducing its substrate with electrons delivered by a membrane-bound pentahemic cytochrome [205,380] from MK and DMK [239], or from UQ pool [241], respectively. This system therefore presents a net balance that does not contribute to the proton gradient formation by itself. The *pmf* generated by this chain [381] thus probably comes from an involved NADH dehydrogenase [382].

4.2. Sulfur cycle

Molybdoenzymes of the Mo-*bis*PGD family have long been reported to participate to the sulfur cycle in prokaryotes which can utilize among electron acceptors, sulfur compounds (elemental sulfur, thiosulfate,

tetrathionate and polysulfide). It is worth mentioning that elemental sulfur is probably the most widespread sulfur species in sediments and geochemical deposits. In fact, the ability to reduce sulfur compounds using H_2 or organic substrates as electron donors is widespread among bacteria and archaea, the latter being mostly hyperthermophilic (see for reviews, [383–386]). Such anaerobic chemolithoautotrophic H_2 oxidation with sulfur reduction can be exemplified with the best-characterized ε-proteobacterium *W. succinogenes* and involves a short electron transport chain composed of two periplasmically-facing membrane-bound enzymes, a [NiFe] hydrogenase and a sulfur reductase also named PsrABC [387–389]. More importantly, dissimilatory reduction of elemental sulfur to hydrogen sulfide is linked with energy conservation as evidenced by growth on H_2 and S^0. Formate can also serve as electron donor to sulfur reduction in *W. succinogenes* yielding similar growth rates [390,391]. A similar situation has been reported in the deep-sea ε-proteobacterium *Sulforovum* sp. NBC37-1 with chemolithoautrophic H_2 oxidation with S^0 reduction catalyzed by an enzymatic complex denoted PsrABC [392]. An identical electron transport chain has been reported in the acidophilic crenarchaeon *Acidianus ambivalens* grown under anaerobic conditions where both enzymes copurified strongly suggesting the existence of a supercomplex [393,394]. The observed decrease of the electron transport activity of a chain using formate or H_2 as electron donor and S^0 as electron acceptor in proteoliposomes of *W. succinogenes* as a function of the degree of dilution by adding phospholipids [395] can also be interpreted as the consequence of a loss of supercomplex stability [396]. Physical association of the hydrogenase and the sulfur reductase denoted SreABC may constitute a common trait as such a supercomplex has been purified and characterized in the hyperthermophilic and microaerophilic bacterium *A. aeolicus* [149]. Most interestingly, the sulfur reductase faces the cytoplasmic side of the membrane owing to the absence of a TAT signal peptide either on SreA and SreB giving rise to opposite locations of the catalytic sites within the supercomplex. However, it remains open what is the exact substrate in vivo (despite that tetrathionate is the best substrate in vitro and thiosulfate is not) and whether such electron transport pathway is energy-conservative [149,386]. To date, the overall yield of the H_2:S^0 oxidoreductase pathway is far from being efficient according to the overall topology of the components. Therefore, generation of an electrochemical gradient would require opposite location of the quinone binding site on each membrane-bound complex as observed in the paradigmatic formate:nitrate respiratory chain in *E. coli* [30]. Quinone reduction at the cytoplasmic side of the inner membrane in the hydrogenase unit coupled with a quinol oxidation step at a periplasmically oriented site in the Psr would allow net translocation of protons across the membrane. Indirect measurement of the H^+/e^- ratio using polysulfide as electron acceptor in *W. succinogenes* indicates a value of 0.5 (Fig. 8) [196,383] which is half that obtained using fumarate respiration. In 2008, Jormakka et al. reported the crystal structure of a putative (based on sequence similarity with PsrABC from *W. succinogenes*) Psr from *T. thermophilus* [88]. Owing to the aerobic growth conditions employed to purify the enzyme complex [397] and the absence of report on polysulfide reduction in *T. thermophilus*, the actual activity of the purified enzyme remains to be determined. However, the crystal structure of this putative PsrABC complex revealed the existence of a quinone binding site at the periplasmic side of the membrane anchor PsrC subunit avoiding charge separation during enzymatic reaction (Fig. 7) [88]. Owing to the low basic pH at which the sulfur reduction occurs in the periplasmically-oriented catalytic dimer PsrAB, such topological organization is in accordance with the H^+/e^- ratio of 0.5 without the need to consider a putative proton-translocation machinery as proposed by Jormakka et al. [88].

The facultative anaerobe γ-proteobacterium *S. oneidensis* MR-1 is able to respire anaerobically inorganic sulfur compounds as terminal electron acceptors such as S^0, SO_3^{2-}, $S_2O_3^{2-}$ and $S_4O_6^{2-}$ using lactate or formate as electron donor [398]. A thiosulfate reductase encoded by an operon denoted *psrABC* but highly homologous to the *phsABC* operon of the enteric γ-proteobacterium *S. enterica*, is responsible for anaerobic respiration of S^0 and $S_2O_3^{2-}$ but not $S_4O_6^{2-}$ [399]. However, while the molecular basis of thiosulfate respiration has been long reported and described in *S. enterica* [150], the exact functioning of the Phs complex remains enigmatic considering the very low redox potential of the acceptor couple [$S_2O_3^{2-}/HS^- + SO_3^{2-}$] of −400 mV (Table 2). As expected, only low potential quinones such as MK were shown to be required for thiosulfate reduction in *S. typhimurium* [242]. To reconcile the observed thiosulfate respiratory capacity of a number of bacteria (mostly sulfate-reducing bacteria) and reported structural organization of PhsABC with the highly endergonic reaction, Stoffels et al. recently showed that the reaction requires the *pmf* suggesting the existence of a reverse redox-loop with MKH_2 oxidation at the cytoplasmic side coupled with thiosulfate reduction in the periplasm of *S. enterica* (Fig. 8) [246]. A similar observation was made with the Psr of *W. succinogenes* showing *pmf*-dependent activity with $MMKH_2$ as electron donor [196] supporting a similar functional trait of these sulfur reductases (PsrABC or PhsABC). Finally, growth on S^0 or $S_2O_3^{2-}$ is only permitted with fermentable carbon sources in *S. enterica* [400] with minor contribution to the overall yield of ATP production [150] suggesting a role for sulfur reduction in redox-balancing of the quinone pool as in the case of Nap (see Section 4.1.3). Accordingly, Stoffels et al. reported that formate oxidation with thiosulfate reduction occurs mainly via the fermentative pathway in *S. enterica* and the participation of hydrogenases [246]. While evidence for chemolithoautotrophic H_2 oxidation with sulfur reduction by hyperthermophilic archaea has long been reported [401], evidence for the existence of a thiosulfate/polysulfide reductase in the hyperthermophilic crenarchaeon *Pyrobaculum islandicum* supporting anaerobic respiration of S^0 or $S_2O_3^{2-}$ has only been provided recently [402]. Transcriptional analyses revealed, under the absence of terminal electron acceptor, the up-regulation of an operon encoding a putative thiosulfate reductase in *P. aerophilum* [327], in accordance with the reported growth on thiosulfate [325]. In this context, the availability of complete genome sequences of several hyperthemophilic crenarchaeon will allow in the near future getting a better understanding on their respiratory capabilities and identification of the involved enzymes [403,404].

The third sulfur reductase having respiratory function is the Ttr, another Mo-*bis*PGD enzyme extensively studied in *S. typhimurium* [148]. Here, formate, H_2 or non-fermentable carbon substrates are used as electron donors for tetrathionate reduction into thiosulfate in accordance with the more positive redox potential of the $S_4O_6^{2-}/S_2O_3^{2-}$ couple between +24 and +170 mV [148] (Table 2). If tetrathionate respiration was reported until now in bacteria taking benefit from this abundant substrate in marine or soil sediments [242], anaerobic tetrathionate respiration of *S. typhimurium* was shown to provide a significant growth advantage over bacteria using fermentation [405]. Moreover, tetrathionate was shown to be produced in the lumen during gut inflammation. Interestingly, Ttr, Phs and Psr from *S. enterica* display strong specificities towards the sulfur compound substrates. The Ttr is able to alternatively use $S_3O_6^{2-}$ but not $S_2O_3^{2-}$ whereas the Phs can use S^0 and $S_2O_3^{2-}$ but not $S_4O_6^{2-}$ using either H_2 or formate as electron donors [400].

In addition to the inorganic sulfur compounds described above, several organosulfur compounds are metabolized by members of the Mo/W-*bis*PGD family. The first one dimethylsulfide (Me_2S; DMS) contributes about 50% of the global biogenic sulfur input to the atmosphere from marine environments and it is recognized that biological activities have a major influence on its level in marine systems. DMS is indeed a substrate of the unique Ddh enzyme characterized so far that catalyzes its oxidation allowing *Rhodovulum sulfidophilum* to grow photoautotrophically with DMS as sole electron donor [406]. In this electron transfer chain, the Ddh oxidizes the DMS in the periplasm, consequently reducing a soluble cytochrome c_2, electron donor to the photosynthetic reaction center [158]. This chain is therefore complementary to the classical cyclic photosynthetic electron transfer chain involving the bc_1 complex, liberating protons in the periplasm and therefore contributing to the generation of the *pmf*.

The reaction catalyzed by the Ddh is formally the reverse of the reaction catalyzed by the more widespread dimethyl sulfoxide

(Me_2SO; DMSO) reductases (see [25] for phylogenetic distribution). These enzymes are anaerobic terminal reductases frequently encountered in bacteria. In the case of heterotrimeric DmsABC, typified by the membrane-bound DMSO reductase from *E. coli* [407], the reduction of DMSO is achieved using electrons delivered by DmsC from the MK and DMK pool [239]. In the case of the monomeric soluble DorA DMSO reductase encountered in *R. capsulatus* and *R. sphaeroides*, the electrons reducing the DMSO are delivered by the membrane-bound pentahemic cytochrome DorC [206] from the UQ pool [210] in the absence of light or during photosynthetic growth. In the case of *S. oneidensis* Dor system, the electrons reducing the DMSO are delivered by the multifunctional tetraheme CymA from the MK pool [408]. DMSO reductases were also reported in *Haloarchaea* such as *Halobacterium salinarum* (formerly *Halobacterium* sp. NRC-1 [409]) where a heterotrimeric DmsABC complex is responsible for both anaerobic DMSO and TMAO respiration using organic substrates as electron donors [164,410]. All the DMSO reduction systems display reaction balances that do not contribute to the proton gradient formation by themselves. The *pmf* generated by these chains comes from the involved NADH dehydrogenase [411].

4.3. Carbon cycle

Two types of Mo/W-*bis*PGD enzymes are known to participate to the carbon cycle through oxidoreduction of C_1 compounds. Formate dehydrogenase (Fdh) catalyzes the reversible conversion of formate to CO_2 while the much less studied formylmethanofuran dehydrogenase (Fmd) catalyzes the covalent attachment of CO_2 to methanofuran, both being either Mo or W enzymes.

Formate can either be the end product of much bacterial fermentation such as the mixed-acid fermentation of enterobacteria or the intermediate of energy metabolism of acetogenic bacteria during the reduction of CO_2 to acetic acid. Thanks to the very low redox potential of formate, its oxidation is coupled to the reduction of a number of terminal electron acceptors ranging from sulfur compounds, to nitrate, fumarate, As(V), Fe(III), Mn(IV) or oxygen. In *E. coli*, three formate dehydrogenases are present, two being involved in respiration (FdnGHI and FdoGHI), the third one (FdhF) being a component of the formate hydrogenlyase (FHL) complex involved in anaerobic fermentation. Basically, FdnGHI or its isoenzyme FdoGHI transfers electrons to the quinone pool which ultimately reduces a number of alternative terminal electron acceptors. As an example, the electron transport chain involving the FdnGHI and NarGHI complexes forms the paradigmatic full proton motive redox loop with a H^+/e^- ratio of 2 based on charge separation at both complexes [296] (Figs. 8 and 9B). These periplasmically-oriented formate dehydrogenases may also be involved in the periplasmic nitrate ammonification pathway of enteric bacteria or *W. succinogenes* that couple quinol oxidation to nitrate reduction by Nap producing nitrite further reduced to ammonium [357]. In this case, the electron transport chain relies on *pmf* generation at the level of electron input into the quinone pool by the Fdh enzyme. On the opposite, H_2 issued from formate oxidation by the FHL complex in the cytoplasm is recycled by the periplasmically-oriented hydrogenases 1 and 2 and electrons reintroduced in the quinone pool [412]. A slightly different situation is encountered in respiratory nitrite ammonification, a strictly periplasmic process [29,357]. Formate oxidation by a membrane-bound formate dehydrogenase (FdhABC) is coupled to nitrite reduction by a cytochrome *c* nitrite reductase (NrfAH) in the ε-proteobacterium *W. succinogenes* [357] while in the δ-proteobacteria *D. desulfuricans* and *D. vulgaris*, formate oxidation is catalyzed by a periplasmic and soluble formate dehydrogenase ($FdhABC_3$) [185,186]. Recently, biochemical studies have allowed a better understanding of how electrons issued from formate oxidation by the periplasmic $FdhABC_3$ of *D. desulfuricans* are ultimately transferred to alternative pathways through a cytochrome *c* network [413]. Formate dehydrogenase appears to be able to reduce several periplasmic cytochrome *c* feeding electrons to alternative terminal electron acceptors such as oxygen, nitrate, nitrite or sulfate. How formate oxidation coupled with nitrite reduction can yield an overall H^+/e^- ratio of 1 remains to be explained [414,415]. Similarly, how electrons issued form formate oxidation ended up to Nap in *D. desulfuricans* remains open. As discussed in Section 4.1.1, the soluble and periplasmic tetrahemic *c*-type cytochrome NapM [362] may provide a rationale for transferring electrons without connection with the quinone pool.

Dissimilatory reduction of Fe(III) or Mn(IV) appears to be major respiratory processes in aquatic environments and is found both in bacteria and archaea. Prominent examples of organisms supporting such respiratory pathway using formate as electron donor are the δ-proteobacteria *Geobacter* sp. or the γ-proteobacterium *S. putrefaciens* (see for review, [416,417]). It was reported that Fe(III) or Mn(IV) reduction involves the multiheme *c*-type cytochrome CymA connecting the quinone pool to the final reductases present in the outer membrane [418,419]. Dissimilatory arsenate reduction coupled with formate oxidation, an energy-conserving process, was reported in the firmicutes *Desulfitobacterium* sp. where formate is not only the electron donor but also the sole carbon source [420]. Bioinformatic analyses of the *D. hafniense* Y51 genome revealed the existence of an operon encoding a periplasmically-oriented formate dehydrogenase (FdoGHI) [4]. Despite the uncertainty about how quinols are oxidized at the ArrC membrane anchor subunit of the Arr complex, energy conservation is ensured through formate oxidation coupled with As(V) reduction at both enzymes level.

More interestingly, formate dehydrogenases have recently been involved in energy conservation during methanogenesis, a pathway allowing reduction of CO_2 to methane using H_2 as reductant. A multiprotein complex composed of heterodisulfide reductase, F420-nonreducing hydrogenase, formate dehydrogenase, and formylmethanofuran dehydrogenase was isolated and characterized in the methanogenic euryarchaeon *Methanococcus maripaludis* [421]. Importantly, when H_2 is limiting, formate can now be used as electron donor for methanogenesis, electrons being transferred to the heterodisulfide reductase. Two molybdoenzymes, namely the formate dehydrogenase and the formylmethanofuran dehydrogenase are thus involved. In contrast to Fdh, much less information is available concerning the latter. The enzyme has been purified from a number of methanogens such as *Methanothermobacter marburgensis* or *Methanosarcina barkeri* giving rise to the isolation of a multimeric complex of varying number of subunits (ranging from 3 to 6) with Mo or W and a high number of [Fe–S] clusters [422–427].

4.4. Diverse or "exotic" metabolisms

In this last section are listed Mo/W-*bis*PGD enzymes which participate in so-called "exotic" metabolisms but, in most cases, without contributing by themselves to the *pmf*.

As a first example, *E. coli* BisC, that shares significant homology with the DMSO and TMAO reductases, is a cytoplasmic enzyme which is not involved in a respiratory chain [146]. Rather, BisC is involved in recycling biotin sulfoxide or methionine sulfoxide [428] for use by cells, accepting electrons from NADH [429] and could thus play a role in protecting cells from oxidative damage [430].

On the other hand, several hydrocarbon compounds, among them, acetylene, pyrogallol, resorcinol, ethylbenzene and cholesterol are substrates of Mo/W-*bis*PGD enzymes, entering thereby into the carbon cycle. Acetylene is hydrated to acetaldehyde by Ah as part of a strict anaerobic degradation pathway of unsaturated hydrocarbon [21]. This reaction, actually known only in *P. acetylenicus*, does not involve any electron transfer and is not bioenergetic at all. All the other listed substrates are aromatic hydrocarbons. Aerobic metabolism, via oxygenases, is often in charge of the degradation of such compounds using reactive molecular oxygen as co-substrate. Prokaryotes have

however recruited multiple Mo/W-*bis*PGD enzymes, catalyzing degradation of such compounds under anaerobic conditions. For instance, the δ-proteobacterium *P. acidigallici* ferments pyrogallol producing its isomer phloroglucinol in the cytoplasm using the enzyme Th [431]. This enzyme is known only in the latter species but BLAST searches revealed that Th is probably encoded by the *Clostridium* sp. SY8519 and *Holophaga faetida* DSM 6591 genomes (YP_004707640/YP_004707641 and ZP_09576407/ZP_09576408, respectively). It is proposed that the reaction consists on a hydroxyl group transfer from 1,2,3,5-tetrahydroxybenzene to pyrogallol producing again 1,2,3,5-tetrahydroxybenzene concomitant to phloroglucinol. This reaction is therefore a net non-redox reaction although the pyrogallol molecule is oxidized to 1,2,3,5-tetrahydroxybenzene and 1,2,3,5-tetrahydroxybenzene is reduced to phloroglucinol. This reaction furthermore does not contribute to the energy conservation. The Th is closely related to another Mo/W-*bis*PGD enzyme contributing to energy generation: resorcinol hydroxylase (Rh) [432].

Resorcinol (1,3-dihydroxybenzene) is produced and utilized in large amounts by the timber, adhesives, and oil industries and enters freshwater environments through the release of effluents. Resorcinol is also an intermediate product of several other hydrocarbon compounds. There have been several reports of bacteria able to utilize resorcinol as carbon and energy sources in the presence or absence of oxygen by different biochemical strategies. Anaerobic metabolisms of resorcinol are found in sulfate-reducing bacteria [433], fermenting bacteria [434], and denitrifiers [434–436]. In the nitrate reducing bacterium *Azoarcus anaerobius*, resorcinol is hydroxylated by Rh at position 4 of the aromatic ring to form hydroxyhydroquinone (HHQ). HHQ is subsequently oxidized with nitrate to 2-hydroxy-1,4-benzoquinone (HBQ). Based on thermodynamic considerations, the electrons from resorcinol and HHQ oxidation can enter the denitrification process and may allow energy conservation by proton translocation as observed in *A. anaerobius* [437]. The question remains how all the whole chain is organized. Whereas sequence of Rh (αβ-type enzyme, Table 1) suggests this enzyme to be soluble in cytoplasm, the activity is detected exclusively in cytoplasmic membrane. The first question is thus the membrane-association mode of the enzyme and if the enzyme is connected to the quinol pool. The second question is the connection way to the nitrate reduction proposed in this metabolism. Although only characterized in A. anaerobius, closely homologous enzymes are revealed by BLAST searches in *Sinorhizobium fredii* HH103 (YP_005191078/YP_005191077), *Rhizobium mesoamericanum* STM3625 (ZP_11265595/ZP_11265594) and numerous Burkholderia.

Ethylbenzene, a pollutant resulting from surface spills of gasoline or leaking underground storage tanks, is a third aromatic hydrocarbon compound to be degraded by prokaryotes. The total mineralization of ethylbenzene to CO_2 provides not only carbon source but also energy [438]. Three bacteria are known to date capable to use this substrate, all belonging to the genus Azoarcus. In these species, the Ebdh is responsible of the anaerobic oxidation of ethylbenzene to (S)-1-phenylethanol in the periplasm [439]. Whereas in itself the oxidation of ethylbenzene in periplasm does not generate pmf, its coupling (the way of which remains unknown) to denitrification [438] or O_2 respiration [440] has been shown energetic. No data is available today on the precise chain involved in these metabolisms but periplasmic cytochrome c has been proposed as natural electron acceptor [440]. This would suggest that instead of nitrate reductase, it would be NO-genic nitrite reductase which could be directly connected to ethylbenzene oxidation under denitrification.

Finally, a last Mo/W-*bis*PGD enzyme, closely related to the Ebdh, has been recently revealed to catalyze one of the initial steps of anaerobic metabolism of cholesterol in the proteobacterial Sterolibacterium denitrificans [167]. The ability of prokaryotes to grow aerobically on cholesterol was well documented, but the steroid C25 dehydrogenase (C25dh) is the first enzyme shown to contribute to a prokaryotic anaerobic growth on cholesterol. In this cholesterol degradation pathway, the membrane-associated C25dh is responsible for the hydroxylation of the tertiary C25 atom of the side chain of cholesta-1,4-dien-3-one at the membrane bilayer surface. C25dh is capable to perform the same reaction in presence of oxygen or nitrate. Commercial cytochrome c has been shown to be able to receive electrons from C25dh [167], the connection with terminal O_2 reductases is therefore straightforward rationalizing an eventual energy production under oxic conditions. As described above for Ebdh, the direct link between cholesterol degradation and denitrification is probably the NO-genic nitrite reductase again via cytochrome c.

Beside compounds containing nitrogen, sulfur or and/or carbon, metabolized also by eukaryotes, numerous compounds considered as toxic for the latter are source of energy for prokaryotes. There are at least eight Mo/W-*bis*PGD enzymes known today to be involved in toxic metabolisms such as arsenics, selenium or oxochlorates.

The use of oxochlorates, i.e. chlorate and perchlorate, as respiratory substrates by prokaryotes has been revealed already in 1925 but these reactions have been resolved in molecular level only recently (see [194] for recent review). Chlorate is well known as toxic for plants being thus used as herbicide and defoliant whereas perchlorate, widely used as oxidizer in solid rocket propellant, is well known as a public health's hazard. In prokaryotes, the two Mo/W-*bis*PGD enzymes responsible for their metabolism are Clr and Pcr, only identified in few organisms [194]. Whereas Pcr is able to reduce both chlorate and perchlorate, Clr is only able to reduce chlorate. Neither of them contributes to the *pmf* formation by themselves. Studies on *Ideonella dechloratans* showed, however, that the Clr is connected to the membranous quinol pool via a soluble cytochrome and a cytochrome bc_1 complex. The soluble cytochrome has been moreover shown to be able to serve as electron donor to a cbb_3 terminal oxidase [441]. Whereas Clr consumes proton in the periplasm, both bc_1 complex and cbb_3 activities contribute to the proton gradient formation, rending this chain globally bioenergetic. Similarly, it has been proposed that in *Dechloromonas* species, whereas the Pcr consumes protons in the periplasm, a connected multihemic cytochrome (NrfH/NapC-type), by its quinol dehydrogenase activity, contributes to the *pmf* formation. The involvement of a cbb_3 oxidase, connected to the Pcr by the PcrC would moreover enhance the energetic efficiency of the chain [194].

Whereas selenium is an essential element used for the synthesis of selenocysteine contained in selenoproteins, high concentration of selenium oxyanions can have detrimental effects on wildlife [442]. Selenium oxyanions have however been shown to be a bioenergetic substrate for numerous bacteria. Several systems have been identified as selenate reductases. The first system, characterized in *E. coli* [443] is the YgfKMN one, where YgfN is a molybdoprotein proposed to belong to the xanthine oxidase family and therefore not from the Mo/W-*bis*PGD family. The second one, characterized in Enterobacter cloacae strain SLD1a-1 [444], is a membrane-bound periplasmic heterotrimeric enzyme allowing the latter strain to reduce selenate aerobically. Protein sequences remain unknown, but biochemical characterization suggests the selenate reductase from E. cloacae to be a Mo-enzyme with a monohemic membrane-bound cyt*b* as γ subunit. It is presently not known if this enzyme is a Mo/W-*bis*PGD enzyme. A *YgfKMN* cluster has however been revealed (YP_003942324-7) in the E. cloacae strain SCF1 and it is not presently known if these two enzymes represent a single and same entity. Whatever the nature of this enzyme, it cannot support anaerobic growth on non-fermentable carbon substrates and seems to have a role only in selenate detoxification [444]. The third one, Ser, characterized in *Thauera selenatis*, is a soluble, periplasmic heterotrimeric Mo/W-*bis*PGD enzyme, harboring a cytb^{III} as γ subunit [193]. This system allows *T. selenatis* to reduce selenate in an anaerobic respiration. Connected to the quinol pool by a soluble c_4 cytochrome and a cytochrome bc_1 complex, the Ser contributes to the generation of the *pmf* using selenate as the sole terminal electron acceptor. The fourth system, Srd, characterized in Bacillus selenatarsenatis [177], is a membrane-bound heterotrimeric Mo/W-*bis*PGD enzyme facing the periplasm. Whereas Ser belongs to the Asp-group of the family, Srd, highly homologous to Ttr from

S. enterica belongs to the Cys-group of the family. Whereas no study has been performed today, the localization of the Srd and the thermodynamics of the MK:selenate oxidoreductase activity allows a possible role of the enzyme in the *pmf* generation if the quinol oxidation site is at the periplasmic side.

Although at low concentrations, arsenic commonly occurs naturally as local geological constituent and has been adopted as bioenergetic substrate by numerous prokaryotes. To the contrary to the preceding metabolisms, the arsenic bioenergetic metabolisms appear to be anything but exotic considering the recent burst in discovered arsenite oxidizing and arsenate respiring microbes (see [182] for recent review). Prokaryotes have been demonstrated to use both As(V) as electron acceptor for respiration, via Arr, or As(III) as electron donor, via Aio or Arx, for energy conservation. Arr funnels reducing equivalents from organic matter (pyruvate, lactate, succinate…) to the terminal acceptor As(V) in an anaerobic respiration involving directly the quinol pool. This metabolism has been discovered as early as 1994 [445] but only ten years later were the genes responsible for this metabolism sequenced [178]. In these respiratory chains, Arr, a membrane-bound heterotrimeric enzyme facing the periplasm, consumes protons in the periplasm when reducing arsenate. Only the quinol dehydrogenase activity of Arr and the proton translocation activity of Complex I make the balance of proton positive.

Most of the characterized As(III) oxidizers are proteobacterial mesophilic aerobes. In these cases, Aio transfers electrons arising from the oxidation of As(III) towards a periplasmic soluble cytochrome ultimately reducing O_2 [176]. There are furthermore several bacterial strains containing *aio* genes which oxidize As(III) under anaerobic conditions. A link between Aio activity and chlorate reduction has also been established in *Dechloromonas* and *Azospira* strains [446]. Although not established it is conceivable that in such a chain, the soluble cytochrome, reduced by Aio, reduces the Clr. Secondly, genomic surveys revealed three photosynthetic bacteria, among them two strict anaerobic photosynthetic *Chlorobium* species, containing *aio* genes. This finding suggests a link between Aio and photosynthesis [147]. The reduction in the periplasm of the photosynthetic reaction center by the electron carrier, reduced itself by Aio, would be *pmf* generating. The single bioenergetic anaerobic photosynthetic oxidation of As(III) established today involves Arx in *Ectothiorhodospiraceae* [447]. Nothing is presently known on the latter enzyme's functioning but biochemical and genomic characterization of Arx [182,448] revealed that this enzyme is very close to Arr. The reversion of Arr's directionality would suggest that Arx transfers electrons arising from the oxidation of As(III) towards the quinone pool. In a similar manner as sulfur compounds, arsenite, from its oxidation, would allow the formation of reductant, NADH, by a reverse electron flow, concomitant to the cyclic electron transfer managed by cytochrome bc_1 and photosynthetic reaction center [182,447] generating *pmf*. A link between arsenite oxidation and denitrification has been moreover established. For example, two proteobacteria are known to use Aio to oxidize As(III) coupled to nitrate (NO_3^-) reduction [449,450]. The fact that Aio reduces periplasmic soluble electron carriers makes the link with nitrate reduction not straightforward and further studies are needed to understand such a chain. To the contrary, a chain involving Arx and Nar allowing *Alkalilimnicola ehrlichii* [305] to produce nitrate from the oxidation of As(III) is easy to imagine (Fig. 9D). The two enzymes would form a redox loop similar to the well known constituted by Fdh and Nar in *E. coli* [182]. Finally, it has been suggested that Arx functioning could be linked to selenate reduction [451] but such a chain remains unknown.

5. Concluding remarks

As presented in Section 4 of the present review, the metabolic diversity of Mo/W-*bis*PGD enzyme-dependent bioenergetic chains in prokaryotes revealed by studies of the last two decades seems to have no limits. As exemplified by the case of ethylbenzene, a pollutant from recent petroleum industry, the time taken by microorganisms to adapt to new substrates is very short. In the vast majority of metabolisms, the involvement of a Mo/W-*bis*PGD enzyme is established revealing this structural motif as the workhorse of prokaryotic catalysis. As exposed in Section 2, prokaryotes can thus be regarded as extraordinary efficient catalyst engineering laboratories. Nevertheless, the associated catalytic mechanisms are presently only partly understood. Notably, it is clear that it is not possible to reveal a unique principle that triggers the reactivity of Mo/W-*bis*PGD enzymes. By the same token, the question of the link between the Mo/W ligand and the reaction specificity is still open. Examination of the wealth of structural, spectroscopic, kinetics and computational data emphasizes the extraordinary high catalytic plasticity of these enzymes that is responsible for their evolutionary success and spreading in prokaryotes. A number of research directions have been proposed in the actual review and will not be listed herein.

Bacteria and Archaea are using all compounds available on earth, even the more toxic of them, e.g. arsenic, for energetic purposes, and have for this aim recruited Mo/W-*bis*PGD enzymes. However, as detailed in Sections 3.4 and 4, the special organization and even the composition of the whole chains giving rise to energy are often still putative. As discussed in Section 3, in the vast majority of cases, the thermodynamics of the overall enzyme reaction appears to only be driven by the redox potential of the physiological substrates. The general rule of energy generation has been announced as early as 1966 by Peter Mitchell under the "chemiosmotic theory": coupling of local chemical reactions through a delocalized, cumulative physicochemical entity, the *pmf* [452]. The molecular details of this theory are however often still unknown and, one of the central question remains the elucidation of quinols/quinones oxido-reduction mechanisms.

In conclusion, despite the progress made, the current knowledge on catalysis of Mo/W-*bis*PGD enzymes and their implications in the bioenergetics in prokaryotes is still very limited, providing ample opportunities for future research.

Acknowledgements

We thank Wolfgang Nitschke, Bénédicte Burlat and Frédéric Biaso for helpful discussions. We acknowledge all colleagues who have contributed to this work directly or through stimulating discussions. We thank the Centre National de la Recherche Scientifique (CNRS), the Agence Nationale de la Recherche (ANR) and the Aix-Marseille University for their financial support.

References

[1] J. Frausto da Silva, R. Williams, The Biological Chemistry of the Elements: The Inorganic Chemistry of Life, Oxford Univ Press, Oxford, UK, 2001.
[2] Y. Zhang, V.N. Gladyshev, Molybdoproteomes and evolution of molybdenum utilization, J. Mol. Biol. 379 (2008) 881–899.
[3] A. Suyama, R. Iwakiri, K. Kai, T. Tokunaga, N. Sera, K. Furukawa, Isolation and characterization of *Desulfitobacterium* sp. strain Y51 capable of efficient dehalogenation of tetrachloroethene and polychloroethanes, Biosci. Biotechnol. Biochem. 65 (2001) 1474–1481.
[4] H. Nonaka, G. Keresztes, Y. Shinoda, Y. Ikenaga, M. Abe, K. Naito, K. Inatomi, K. Furukawa, M. Inui, H. Yukawa, Complete genome sequence of the dehalorespiring bacterium *Desulfitobacterium hafniense* Y51 and comparison with *Dehalococcoides ethenogenes* 195, J. Bacteriol. 188 (2006) 2262–2274.
[5] A. Cvetkovic, A.L. Menon, M.P. Thorgersen, J.W. Scott, F.L. Poole II, F.E. Jenney Jr., W.A. Lancaster, J.L. Praissman, S. Shanmukh, B.J. Vaccaro, S.A. Trauger, E. Kalisiak, J.V. Apon, G. Siuzdak, S.M. Yannone, J.A. Tainer, M.W. Adams, Microbial metalloproteomes are largely uncharacterized, Nature 466 (2010) 779–782.
[6] M.K. Johnson, D.C. Rees, M.W. Adams, Tungstoenzymes, Chem. Rev. 96 (1996) 2817–2840.
[7] A. Kletzin, M.W. Adams, Tungsten in biological systems, FEMS Microbiol. Rev. 18 (1996) 5–63.
[8] E.J. Dridge, C.S. Butler, Thermostable properties of the periplasmic selenate reductase from *Thauera selenatis*, Biochimie 92 (2010) 1268–1273.
[9] A.D. Anbar, Oceans. Elements and evolution, Science 322 (2008) 1481–1483.
[10] O. Einsle, F.A. Tezcan, S.L. Andrade, B. Schmid, M. Yoshida, J.B. Howard, D.C. Rees, Nitrogenase MoFe-protein at 1.16 A resolution: a central ligand in the FeMo-cofactor, Science 297 (2002) 1696–1700.

[11] J. Wilcoxen, B. Zhang, R. Hille, Reaction of the molybdenum- and copper-containing carbon monoxide dehydrogenase from *Oligotropha carboxydovorans* with quinones, Biochemistry 50 (2011) 1910–1916.
[12] R. Hille, The mononuclear molybdenum enzymes, Chem. Rev. 96 (1996) 2757–2816.
[13] G. Schwarz, R.R. Mendel, M.W. Ribbe, Molybdenum cofactors, enzymes and pathways, Nature 460 (2009) 839–847.
[14] Y. Zhang, S. Rump, V.N. Gladyshev, Comparative genomics and evolution of molybdenum utilization, Coord. Chem. Rev. 255 (2011) 1206–1217.
[15] F. Schneider, J. Lowe, R. Huber, H. Schindelin, C. Kisker, J. Knablein, Crystal structure of dimethyl sulfoxide reductase from *Rhodobacter capsulatus* at 1.88 A resolution, J. Mol. Biol. 263 (1996) 53–69.
[16] R.A. Rothery, G.J. Workun, J.H. Weiner, The prokaryotic complex iron–sulfur molybdoenzyme family, Biochim. Biophys. Acta 1778 (2008) 1897–1929.
[17] H. Dobbek, Structural aspects of mononuclear Mo/W enzymes, Coord. Chem. Rev. 255 (2011) 1104–1116.
[18] R.H. Holm, E.I. solomon, A. Majumdar, A. Tenderhold, Comparative molecular chemistry of molybdenum and tungsten and its relation to hydroxylase and oxotransferase enzymes, Coord. Chem. Rev. 255 (2011) 22.
[19] A. Magalon, J.G. Fedor, A. Walburger, J.H. Weiner, Molybdenum enzymes in bacteria and their maturation, Coord. Chem. Rev. 255 (2011) 19.
[20] M.J. Romao, Molybdenum and tungsten enzymes: a crystallographic and mechanistic overview, Dalton Trans. (2009) 4053–4068.
[21] B. Schink, Fermentation of acetylene by an obligate anaerobe, *Pelobacter acetylenicus* sp. nov. Arch. Microbiol. 142 (1985) 295–301.
[22] A. Messerschmidt, H. Niessen, D. Abt, O. Einsle, B. Schink, P.M. Kroneck, Crystal structure of pyrogallol–phloroglucinol transhydroxylase, an Mo enzyme capable of intermolecular hydroxyl transfer between phenols, Proc. Natl. Acad. Sci. U. S. A. 101 (2004) 11571–11576.
[23] F. Baymann, E. Lebrun, M. Brugna, B. Schoepp-Cothenet, M.T. Giudici-Orticoni, W. Nitschke, The redox protein construction kit: pre-last universal common ancestor evolution of energy-conserving enzymes, Philos. Trans. R. Soc. Lond. B Biol. Sci. 358 (2003) 267–274.
[24] B. Schoepp-Cothenet, R. van Lis, A. Atteia, F. Baymann, L. Capowiez, A.L. Ducluzeau, S. Duval, F. Ten Brink, M.J. Russell, W. Nitschke, On the universal core of bioenergetics, Biochim. Biophys. Acta 1827 (2013) 79–93.
[25] B. Schoepp-Cothenet, R. van Lis, P. Philippot, A. Magalon, M.J. Russell, W. Nitschke, The ineluctable requirement for the trans-iron elements molybdenum and/or tungsten in the origin of life, Sci. Rep. 2 (2012) 263.
[26] M.J. Russell, A.J. Hall, The emergence of life from iron monosulphide bubbles at a submarine hydrothermal redox and pH front, J. Geol. Soc. London 154 (1997) 377–402.
[27] B.E. Erickson, G.R. Helz, Molybdenum(VI) speciation in sulfidic waters: stability and lability of thiomolybdates, Geochim. Cosmochim. Acta 64 (2000) 1149–1158.
[28] W. Nitschke, M.J. Russell, Hydrothermal focusing of chemical and chemiosmotic energy, supported by delivery of catalytic Fe, Ni, Mo/W, Co, S and Se, forced life to emerge, J. Mol. Evol. 69 (2009) 481–496.
[29] J. Simon, M.G. Klotz, Diversity and evolution of bioenergetic systems involved in microbial nitrogen compound transformations, Biochim. Biophys. Acta 1827 (2013) 114–135.
[30] J. Simon, R.J. van Spanning, D.J. Richardson, The organisation of proton motive and non-proton motive redox loops in prokaryotic respiratory systems, Biochim. Biophys. Acta 1777 (2008) 1480–1490.
[31] J.A. Dumesic, G.W. Huber, M. Boudart, Handbook of Heterogeneous Catalysis, 2nd ed., 2008, pp. 1–15.
[32] G.A. Somorjai, Y. Li, Introduction to Surface Chemistry and Catalysis, 2nd ed., John Wiley & Sons, Hoboken, NJ, 2010.
[33] M.R. Smith, U.S. Ozkan, Transient isotopic labeling studies under steady-state conditions in partial oxidation of methane to formaldehyde over MoO_3 catalysts, J. Catal. 142 (1993) 226–236.
[34] M. Pourbaix, Atlas of Electrochemical Equilibria in Aqueous Solutions, 2nd ed. National Association of Corrosion Engineers (NACE International), Houston, 1974.
[35] C.A. Trieber, R.A. Rothery, J.H. Weiner, Engineering a novel iron–sulfur cluster into the catalytic subunit of *Escherichia coli* dimethyl-sulfoxide reductase, J. Biol. Chem. 271 (1996) 4620–4626.
[36] L.E. Bevers, P.L. Hagedoorn, W.R. Hagen, The bioinorganic chemistry of tungsten, Coord. Chem. Rev. 253 (2009) 269–290.
[37] M.J. Pushie, G.N. George, Spectroscopic studies of molybdenum and tungsten enzymes, Coord. Chem. Rev. 255 (2011) 1055–1084.
[38] S. Metz, W. Thiel, Theoretical studies on the reactivity of molybdenum enzymes, Coord. Chem. Rev. 255 (2011) 1085–1103.
[39] H. Schindelin, C. Kisker, J. Hilton, K.V. Rajagopalan, D.C. Rees, Crystal structure of DMSO reductase: redox-linked changes in molybdopterin coordination, Science 272 (1996) 1615–1621.
[40] A.S. McAlpine, A.G. McEwan, A.L. Shaw, S. Bailey, Molybdenum active centre of DMSO reductase from *Rhodobacter capsulatus*: crystal structure of the oxidised enzyme at 1.82-A resolution and the ditionite-reduced enzyme at 2.8-A resolution, J. Biol. Inorg. Chem. 2 (1997) 690–701.
[41] M. Czjzek, J.P. Dos Santos, J. Pommier, G. Giordano, V. Mejean, R. Haser, Crystal structure of oxidized trimethylamine N-oxide reductase from *Shewanella massilia* at 2.5 A resolution, J. Mol. Biol. 284 (1998) 435–447.
[42] H.-K. Li, C. Temple, K.V. Rajagopalan, H. Schindelin, The 1.3 A crystal structure of *Rhodobacter sphaeroides* dimethyl sulfoxide reductase reveals two distinct molybdenum coordination environments, J. Am. Chem. Soc. 122 (2000) 7673–7680.
[43] G.N. George, J. Hilton, K.V. Rajagoapalan, X-ray absorption spectroscopy of dimethyl sulfoxide reductase from *Rhodobacter sphaeroides*, J. Am. Chem. Soc. 118 (1996) 1113–1117.
[44] G.N. George, J. Hilton, C. Temple, R.C. Prince, K.V. Rajagoapalan, Structure of the molybdenum site of dimethyl sulfoxide reductase, J. Am. Chem. Soc. 121 (1999) 1256–1266.
[45] S.D. Garton, J. Hilton, H. Oku, B.R. Crouse, K.V. Rajagoapalan, M.K. Johnson, Active site structures and catalytic mechanism of *Rhodobacter sphaeroides* dimethyl sulfoxide reductase as revealed by resonance Raman spectroscopy, J. Am. Chem. Soc. 119 (1997) 12906–12916.
[46] L. Zhang, K.J. Nelson, K.V. Rajagopalan, G.N. George, Structure of the molybdenum site of *Escherichia coli* trimethylamine N-oxide reductase, Inorg. Chem. 47 (2008) 1074–1078.
[47] V. Fourmond, B. Burlat, S. Dementin, P. Arnoux, M. Sabaty, S. Boiry, B. Guigliarelli, P. Bertrand, D. Pignol, C. Leger, Major Mo(V) EPR signature of *Rhodobacter sphaeroides* periplasmic nitrate reductase arising from a dead-end species that activates upon reduction. Relation to other molybdoenzymes from the DMSO reductase family, J. Phys. Chem. B 112 (2008) 15478–15486.
[48] R.C. Bray, B. Adams, A.T. Smith, B. Bennett, S. Bailey, Reversible dissociation of thiolate ligands from molybdenum in an enzyme of the dimethyl sulfoxide reductase family, Biochemistry 39 (2000) 11258–11269.
[49] A.S. McAlpine, A.G. McEwan, S. Bailey, The high resolution crystal structure of DMSO reductase in complex with DMSO, J. Mol. Biol. 275 (1998) 613–623.
[50] C.E. Webster, M.B. Hall, The theoretical transition state structure of a model complex bears a striking resemblance to the active site structure of DMSO reductase, J. Am. Chem. Soc. 123 (2001) 5820–5821.
[51] A. Thapper, R.J. Deeth, E. Nordlander, A density functional study of oxygen atom transfer reactions between biological oxygen atom donors and molybdenum(IV) bis(dithiolene) complexes, Inorg. Chem. 41 (2002) 6695–6702.
[52] J.P. McNamara, J.A. Joule, I.H. Hillier, C.D. Garner, Promotion of oxygen atom transfer in Mo and W enzymes by bicyclic forms of the pterin cofactor, Chem. Commun. (Camb.) (2005) 177–179.
[53] N. Cobb, T. Conrads, R. Hille, Mechanistic studies of *Rhodobacter sphaeroides* Me_2SO reductase, J. Biol. Chem. 280 (2005) 11007–11017.
[54] N.R. Bastian, C.J. Kay, M.J. Barber, K.V. Rajagopalan, Spectroscopic studies of the molybdenum-containing dimethyl sulfoxide reductase from *Rhodobacter sphaeroides f.* sp. *denitrificans*, J. Biol. Chem. 266 (1991) 45–51.
[55] B. Bennett, N. Benson, A.G. McEwan, R.C. Bray, Multiple states of the molybdenum centre of dimethylsulphoxide reductase from *Rhodobacter capsulatus* revealed by EPR spectroscopy, Eur. J. Biochem. 225 (1994) 321–331.
[56] A.M. Raitsimring, A.V. Astashkin, C. Feng, J.H. Enemark, K.J. Nelson, K.V. Rajagopalan, Pulsed EPR studies of the exchangeable proton at the molybdenum center of dimethyl sulfoxide reductase, J. Biol. Inorg. Chem. 8 (2003) 95–104.
[57] P. Bertrand, B. Guigliarelli, J.P. Gayda, P. Beardwood, J.F. Gibson, A ligand-field model to describe a new class of 2Fe–2S clusters in proteins and their synthetic analogues, Biochim. Biophys. Acta 831 (1985) 261–266.
[58] F. Biaso, B. Burlat, B. Guigliarelli, DFT investigation of the molybdenum cofactor in periplasmic nitrate reductases: structure of the Mo(V) EPR-active species, Inorg. Chem. 51 (2012) 3409–3419.
[59] R.P. Mtei, G. Lyashenko, B. Stein, N. Rubie, R. Hille, M.L. Kirk, Spectroscopic and electronic structure studies of a dimethyl sulfoxide reductase catalytic intermediate: implications for electron- and atom-transfer reactivity, J. Am. Chem. Soc. 133 (2011) 9762–9774.
[60] J.L. Simala-Grant, J.H. Weiner, Modulation of the substrate specificity of *Escherichia coli* dimethylsulfoxide reductase, Eur. J. Biochem. 251 (1998) 510–515.
[61] J.P. Ridge, K.F. Aguey-Zinsou, P.V. Bernhardt, G.R. Hanson, A.G. McEwan, The critical role of tryptophan-116 in the catalytic cycle of dimethylsulfoxide reductase from *Rhodobacter capsulatus*, FEBS Lett. 563 (2004) 197–202.
[62] N. Cobb, C. Hemann, G.A. Polsinelli, J.P. Ridge, A.G. McEwan, R. Hille, Spectroscopic and kinetic studies of Y114F and W116F mutants of Me_2SO reductase from *Rhodobacter capsulatus*, J. Biol. Chem. 282 (2007) 35519–35529.
[63] V.V. Pollock, R.C. Conover, M.K. Johnson, M.J. Barber, Biotin sulfoxide reductase: tryptophan 90 is required for efficient substrate utilization, Arch. Biochem. Biophys. 409 (2003) 315–326.
[64] K.E. Johnson, K.V. Rajagopalan, An active site tyrosine influences the ability of the dimethyl sulfoxide reductase family of molybdopterin enzymes to reduce S-oxides, J. Biol. Chem. 276 (2001) 13178–13185.
[65] J. Buc, C.L. Santini, R. Giordani, M. Czjzek, L.F. Wu, G. Giordano, Enzymatic and physiological properties of the tungsten-substituted molybdenum TMAO reductase from *Escherichia coli*, Mol. Microbiol. 32 (1999) 159–168.
[66] J.P. Ridge, K.F. Aguey-Zinsou, P.V. Bernhardt, I.M. Brereton, G.R. Hanson, A.G. McEwan, Site-directed mutagenesis of dimethyl sulfoxide reductase from *Rhodobacter capsulatus*: characterization of a Y114→F mutant, Biochemistry 41 (2002) 15762–15769.
[67] J.M. Dias, M.E. Than, A. Humm, R. Huber, G.P. Bourenkov, H.D. Bartunik, S. Bursakov, J. Calvete, J. Caldeira, C. Carneiro, J.J. Moura, I. Moura, M.J. Romao, Crystal structure of the first dissimilatory nitrate reductase at 1.9 A solved by MAD methods, Struct. Fold. Des. 7 (1999) 65–79.
[68] P. Arnoux, M. Sabaty, J. Alric, B. Frangioni, B. Guigliarelli, J.M. Adriano, D. Pignol, Structural and redox plasticity in the heterodimeric periplasmic nitrate reductase, Nat. Struct. Biol. 10 (2003) 928–934.
[69] B.J. Jepson, S. Mohan, T.A. Clarke, A.J. Gates, J.A. Cole, C.S. Butler, J.N. Butt, A.M. Hemmings, D.J. Richardson, Spectropotentiometric and structural analysis of the periplasmic nitrate reductase from *Escherichia coli*, J. Biol. Chem. 282 (2007) 6425–6437.
[70] S. Najmudin, P.J. Gonzalez, J. Trincao, C. Coelho, A. Mukhopadhyay, N.M. Cerqueira, C.C. Romao, I. Moura, J.J. Moura, C.D. Brondino, M.J. Romao, Periplasmic nitrate reductase revisited: a sulfur atom completes the sixth coordination of the catalytic molybdenum, J. Biol. Inorg. Chem. 13 (2008) 737–753.

[71] C. Coelho, P.J. Gonzalez, J.G. Moura, I. Moura, J. Trincao, M. Joao Romao, The crystal structure of *Cupriavidus necator* nitrate reductase in oxidized and partially reduced states, J. Mol. Biol. 408 (2011) 932–948.

[72] M. Leopoldini, N. Russo, M. Toscano, M. Dulak, T.A. Wesolowski, Mechanism of nitrate reduction by *Desulfovibrio desulfuricans* nitrate reductase—a theoretical investigation, Chemistry 12 (2006) 2532–2541.

[73] M. Hoffmann, Density functional theory studies of model complexes for molybdenum-dependent nitrate reductase active sites, J. Biol. Inorg. Chem. 12 (2007) 989–1001.

[74] P.J. Gonzalez, M.G. Rivas, C.D. Brondino, S.A. Bursakov, I. Moura, J.J. Moura, EPR and redox properties of periplasmic nitrate reductase from *Desulfovibrio desulfuricans* ATCC 27774, J. Biol. Inorg. Chem. 11 (2006) 609–616.

[75] C.S. Butler, J.M. Charnock, B. Bennett, H.J. Sears, A.J. Reilly, S.J. Ferguson, C.D. Garner, D.J. Lowe, A.J. Thomson, B.C. Berks, D.J. Richardson, Models for molybdenum coordination during the catalytic cycle of periplasmic nitrate reductase from *Paracoccus denitrificans* derived from EPR and EXAFS spectroscopy, Biochemistry 38 (1999) 9000–9012.

[76] C.S. Butler, S.A. Fairhurst, S.J. Ferguson, A.J. Thomson, B.C. Berks, D.J. Richardson, D.J. Lowe, Mo(V) co-ordination in the periplasmic nitrate reductase from *Paracoccus pantotrophus* probed by electron nuclear double resonance (ENDOR) spectroscopy, Biochem. J. 363 (2002) 817–823.

[77] C. Leger, S.J. Elliott, K.R. Hoke, L.J. Jeuken, A.K. Jones, F.A. Armstrong, Enzyme electrokinetics: using protein film voltammetry to investigate redox enzymes and their mechanisms, Biochemistry 42 (2003) 8653–8662.

[78] L.J. Anderson, D.J. Richardson, J.N. Butt, Catalytic protein film voltammetry from a respiratory nitrate reductase provides evidence for complex electrochemical modulation of enzyme activity, Biochemistry 40 (2001) 11294–11307.

[79] B. Frangioni, P. Arnoux, M. Sabaty, D. Pignol, P. Bertrand, B. Guigliarelli, C. Leger, In *Rhodobacter sphaeroides* respiratory nitrate reductase, the kinetics of substrate binding favors intramolecular electron transfer, J. Am. Chem. Soc. 126 (2004) 1328–1329.

[80] P. Bertrand, B. Frangioni, S. Dementin, M. Sabaty, P. Arnoux, B. Guigliarelli, D. Pignol, C. Leger, Effects of slow substrate binding and release in redox enzymes: theory and application to periplasmic nitrate reductase, J. Phys. Chem. B 111 (2007) 10300–10311.

[81] N.M. Cerqueira, P.J. Gonzalez, C.D. Brondino, M.J. Romao, C.C. Romao, I. Moura, J.J. Moura, The effect of the sixth sulfur ligand in the catalytic mechanism of periplasmic nitrate reductase, J. Comput. Chem. 30 (2009) 2466–2484.

[82] M. Hofmann, Density functional theory study of model complexes for the revised nitrate reductase active site in *Desulfovibrio desulfuricans* NapA, J. Biol. Inorg. Chem. 14 (2009) 1023–1035.

[83] H. Xie, Z. Cao, Enzymatic reduction of nitrate to nitrite: insight from density functional calculations, Organometallics 29 (2010) 436–441.

[84] S. Dementin, P. Arnoux, B. Frangioni, S. Grosse, C. Leger, B. Burlat, B. Guigliarelli, M. Sabaty, D. Pignol, Access to the active site of periplasmic nitrate reductase: insights from site-directed mutagenesis and zinc inhibition studies, Biochemistry 46 (2007) 9713–9721.

[85] V. Fourmond, B. Burlat, S. Dementin, M. Sabaty, P. Arnoux, E. Etienne, B. Guigliarelli, P. Bertrand, D. Pignol, C. Leger, Dependence of catalytic activity on driving force in solution assays and protein film voltammetry: insights from the comparison of nitrate reductase mutants, Biochemistry 49 (2010) 2424–2432.

[86] T. Hettmann, R.A. Siddiqui, C. Frey, T. Santos-Silva, M.J. Romao, S. Diekmann, Mutagenesis study on amino acids around the molybdenum centre of the periplasmic nitrate reductase from *Ralstonia eutropha*, Biochem. Biophys. Res. Commun. 320 (2004) 1211–1219.

[87] B.J. Jepson, L.J. Anderson, L.M. Rubio, C.J. Taylor, C.S. Butler, E. Flores, A. Herrero, J.N. Butt, D.J. Richardson, Tuning a nitrate reductase for function. The first spectropotentiometric characterization of a bacterial assimilatory nitrate reductase reveals novel redox properties, J. Biol. Chem. 279 (2004) 32212–32218.

[88] M. Jormakka, K. Yokoyama, T. Yano, M. Tamakoshi, S. Akimoto, T. Shimamura, P. Curmi, S. Iwata, Molecular mechanism of energy conservation in polysulfide respiration, Nat. Struct. Mol. Biol. 15 (2008) 730–737.

[89] T. Prisner, S. Lyubenova, Y. Atabay, F. MacMillan, A. Kroger, O. Klimmek, Multifrequency cw-EPR investigation of the catalytic molybdenum cofactor of polysulfide reductase from *Wolinella succinogenes*, J. Biol. Inorg. Chem. 8 (2003) 419–426.

[90] S. Lyubenova, T. Maly, K. Zwicker, U. Brandt, B. Ludwig, T. Prisner, Multifrequency pulsed electron paramagnetic resonance on metalloproteins, Acc. Chem. Res. 43 (2010) 181–189.

[91] J.C. Boyington, V.N. Gladyshev, S.V. Khangulov, T.C. Stadtman, P.D. Sun, Crystal structure of formate dehydrogenase H: catalysis involving Mo, molybdopterin, selenocysteine, and an Fe_4S_4 cluster, Science 275 (1997) 1305–1308.

[92] M. Jormakka, S. Tornroth, B. Byrne, S. Iwata, Molecular basis of proton motive force generation: structure of formate dehydrogenase-N, Science 295 (2002) 1863–1868.

[93] H. Raaijmakers, S. Macieira, J.M. Dias, S. Teixeira, S. Bursakov, R. Huber, J.J. Moura, I. Moura, M.J. Romao, Gene sequence and the 1.8 A crystal structure of the tungsten-containing formate dehydrogenase from *Desulfovibrio gigas*, Structure 10 (2002) 1261–1272.

[94] H.C. Raaijmakers, M.J. Romao, Formate-reduced *E. coli* formate dehydrogenase H: the reinterpretation of the crystal structure suggests a new reaction mechanism, J. Biol. Inorg. Chem. 11 (2006) 849–854.

[95] G.N. George, C.M. Colangelo, J. Dong, R.A. Scott, S.V. Khangulov, V.N. Gladyshev, T.C. Stadtman, X-ray absorption spectroscopy of the molybdenum site of *Escherichia coli* formate dehydrogenase, J. Am. Chem. Soc. 120 (1998) 1267–1273.

[96] R. Thome, A. Gust, R. Toci, R. Mendel, F. Bittner, A. Magalon, A. Walburger, A sulfurtransferase is essential for activity of formate dehydrogenases in *Escherichia coli*, J. Biol. Chem. 287 (2012) 4671–4678.

[97] S.V. Khangulov, V.N. Gladyshev, G.C. Dismukes, T.C. Stadtman, Selenium-containing formate dehydrogenase H from *Escherichia coli*: a molybdopterin enzyme that catalyzes formate oxidation without oxygen transfer, Biochemistry 37 (1998) 3518–3528.

[98] M.G. Rivas, P.J. Gonzalez, C.D. Brondino, J.J. Moura, I. Moura, EPR characterization of the molybdenum(V) forms of formate dehydrogenase from *Desulfovibrio desulfuricans* ATCC 27774 upon formate reduction, J. Inorg. Biochem. 101 (2007) 1617–1622.

[99] L. De Gioia, P. Fantucci, B. Guigliarelli, P. Bertrand, Ab initio investigation of the structural and electronic differences between active-site models of [NiFe] and [NiFeSe] hydrogenases, Int. J. Quantum Chem. 73 (1999) 187–195.

[100] M.J. Axley, A. Bock, T.C. Stadtman, Catalytic properties of an *Escherichia coli* formate dehydrogenase mutant in which sulfur replaces selenium, Proc. Natl. Acad. Sci. U. S. A. 88 (1991) 8450–8454.

[101] M. Leopoldini, S.G. Chiodo, M. Toscano, N. Russo, Reaction mechanism of molybdoenzyme formate dehydrogenase, Chemistry 14 (2008) 8674–8681.

[102] C.S. Mota, M.G. Rivas, C.D. Brondino, I. Moura, J.J. Moura, P.J. Gonzalez, N.M. Cerqueira, The mechanism of formate oxidation by metal-dependent formate dehydrogenases, J. Biol. Inorg. Chem. 16 (2011) 1255–1268.

[103] M. Tiberti, E. Papaleo, N. Russo, L. De Gioia, G. Zampella, Evidence for the formation of a Mo–H intermediate in the catalytic cycle of formate dehydrogenase, Inorg. Chem. 51 (2012) 8331–8339.

[104] G.B. Seiffert, G.M. Ullmann, A. Messerschmidt, B. Schink, P.M. Kroneck, O. Einsle, Structure of the non-redox-active tungsten/[4Fe:4S] enzyme acetylene hydratase, Proc. Natl. Acad. Sci. U. S. A. 104 (2007) 3073–3077.

[105] F. Tenbrink, B. Schink, P.M. Kroneck, Exploring the active site of the tungsten, iron–sulfur enzyme acetylene hydratase, J. Bacteriol. 193 (2011) 1229–1236.

[106] S. Antony, C.A. Bayse, Theoretical studies of models of the active site of the tungstoenzyme acetylene hydratase, Organometallics 28 (2009) 4938–4944.

[107] M.A. Vincent, I.H. Hillier, G. Periyasamy, N.A. Burton, A DFT study of the possible role of vinylidene and carbene intermediates in the mechanism of the enzyme acetylene hydratase, Dalton Trans. 39 (2010) 3816–3822.

[108] R.Z. Liao, J.G. Yu, F. Himo, Mechanism of tungsten-dependent acetylene hydratase from quantum chemical calculations, Proc. Natl. Acad. Sci. U. S. A. 107 (2010) 22523–22527.

[109] Y.F. Liu, R.Z. Liao, W.J. Ding, J.G. Yu, R.Z. Liu, Theoretical investigation of the first-shell mechanism of acetylene hydration catalyzed by a biomimetic tungsten complex, J. Biol. Inorg. Chem. 16 (2011) 745–752.

[110] R.C. Bray, S.P. Vincent, D.J. Lowe, R.A. Clegg, P.B. Garland, Electron-paramagnetic-resonance studies on the molybdenum of nitrate reductase from *Escherichia coli* K12, Biochem. J. 155 (1976) 201–203.

[111] B. Guigliarelli, M. Asso, C. More, V. Augier, F. Blasco, J. Pommier, G. Giordano, P. Bertrand, EPR and redox characterization of iron–sulfur centers in nitrate reductases A and Z from *Escherichia coli*. Evidence for a high-potential and a low-potential class and their relevance in the electron-transfer mechanism, Eur. J. Biochem. 207 (1992) 61–68.

[112] B. Guigliarelli, A. Magalon, M. Asso, P. Bertrand, C. Frixon, G. Giordano, F. Blasco, Complete coordination of the four Fe–S centers of the beta subunit from *Escherichia coli* nitrate reductase. Physiological, biochemical, and EPR characterization of site-directed mutants lacking the highest or lowest potential [4Fe–4S] clusters, Biochemistry 35 (1996) 4828–4836.

[113] F. Blasco, B. Guigliarelli, A. Magalon, M. Asso, G. Giordano, R.A. Rothery, The coordination and function of the redox centres of the membrane-bound nitrate reductases, Cell. Mol. Life Sci. 58 (2001) 179–193.

[114] M.G. Bertero, R.A. Rothery, M. Palak, C. Hou, D. Lim, F. Blasco, J.H. Weiner, N.C. Strynadka, Insights into the respiratory electron transfer pathway from the structure of nitrate reductase A, Nat. Struct. Biol. 10 (2003) 681–687.

[115] M. Jormakka, D. Richardson, B. Byrne, S. Iwata, Architecture of NarGH reveals a structural classification of Mo-bisMGD enzymes, Structure (Camb) 12 (2004) 95–104.

[116] C. Avazeri, R.J. Turner, J. Pommier, J.H. Weiner, G. Giordano, A. Vermeglio, Tellurite reductase activity of nitrate reductase is responsible for the basal resistance of *Escherichia coli* to tellurite, Microbiology 143 (Pt 4) (1997) 1181–1189.

[117] M. Sabaty, C. Avazeri, D. Pignol, A. Vermeglio, Characterization of the reduction of selenate and tellurite by nitrate reductases, Appl. Environ. Microbiol. 67 (2001) 5122–5126.

[118] S.J. Nieter Burgmayer, D.L. Pearsall, S.M. Blaney, E.M. Moore, C. Sauk-Schubert, Redox reactions of the pyranopterin system of the molybdenum cofactor, J. Biol. Inorg. Chem. 9 (2004) 59–66.

[119] S.P. Vincent, R.C. Bray, Electron-paramagnetic-resonance studies on nitrate reductase from *Escherichia coli* K12, Biochem. J. 171 (1978) 639–647.

[120] G.N. George, R.C. Bray, F.F. Morpeth, D.H. Boxer, Complexes with halide and other anions of the molybdenum centre of nitrate reductase from *Escherichia coli*, Biochem. J. 227 (1985) 925–931.

[121] G.N. George, N.A. Turner, R.C. Bray, F.F. Morpeth, D.H. Boxer, S.P. Cramer, X-ray-absorption and electron-paramagnetic-resonance spectroscopic studies of the environment of molybdenum in high-pH and low-pH forms of *Escherichia coli* nitrate reductase, Biochem. J. 259 (1989) 693–700.

[122] A. Magalon, M. Asso, B. Guigliarelli, R.A. Rothery, P. Bertrand, G. Giordano, F. Blasco, Molybdenum cofactor properties and [Fe–S] cluster coordination in *Escherichia coli* nitrate reductase A: investigation by site-directed mutagenesis of the conserved his-50 residue in the NarG subunit, Biochemistry 37 (1998) 7363–7370.

[123] R.A. Rothery, M.G. Bertero, T. Spreter, N. Bouromand, N.C. Strynadka, J.H. Weiner, Protein crystallography reveals a Role for the FS0 cluster of *Escherichia coli* nitrate reductase A (NarGHI) in enzyme maturation, J. Biol. Chem. 285 (2010) 8801–8807.

[124] N. Turner, A.L. Ballard, R.C. Bray, S. Ferguson, Investigation by electron paramagnetic resonance spectroscopy of the molybdenum centre of respiratory nitrate reductase from *Paracoccus denitrificans*, Biochem. J. 252 (1988) 925–926.

[125] C. Correia, S. Besson, C.D. Brondino, P.J. Gonzalez, G. Fauque, J. Lampreia, I. Moura, J.J. Moura, Biochemical and spectroscopic characterization of the membrane-bound nitrate reductase from *Marinobacter hydrocarbonoclasticus* 617, J. Biol. Inorg. Chem. 13 (2008) 1321–1333.

[126] S.J. Field, N.P. Thornton, L.J. Anderson, A.J. Gates, A. Reilly, B.J. Jepson, D.J. Richardson, S.J. George, M.R. Cheesman, J.N. Butt, Reductive activation of nitrate reductases, Dalton Trans. (2005) 3580–3586.

[127] J. Marangon, P.M. Paes de Sousa, I. Moura, C.D. Brondino, J.J. Moura, P.J. Gonzalez, Substrate-dependent modulation of the enzymatic catalytic activity: reduction of nitrate, chlorate and perchlorate by respiratory nitrate reductase from *Marinobacter hydrocarbonoclasticus* 617, Biochim. Biophys. Acta 1817 (2012) 1072–1082.

[128] C.E. Vine, S.K. Purewal, J.A. Cole, NsrR-dependent method for detecting nitric oxide accumulation in the *Escherichia coli* cytoplasm and enzymes involved in NO production, FEMS Microbiol. Lett. 325 (2011) 108–114.

[129] N.J. Gilberthorpe, R.K. Poole, Nitric oxide homeostasis in *Salmonella typhimurium*: roles of respiratory nitrate reductase and flavohemoglobin, J. Biol. Chem. 283 (2008) 11146–11154.

[130] G. Rowley, D. Hensen, H. Felgate, A. Arkenberg, C. Appia-Ayme, K. Prior, C. Harrington, S.J. Field, J.N. Butt, E. Baggs, D.J. Richardson, Resolving the contributions of the membrane-bound and periplasmic nitrate reductase systems to nitric oxide and nitrous oxide production in *Salmonella enterica* serovar Typhimurium, Biochem. J. 441 (2012) 755–762.

[131] D.P. Kloer, C. Hagel, J. Heider, G.E. Schulz, Crystal structure of ethylbenzene dehydrogenase from *Aromatoleum aromaticum*, Structure 14 (2006) 1377–1388.

[132] D. Knack, C. Hagel, M. Szaleniec, A. Dudzik, A. Salwinski, J. Heider, Substrate and inhibitor spectra of ethylbenzene dehydrogenase: perspectives on application potential and catalytic mechanism, Appl. Environ. Microbiol. 78 (2012) 6475–6482.

[133] M. Szaleniec, T. Borowski, K. Schuhle, M. Witko, J. Heider, Ab initio modeling of ethylbenzene dehydrogenase reaction mechanism, J. Am. Chem. Soc. 132 (2010) 6014–6024.

[134] J. Caldeira, V. Belle, M. Asso, B. Guigliarelli, I. Moura, J.J.G. Moura, P. Bertrand, Analysis of the electron paramagnetic resonance properties of the $[2Fe–2S]^{1+}$ centers in molybdenum enzymes of the xanthine oxidase family: assignment of signals I and II, Biochemistry 39 (2000) 2700–2707.

[135] P. Bertrand, C. More, B. Guigliarelli, A. Fournel, B. Bennett, B. Howes, Biological polynuclear clusters coupled by magnetic interactions: from the point dipole approximation to a local spin model, J. Am. Chem. Soc. 116 (1994) 3078–3086.

[136] A.V. Astashkin, A. Rajapakshe, M.J. Cornelison, K. Johnson-Winters, J.H. Enemark, Determination of the distance between the Mo(V) and Fe(III) heme centers of wild type human sulfite oxidase by pulsed EPR spectroscopy, J. Phys. Chem. B 116 (2012) 1942–1950.

[137] S. Stoll, Y. NejatyJahromy, J.J. Woodward, A. Ozarowski, M.A. Marletta, R.D. Britt, Nitric oxide synthase stabilizes the tetrahydrobiopterin cofactor radical by controlling its protonation state, J. Am. Chem. Soc. 132 (2012) 11812–11823.

[138] A. Brunel, J. Santolini, P. Dorlet, Electron paramagnetic resonance characterization of tetrahydrobiopterin radical formation in bacterial nitric oxide synthase compared to mammalian nitric oxide synthase, Biophys. J. 103 (2012) 109–117.

[139] R.A. Rothery, B. Stein, M. Solomonson, M.L. Kirk, J.H. Weiner, Pyranopterin conformation defines the function of molybdenum and tungsten enzymes, Proc. Natl. Acad. Sci. U. S. A. 109 (2012) 14773–14778.

[140] M.C. Lett, D. Muller, D. Lievremont, S. Silver, J. Santini, Unified nomenclature for genes involved in prokaryotic aerobic arsenite oxidation, J. Bacteriol. 194 (2012) 207–208.

[141] D. Muller, D. Lievremont, D.D. Simeonova, J.C. Hubert, M.C. Lett, Arsenite oxidase aox genes from a metal-resistant beta-proteobacterium, J. Bacteriol. 185 (2003) 135–141.

[142] V. Bonnefoy, J. Ratouchniak, F. Blasco, M. Chippaux, Organization of the nar genes at the chlZ locus, FEMS Microbiol. Lett. 147 (1997) 147–149.

[143] V.M. Luque-Almagro, A.J. Gates, C. Moreno-Vivian, S.J. Ferguson, D.J. Richardson, M.D. Roldan, Bacterial nitrate assimilation: gene distribution and regulation, Biochem. Soc. Trans. 39 (2011) 1838–1843.

[144] F.F. Morpeth, D.H. Boxer, Kinetic analysis of respiratory nitrate reductase from *Escherichia coli* K12, Biochemistry 24 (1985) 40–46.

[145] S. Gon, J.C. Patte, V. Mejean, C. Iobbi-Nivol, The torYZ (yecK bisZ) operon encodes a third respiratory trimethylamine N-oxide reductase in *Escherichia coli*, J. Bacteriol. 182 (2000) 5779–5786.

[146] V.V. Pollock, M.J. Barber, Biotin sulfoxide reductase. Heterologous expression and characterization of a functional molybdopterin guanine dinucleotide-containing enzyme, J. Biol. Chem. 272 (1997) 3355–3362.

[147] S. Duval, A.L. Ducluzeau, W. Nitschke, B. Schoepp-Cothenet, Enzyme phylogenies as markers for the oxidation state of the environment: the case of respiratory arsenate reductase and related enzymes, BMC Evol. Biol. 8 (2008) 206.

[148] M. Hensel, A.P. Hinsley, T. Nikolaus, G. Sawers, B.C. Berks, The genetic basis of tetrathionate respiration in *Salmonella typhimurium*, Mol. Microbiol. 32 (1999) 275–287.

[149] M. Guiral, P. Tron, C. Aubert, A. Gloter, C. Iobbi-Nivol, M.T. Giudici-Orticoni, A membrane-bound multienzyme, hydrogen-oxidizing, and sulfur-reducing complex from the hyperthermophilic bacterium *Aquifex aeolicus*, J. Biol. Chem. 280 (2005) 42004–42015.

[150] N.K. Heinzinger, S.Y. Fujimoto, M.A. Clark, M.S. Moreno, E.L. Barrett, Sequence analysis of the phs operon in *Salmonella typhimurium* and the contribution of thiosulfate reduction to anaerobic energy metabolism, J. Bacteriol. 177 (1995) 2813–2820.

[151] B.J. Jepson, A. Marietou, S. Mohan, J.A. Cole, C.S. Butler, D.J. Richardson, Evolution of the soluble nitrate reductase: defining the monomeric periplasmic nitrate reductase subgroup, Biochem. Soc. Trans. 34 (2006) 122–126.

[152] K. Ogawa, E. Akagawa, K. Yamane, Z.W. Sun, M. LaCelle, P. Zuber, M.M. Nakano, The nasB operon and nasA gene are required for nitrate/nitrite assimilation in *Bacillus subtilis*, J. Bacteriol. 177 (1995) 1409–1413.

[153] J.T. Lin, B.S. Goldman, V. Stewart, Structures of genes nasA and nasB, encoding assimilatory nitrate and nitrite reductases in *Klebsiella pneumoniae* M5al, J. Bacteriol. 175 (1993) 2370–2378.

[154] A.J. Gates, V.M. Luque-Almagro, A.D. Goddard, S.J. Ferguson, M.D. Roldan, D.J. Richardson, A composite biochemical system for bacterial nitrate and nitrite assimilation as exemplified by *Paracoccus denitrificans*, Biochem. J. 435 (2011) 743–753.

[155] P. Lanciano, A. Savoyant, S. Grimaldi, A. Magalon, B. Guigliarelli, P. Bertrand, New method for the spin quantitation of $[4Fe–4S]^{+}$ clusters with $S=(3)/(2)$. Application to the FS0 center of the NarGHI nitrate reductase from *Escherichia coli*, J. Phys. Chem. B 111 (2007) 13632–13637.

[156] R.A. Rothery, M.G. Bertero, R. Cammack, M. Palak, F. Blasco, N.C. Strynadka, J.H. Weiner, The catalytic subunit of *Escherichia coli* nitrate reductase A contains a novel [4Fe–4S] cluster with a high-spin ground state, Biochemistry 43 (2004) 5324–5333.

[157] T. Krafft, A. Bowen, F. Theis, J.M. Macy, Cloning and sequencing of the genes encoding the periplasmic-cytochrome B-containing selenate reductase of *Thauera selenatis*, DNA Seq. 10 (2000) 365–377.

[158] C.A. McDevitt, P. Hugenholtz, G.R. Hanson, A.G. McEwan, Molecular analysis of dimethyl sulphide dehydrogenase from *Rhodovulum sulfidophilum*: its place in the dimethyl sulphoxide reductase family of microbial molybdopterin-containing enzymes, Mol. Microbiol. 44 (2002) 1575–1587.

[159] H.D. Thorell, K. Stenklo, J. Karlsson, T. Nilsson, A gene cluster for chlorate metabolism in *Ideonella dechloratans*, Appl. Environ. Microbiol. 69 (2003) 5585–5592.

[160] N.L. Creevey, A.G. McEwan, G.R. Hanson, P.V. Bernhardt, Thermodynamic characterization of the redox centers within dimethylsulfide dehydrogenase, Biochemistry 47 (2008) 3770–3776.

[161] E.J. Dridge, C.A. Watts, B.J. Jepson, K. Line, J.M. Santini, D.J. Richardson, C.S. Butler, Investigation of the redox centres of periplasmic selenate reductase from *Thauera selenatis* by EPR spectroscopy, Biochem. J. 408 (2007) 19–28.

[162] C.A. McDevitt, G.R. Hanson, C.J. Noble, M.R. Cheesman, A.G. McEwan, Characterization of the redox centers in dimethyl sulfide dehydrogenase from *Rhodovulum sulfidophilum*, Biochemistry 41 (2002) 15234–15244.

[163] H. Tang, R.A. Rothery, J.E. Voss, J.H. Weiner, Correct assembly of iron–sulfur cluster FS0 into *Escherichia coli* dimethyl sulfoxide reductase (DmsABC) is a prerequisite for molybdenum cofactor insertion, J. Biol. Chem. 286 (2011) 15147–15154.

[164] J.A. Muller, S. DasSarma, Genomic analysis of anaerobic respiration in the archaeon *Halobacterium* sp. strain NRC-1: dimethyl sulfoxide and trimethylamine N-oxide as terminal electron acceptors, J. Bacteriol. 187 (2005) 1659–1667.

[165] S. Lucker, M. Wagner, F. Maixner, E. Pelletier, H. Koch, B. Vacherie, T. Rattei, J.S. Damste, E. Spieck, D. Le Paslier, H. Daims, A *Nitrospira* metagenome illuminates the physiology and evolution of globally important nitrite-oxidizing bacteria, Proc. Natl. Acad. Sci. U. S. A. 107 (2010) 13479–13484.

[166] R.M. Martinez-Espinosa, E.J. Dridge, M.J. Bonete, J.N. Butt, C.S. Butler, F. Sargent, D.J. Richardson, Look on the positive side! The orientation, identification and bioenergetics of 'Archaeal' membrane-bound nitrate reductases, FEMS Microbiol. Lett. 276 (2007) 129–139.

[167] J. Dermer, G. Fuchs, Molybdoenzyme that catalyzes the anaerobic hydroxylation of a tertiary carbon atom in the side chain of cholesterol, J. Biol. Chem. 287 (2012) 36905–36916.

[168] D.Y. Sorokin, S. Lucker, D. Vejmelkova, N.A. Kostrikina, R. Kleerebezem, W.I. Rijpstra, J.S. Damste, D. Le Paslier, G. Muyzer, M. Wagner, M.C. van Loosdrecht, H. Daims, Nitrification expanded: discovery, physiology and genomics of a nitrite-oxidizing bacterium from the phylum Chloroflexi, ISME J. 6 (2012) 2245–2256.

[169] P.J. Ellis, T. Conrads, R. Hille, P. Kuhn, Crystal structure of the 100 kDa arsenite oxidase from *Alcaligenes faecalis* in two crystal forms at 1.64 A and 2.03 A, Structure 9 (2001) 125–132.

[170] S.J. Coulthurst, A. Dawson, W.N. Hunter, F. Sargent, Conserved signal peptide recognition systems across the prokaryotic domains, Biochemistry 51 (2012) 1678–1686.

[171] A.P. Hinsley, N.R. Stanley, T. Palmer, B.C. Berks, A naturally occurring bacterial Tat signal peptide lacking one of the 'invariant' arginine residues of the consensus targeting motif, FEBS Lett. 497 (2001) 45–49.

[172] F. Reyes, M.D. Roldan, W. Klipp, F. Castillo, C. Moreno-Vivian, Isolation of periplasmic nitrate reductase genes from *Rhodobacter sphaeroides* DSM 158: structural and functional differences among prokaryotic nitrate reductases, Mol. Microbiol. 19 (1996) 1307–1318.

[173] B. Ize, S.J. Coulthurst, K. Hatzixanthis, I. Caldelari, G. Buchanan, E.C. Barclay, D.J. Richardson, T. Palmer, F. Sargent, Remnant signal peptides on non-exported enzymes: implications for the evolution of prokaryotic respiratory chains, Microbiology 155 (2009) 3992–4004.

[174] R.J. Turner, A.L. Papish, F. Sargent, Sequence analysis of bacterial redox enzyme maturation proteins (REMPs), Can. J. Microbiol. 50 (2004) 225–238.

[175] A. Lieutaud, R. van Lis, S. Duval, L. Capowiez, D. Muller, R. Lebrun, S. Lignon, M.L. Fardeau, M.C. Lett, W. Nitschke, B. Schoepp-Cothenet, Arsenite oxidase from *Ralstonia* sp. 22: characterization of the enzyme and its interaction with soluble cytochromes, J. Biol. Chem. 285 (2010) 20433–20441.

[176] J.M. Santini, R.N. vanden Hoven, Molybdenum-containing arsenite oxidase of the chemolithoautotrophic arsenite oxidizer NT-26, J. Bacteriol. 186 (2004) 1614–1619.

[177] M. Kuroda, M. Yamashita, E. Miwa, K. Imao, N. Fujimoto, H. Ono, K. Nagano, K. Sei, M. Ike, Molecular cloning and characterization of the srdBCA operon, encoding the respiratory selenate reductase complex, from the selenate-reducing bacterium *Bacillus selenatarsenatis* SF-1, J. Bacteriol. 193 (2011) 2141–2148.
[178] C.W. Saltikov, D.K. Newman, Genetic identification of a respiratory arsenate reductase, Proc. Natl. Acad. Sci. U. S. A. 100 (2003) 10983–10988.
[179] J.T. Lin, B.S. Goldman, V. Stewart, The nasFEDCBA operon for nitrate and nitrite assimilation in *Klebsiella pneumoniae* M5al, J. Bacteriol. 176 (1994) 2551–2559.
[180] E. Lebrun, J.M. Santini, M. Brugna, A.L. Ducluzeau, S. Ouchane, B. Schoepp-Cothenet, F. Baymann, W. Nitschke, The Rieske protein: a case study on the pitfalls of multiple sequence alignments and phylogenetic reconstruction, Mol. Biol. Evol. 23 (2006) 1180–1191.
[181] S. Duval, J.M. Santini, W. Nitschke, R. Hille, B. Schoepp-Cothenet, The small subunit AroB of arsenite oxidase: lessons on the [2Fe–2S] Rieske protein superfamily, J. Biol. Chem. 285 (2010) 20442–20451.
[182] R. van Lis, W. Nitschke, S. Duval, B. Schoepp-Cothenet, Arsenics as bioenergetic substrates, Biochim. Biophys. Acta 1827 (2013) 176–188.
[183] R. van Lis, W. Nitschke, T.P. Warelow, L. Capowiez, J.M. Santini, B. Schoepp-Cothenet, Heterologously expressed arsenite oxidase: a system to study biogenesis and structure/function relationships of the enzyme family, Biochim. Biophys. Acta 1817 (2012) 1701–1708.
[184] R. Blasco, F. Castillo, M. Martinez-Luque, The assimilatory nitrate reductase from the phototrophic bacterium, *Rhodobacter capsulatus* E1F1, is a flavoprotein, FEBS Lett. 414 (1997) 45–49.
[185] C. Costa, M. Teixeira, J. LeGall, J.J.G. Moura, I. Moura, Formate dehydrogenase from *Desulfovibrio desulfuricans* ATCC 27774: isolation and spectroscopic characterization of the active sites (heme, iron–sulfur centers and molybdenum), J. Biol. Inorg. Chem. 2 (1997) 198–208.
[186] C. Sebban, L. Blanchard, M. Bruschi, F. Guerlesquin, Purification and characterization of the formate dehydrogenase from *Desulfovibrio vulgaris* Hildenborough, FEMS Microbiol. Lett. 133 (1995) 143–149.
[187] K.S. Bender, C. Shang, R. Chakraborty, S.M. Belchik, J.D. Coates, L.A. Achenbach, Identification, characterization, and classification of genes encoding perchlorate reductase, J. Bacteriol. 187 (2005) 5090–5096.
[188] F. Cava, O. Zafra, J. Berenguer, A cytochrome *c* containing nitrate reductase plays a role in electron transport for denitrification in *Thermus thermophilus* without involvement of the *bc* respiratory complex, Mol. Microbiol. 70 (2008) 507–518.
[189] O. Zafra, F. Cava, F. Blasco, A. Magalon, J. Berenguer, Membrane-associated maturation of the heterotetrameric nitrate reductase of *Thermus thermophilus*, J. Bacteriol. 187 (2005) 3990–3996.
[190] O. Zafra, S. Ramirez, P. Castan, R. Moreno, F. Cava, C. Valles, E. Caro, J. Berenguer, A cytochrome c encoded by the nar operon is required for the synthesis of active respiratory nitrate reductase in *Thermus thermophilus*, FEBS Lett. 523 (2002) 99–102.
[191] S. Afshar, E. Johnson, S. de Vries, I. Schroder, Properties of a thermostable nitrate reductase from the hyperthermophilic archaeon *Pyrobaculum aerophilum*, J. Bacteriol. 183 (2001) 5491–5495.
[192] S. de Vries, M. Momcilovic, M.J. Strampraad, J.P. Whitelegge, A. Baghai, I. Schroder, Adaptation to a high-tungsten environment: *Pyrobaculum aerophilum* contains an active tungsten nitrate reductase, Biochemistry 49 (2010) 9911–9921.
[193] I. Schroder, S. Rech, T. Krafft, J.M. Macy, Purification and characterization of the selenate reductase from *Thauera selenatis*, J. Biol. Chem. 272 (1997) 23765–23768.
[194] T. Nilsson, M. Rova, A. Smedja Backlund, Microbial metabolism of oxochlorates: a bioenergetic perspective, Biochim. Biophys. Acta 1827 (2013) 189–197.
[195] H. Hussain, J. Grove, L. Griffiths, S. Busby, J. Cole, A seven-gene operon essential for formate-dependent nitrite reduction to ammonia by enteric bacteria, Mol. Microbiol. 12 (1994) 153–163.
[196] W. Dietrich, O. Klimmek, The function of methyl-menaquinone-6 and polysulfide reductase membrane anchor (PsrC) in polysulfide respiration of *Wolinella succinogenes*, Eur. J. Biochem. 269 (2002) 1086–1095.
[197] J.H. Weiner, G. Shaw, R.J. Turner, C.A. Trieber, The topology of the anchor subunit of dimethyl sulfoxide reductase of *Escherichia coli*, J. Biol. Chem. 268 (1993) 3238–3244.
[198] L. Pieulle, X. Morelli, P. Gallice, E. Lojou, P. Barbier, M. Czjzek, P. Bianco, F. Guerlesquin, E.C. Hatchikian, The type I/type II cytochrome c3 complex: an electron transfer link in the hydrogen-sulfate reduction pathway, J. Mol. Biol. 354 (2005) 73–90.
[199] R.O. Louro, Proton thrusters: overview of the structural and functional features of soluble tetrahaem cytochromes c3, J. Biol. Inorg. Chem. 12 (2007) 1–10.
[200] T.M. Iverson, D.M. Arciero, A.B. Hooper, D.C. Rees, High-resolution structures of the oxidized and reduced states of cytochrome c554 from *Nitrosomonas europaea*, J. Biol. Inorg. Chem. 6 (2001) 390–397.
[201] S.R. Starkenburg, P.S. Chain, L.A. Sayavedra-Soto, L. Hauser, M.L. Land, F.W. Larimer, S.A. Malfatti, M.G. Klotz, P.J. Bottomley, D.J. Arp, W.J. Hickey, Genome sequence of the chemolithoautotrophic nitrite-oxidizing bacterium *Nitrobacter winogradskyi* Nb-255, Appl. Environ. Microbiol. 72 (2006) 2050–2063.
[202] S.R. Starkenburg, F.W. Larimer, L.Y. Stein, M.G. Klotz, P.S. Chain, L.A. Sayavedra-Soto, A.T. Poret-Peterson, M.E. Gentry, D.J. Arp, B. Ward, P.J. Bottomley, Complete genome sequence of *Nitrobacter hamburgensis* X14 and comparative genomic analysis of species within the genus *Nitrobacter*, Appl. Environ. Microbiol. 74 (2008) 2852–2863.
[203] P.N. Refojo, M. Teixeira, M.M. Pereira, The alternative complex III: properties and possible mechanisms for electron transfer and energy conservation, Biochim. Biophys. Acta 1817 (2012) 1852–1859.
[204] M.L. Rodrigues, T.F. Oliveira, I.A. Pereira, M. Archer, X-ray structure of the membrane-bound cytochrome c quinol dehydrogenase NrfH reveals novel haem coordination, EMBO J. 25 (2006) 5951–5960.
[205] V. Mejean, C. Iobbi-Nivol, M. Lepelletier, G. Giordano, M. Chippaux, M.C. Pascal, TMAO anaerobic respiration in *Escherichia coli*: involvement of the tor operon, Mol. Microbiol. 11 (1994) 1169–1179.
[206] T. Ujiiye, I. Yamamoto, H. Nakama, A. Okubo, S. Yamazaki, T. Satoh, Nucleotide sequence of the genes, encoding the pentaheme cytochrome (dmsC) and the transmembrane protein (dmsB), involved in dimethyl sulfoxide respiration from *Rhodobacter sphaeroides* f. sp. *denitrificans*, Biochim. Biophys. Acta 1277 (1996) 1–5.
[207] M.D. Roldan, H.J. Sears, M.R. Cheesman, S.J. Ferguson, A.J. Thomson, B.C. Berks, D.J. Richardson, Spectroscopic characterization of a novel multiheme c-type cytochrome widely implicated in bacterial electron transport, J. Biol. Chem. 273 (1998) 28785–28790.
[208] J.N. Murphy, C.W. Saltikov, The cymA gene, encoding a tetraheme c-type cytochrome, is required for arsenate respiration in *Shewanella* species, J. Bacteriol. 189 (2007) 2283–2290.
[209] S. Gon, M.T. Giudici-Orticoni, V. Mejean, C. Iobbi-Nivol, Electron transfer and binding of the c-type cytochrome TorC to the trimethylamine N-oxide reductase in *Escherichia coli*, J. Biol. Chem. 276 (2001) 11545–11551.
[210] A.L. Shaw, A. Hochkoeppler, P. Bonora, D. Zannoni, G.R. Hanson, A.G. McEwan, Characterization of DorC from *Rhodobacter capsulatus*, a c-type cytochrome involved in electron transfer to dimethyl sulfoxide reductase, J. Biol. Chem. 274 (1999) 9911–9914.
[211] T.H. Brondijk, A. Nilavongse, N. Filenko, D.J. Richardson, J.A. Cole, NapGH components of the periplasmic nitrate reductase of *Escherichia coli* K-12: location, topology and physiological roles in quinol oxidation and redox balancing, Biochem. J. 379 (2004) 47–55.
[212] M. Kern, J. Simon, Characterization of the NapGH quinol dehydrogenase complex involved in *Wolinella succinogenes* nitrate respiration, Mol. Microbiol. 69 (2008) 1137–1152.
[213] B. Schoepp-Cothenet, C. Lieutaud, F. Baymann, A. Vermeglio, T. Friedrich, D.M. Kramer, W. Nitschke, Menaquinone as pool quinone in a purple bacterium, Proc. Natl. Acad. Sci. U. S. A. 106 (2009) 8549–8554.
[214] W. Nitschke, D.M. Kramer, A. Riedel, U. Liebl, From naphto- to benzoquinones, (r)evolutionary reorganisation of electron transfer chains, in: P. Mathis (Ed.), Photosynthesis: From Light to Biosphere, Kluwer Academic Publishers, Dortrecht, 1995, pp. 945–950.
[215] M.D. Collins, D. Jones, Distribution of isoprenoid quinone structural types in bacteria and their taxonomic implication, Microbiol. Rev. 45 (1981) 316–354.
[216] S. Grimaldi, P. Lanciano, P. Bertrand, F. Blasco, B. Guigliarelli, Evidence for an EPR-detectable semiquinone intermediate stabilized in the membrane-bound subunit NarI of nitrate reductase A (NarGHI) from *Escherichia coli*, Biochemistry 44 (2005) 1300–1308.
[217] S. Grimaldi, R. Arias-Cartin, P. Lanciano, S. Lyubenova, R. Szenes, B. Endeward, T.F. Prisner, B. Guigliarelli, A. Magalon, Determination of the proton environment of high stability Menasemiquinone intermediate in *Escherichia coli* nitrate reductase A by pulsed EPR, J. Biol. Chem. 287 (2012) 4662–4670.
[218] R. Arias-Cartin, S. Grimaldi, J. Pommier, P. Lanciano, C. Schaefer, P. Arnoux, G. Giordano, B. Guigliarelli, A. Magalon, Cardiolipin-based respiratory complex activation in bacteria, Proc. Natl. Acad. Sci. U. S. A. 108 (2011) 7781–7786.
[219] P. Lanciano, A. Magalon, P. Bertrand, B. Guigliarelli, S. Grimaldi, High-stability semiquinone intermediate in nitrate reductase A (NarGHI) from *Escherichia coli* is located in a quinol oxidation site close to heme bD, Biochemistry 46 (2007) 5323–5329.
[220] S. Grimaldi, R. Arias-Cartin, P. Lanciano, S. Lyubenova, B. Endeward, T.F. Prisner, A. Magalon, B. Guigliarelli, Direct evidence for nitrogen ligation to the high stability semiquinone intermediate in *Escherichia coli* nitrate reductase A, J. Biol. Chem. 285 (2010) 179–187.
[221] R. Arias-Cartin, S. Lyubenova, P. Ceccaldi, T. Prisner, A. Magalon, B. Guigliarelli, S. Grimaldi, HYSCORE evidence that endogenous mena- and ubisemiquinone bind at the same Q site (Q(D)) of *Escherichia coli* nitrate reductase A, J. Am. Chem. Soc. 132 (2010) 5942–5943.
[222] U. Liebl, S. Pezennec, A. Riedel, E. Kellner, W. Nitschke, The Rieske FeS center from the gram-positive bacterium PS3 and its interaction with the menaquinone pool studied by EPR, J. Biol. Chem. 267 (1992) 14068–14072.
[223] G.M. Carlone, F.A. Anet, Detection of menaquinone-6 and a novel methyl-substituted menaquinone-6 in *Campylobacter jejuni* and *Campylobacter fetus* subsp. *fetus*, J. Gen. Microbiol. 129 (1983) 3385–3393.
[224] M.D. Collins, F. Fernandez, Menaquinone-6 and thermoplasma-quinone-6 in *Wolinella succinogenes*, FEMS Microbiol. Lett. 22 (1984) 273–276.
[225] T. Itoh, H. Funabashi, Y. Katayama-Fujimura, S. Iwasaki, H. Kuraishi, Structure of methylmenaquinone-7 isolated from *Alteromonas putrefaciens*, Biochim. Biophys. Acta 840 (1985) 51–55.
[226] M. Akagawa-Matsushita, T. Itoh, Y. Katayama, H. Kuraishi, K. Yamasato, Isoprenoid quinone composition of some marine *Alteromonas*, *Marinomonas*, *Deleya*, *Pseudomonas* and *Shewanella* species, J. Gen. Microbiol. 138 (1992) 2275–2281.
[227] R. Thummer, O. Klimmek, R.A. Schmitz, Biochemical studies of *Klebsiella pneumoniae* NifL reduction using reconstituted partial anaerobic respiratory chains of *Wolinella succinogenes*, J. Biol. Chem. 282 (2007) 12517–12526.
[228] B. Nowicka, J. Kruk, Occurrence, biosynthesis and function of isoprenoid quinones, Biochim. Biophys. Acta 1797 (2010) 1587–1605.
[229] A.I. Shestopalov, A.V. Bogachev, R.A. Murtazina, M.B. Viryasov, V.P. Skulachev, Aeration-dependent changes in composition of the quinone pool in *Escherichia coli*. Evidence of post-transcriptional regulation of the quinone biosynthesis, FEBS Lett. 404 (1997) 272–274.
[230] B.J. Wallace, I.G. Young, Role of quinones in electron transport to oxygen and nitrate in *Escherichia coli*. Studies with a ubiA–menA– double quinone mutant, Biochim. Biophys. Acta 461 (1977) 84–100.

[231] M. Bekker, G. Kramer, A.F. Hartog, M.J. Wagner, C.G. de Koster, K.J. Hellingwerf, M.J. de Mattos, Changes in the redox state and composition of the quinone pool of *Escherichia coli* during aerobic batch-culture growth, Microbiology 153 (2007) 1974–1980.

[232] R. Meganathan, O. Kwon, Biosynthesis of menaquinone (vitamin K_2) and ubiquinone (coenzyme Q), in: R. Curtiss III, J.B. Kaper, C.L. Squires, P.D. Karp, F.C. Neidhardt, J.M. Slauch (Eds.), EcoSal, ASM Press, Washington DC, 2009.

[233] D.J. Richardson, Bacterial respiration: a flexible process for a changing environment, Microbiology 146 (Pt 3) (2000) 551–571.

[234] G. Unden, J. Bongaerts, Alternative respiratory pathways of *Escherichia coli*: energetics and transcriptional regulation in response to electron acceptors, Biochim. Biophys. Acta 1320 (1997) 217–234.

[235] G. Unden, P. Dünnwald, The aerobic and anaerobic respiratory chain of *Escherichia coli* and *Salmonella enterica*: enzymes and energetics, in: R. Curtiss III, J.B. Kaper, C.L. Squires, P.D. Karp, F.C. Neidhardt, J.M. Slauch (Eds.), EcoSal, ASM Press, Washington, DC, 2008.

[236] B. Soballe, R.K. Poole, Microbial ubiquinones: multiple roles in respiration, gene regulation and oxidative stress management, Microbiology 145 (Pt 8) (1999) 1817–1830.

[237] H.S. Kwan, E.L. Barrett, Roles for menaquinone and the two trimethylamine oxide (TMAO) reductases in TMAO respiration in *Salmonella typhimurium*: Mu d(Apr lac) insertion mutations in men and tor, J. Bacteriol. 155 (1983) 1147–1155.

[238] U. Wissenbach, A. Kroger, G. Unden, The specific functions of menaquinone and demethylmenaquinone in anaerobic respiration with fumarate, dimethylsulfoxide, trimethylamine N-oxide and nitrate by *Escherichia coli*, Arch. Microbiol. 154 (1990) 60–66.

[239] U. Wissenbach, D. Ternes, G. Unden, An *Escherichia coli* mutant containing only demethylmenaquinone, but no menaquinone: effects on fumarate, dimethylsulfoxide, trimethylamine N-oxide and nitrate respiration, Arch. Microbiol. 158 (1992) 68–73.

[240] R. Meganathan, Inability of *men* mutants of *Escherichia coli* to use trimethylamine-N-oxide as an electron acceptor, FEMS Microbiol. Lett. 24 (1984) 57–62.

[241] C.R. Myers, J.M. Myers, Role of menaquinone in the reduction of fumarate, nitrate, iron(III) and manganese(IV) by *Shewanella putrefaciens* MR-1, FEMS Microbiol. Lett. 114 (1993) 215–222.

[242] E.L. Barrett, M.A. Clark, Tetrathionate reduction and production of hydrogen sulfide from thiosulfate, Microbiol. Rev. 51 (1987) 192–205.

[243] C. Novotny, F. Kapralek, Participation of quinone and cytochrome b in tetrathionate reductase respiratory chain of *Citrobacter freundii*, Biochem. J. 178 (1979) 237–240.

[244] E. Maklashina, G. Cecchini, Comparison of catalytic activity and inhibitors of quinone reactions of succinate dehydrogenase (Succinate-ubiquinone oxidoreductase) and fumarate reductase (Menaquinol-fumarate oxidoreductase) from *Escherichia coli*, Arch. Biochem. Biophys. 369 (1999) 223–232.

[245] H.S. Kwan, E.L. Barrett, Map locations and functions of *Salmonella typhimurium* men genes, J. Bacteriol. 159 (1984) 1090–1092.

[246] L. Stoffels, M. Krehenbrink, B.C. Berks, G. Unden, Thiosulfate reduction in *Salmonella enterica* is driven by the proton motive force, J. Bacteriol. 194 (2012) 475–485.

[247] K. Tyson, R. Metheringham, L. Griffiths, J. Cole, Characterisation of *Escherichia coli* K-12 mutants defective in formate-dependent nitrite reduction: essential roles for hemN and the menFDBCE operon, Arch. Microbiol. 168 (1997) 403–411.

[248] T.H. Brondijk, D. Fiegen, D.J. Richardson, J.A. Cole, Roles of NapF, NapG and NapH, subunits of the *Escherichia coli* periplasmic nitrate reductase, in ubiquinol oxidation, Mol. Microbiol. 44 (2002) 245–255.

[249] L.C. Potter, J.A. Cole, Essential roles for the products of the napABCD genes, but not napFGH, in periplasmic nitrate reduction by *Escherichia coli* K-12, Biochem. J. 344 (Pt 1) (1999) 69–76.

[250] J. Simon, M. Sanger, S.C. Schuster, R. Gross, Electron transport to periplasmic nitrate reductase (NapA) of *Wolinella succinogenes* is independent of a NapC protein, Mol. Microbiol. 49 (2003) 69–79.

[251] M. Kern, A.M. Mager, J. Simon, Role of individual nap gene cluster products in NapC-independent nitrate respiration of *Wolinella succinogenes*, Microbiology 153 (2007) 3739–3747.

[252] G. Unden, Differential roles for menaquinone and demethylmenaquinone in anaerobic electron transport of *E. coli* and their fnr-independent expression, Arch. Microbiol. 150 (1988) 499–503.

[253] B. Soballe, R.K. Poole, Requirement for ubiquinone downstream of cytochrome(s) b in the oxygen-terminated respiratory chains of *Escherichia coli* K-12 revealed using a null mutant allele of ubiCA, Microbiology 144 (Pt 2) (1998) 361–373.

[254] M.Y. Okamura, M.L. Paddock, M.S. Graige, G. Feher, Proton and electron transfer in bacterial reaction centers, Biochim. Biophys. Acta 1458 (2000) 148–163.

[255] M. Sato-Watanabe, T. Mogi, H. Miyoshi, Y. Anraku, Characterization and functional role of the QH site of bo-type ubiquinol oxidase from *Escherichia coli*, Biochemistry 37 (1998) 5356–5361.

[256] M. Sato-Watanabe, T. Mogi, T. Ogura, T. Kitagawa, H. Miyoshi, H. Iwamura, Y. Anraku, Identification of a novel quinone-binding site in the cytochrome bo complex from *Escherichia coli*, J. Biol. Chem. 269 (1994) 28908–28912.

[257] L.L. Yap, M.T. Lin, H. Ouyang, R.I. Samoilova, S.A. Dikanov, R.B. Gennis, The quinone-binding sites of the cytochrome bo3 ubiquinol oxidase from *Escherichia coli*, Biochim. Biophys. Acta 1797 (2010) 1924–1932.

[258] S.J. Marritt, T.G. Lowe, J. Bye, D.G. McMillan, L. Shi, J. Fredrickson, J. Zachara, D.J. Richardson, M.R. Cheesman, L.J. Jeuken, J.N. Butt, A functional description of CymA, an electron-transfer hub supporting anaerobic respiratory flexibility in *Shewanella*, Biochem. J. 444 (2012) 465–474.

[259] D.G. McMillan, S.J. Marritt, J.N. Butt, L.J. Jeuken, Menaquinone-7 is specific cofactor in tetraheme quinol dehydrogenase CymA, J. Biol. Chem. 287 (2012) 14215–14225.

[260] M.G. Bertero, R.A. Rothery, N. Boroumand, M. Palak, F. Blasco, N. Ginet, J.H. Weiner, N.C. Strynadka, Structural and biochemical characterization of a quinol binding site of *Escherichia coli* nitrate reductase A, J. Biol. Chem. 280 (2005) 14836–14843.

[261] R. Arias-Cartin, S. Grimaldi, P. Arnoux, B. Guigliarelli, A. Magalon, Cardiolipin binding in bacterial respiratory complexes: structural and functional implications, Biochim. Biophys. Acta 1817 (2012) 1937–1949.

[262] R. Giordani, J. Buc, A. Cornish-Bowden, M.L. Cardenas, Kinetics of membrane-bound nitrate reductase A from *Escherichia coli* with analogues of physiological electron donors—different reaction sites for menadiol and duroquinol, Eur. J. Biochem. 250 (1997) 567–577.

[263] Z. Zhao, R.A. Rothery, J.H. Weiner, Transient kinetic studies of heme reduction in *Escherichia coli* nitrate reductase A (NarGHI) by menaquinol, Biochemistry 42 (2003) 5403–5413.

[264] R. Giordani, J. Buc, Evidence for two different electron transfer pathways in the same enzyme, nitrate reductase A from *Escherichia coli*, Eur. J. Biochem. 271 (2004) 2400–2407.

[265] R.A. Rothery, J.H. Weiner, Interaction of an engineered [3Fe–4S] cluster with a menaquinol binding site of *Escherichia coli* DMSO reductase, Biochemistry 35 (1996) 3247–3257.

[266] Z. Zhao, J.H. Weiner, Interaction of 2-n-heptyl-4-hydroxyquinoline-N-oxide with dimethyl sulfoxide reductase of *Escherichia coli*, J. Biol. Chem. 273 (1998) 20758–20763.

[267] P. Geijer, J.H. Weiner, Glutamate 87 is important for menaquinol binding in DmsC of the DMSO reductase (DmsABC) from *Escherichia coli*, Biochim. Biophys. Acta 1660 (2004) 66–74.

[268] M.L. Rodrigues, K.A. Scott, M.S. Sansom, I.A. Pereira, M. Archer, Quinol oxidation by c-type cytochromes: structural characterization of the menaquinol binding site of NrfHA, J. Mol. Biol. 381 (2008) 341–350.

[269] K. Zargar, C.W. Saltikov, Lysine-91 of the tetraheme c-type cytochrome CymA is essential for quinone interaction and arsenate respiration in *Shewanella* sp. strain ANA-3, Arch. Microbiol. 191 (2009) 797–806.

[270] N. Fisher, P.R. Rich, A motif for quinone binding sites in respiratory and photosynthetic systems, J. Mol. Biol. 296 (2000) 1153–1162.

[271] V.W. Cheng, R.A. Rothery, M.G. Bertero, N.C. Strynadka, J.H. Weiner, Investigation of the environment surrounding iron–sulfur cluster 4 of *Escherichia coli* dimethylsulfoxide reductase, Biochemistry 44 (2005) 8068–8077.

[272] S. Grimaldi, R. Arias-Cartin, B. Guigliarelli, A. Magalon, unpublished results.

[273] A. Hochman, A. Nissany, M. Amizur, Nitrate reduction and assimilation by a moderately halophilic, halotolerant bacterium BA-1, Biochim. Biophys. Acta 965 (1988) 82–89.

[274] C. Moreno-Vivian, P. Cabello, M. Martinez-Luque, R. Blasco, F. Castillo, Prokaryotic nitrate reduction: molecular properties and functional distinction among bacterial nitrate reductases, J. Bacteriol. 181 (1999) 6573–6584.

[275] E. Flores, J.E. Frias, L.M. Rubio, A. Herrero, Photosynthetic nitrate assimilation in cyanobacteria, Photosynth. Res. 83 (2005) 117–133.

[276] M.J. Bonete, R.M. Martinez-Espinosa, C. Pire, B. Zafrilla, D.J. Richardson, Nitrogen metabolism in haloarchaea, Saline Syst. 4 (2008) 9.

[277] I. Luque, A. Herrero, E. Flores, F. Madueno, Clustering of genes involved in nitrate assimilation in the cyanobacterium *Synechococcus*, Mol. Gen. Genet. 232 (1992) 7–11.

[278] J.E. Frias, E. Flores, A. Herrero, Nitrate assimilation gene cluster from the heterocyst-forming cyanobacterium *Anabaena* sp. strain PCC 7120, J. Bacteriol. 179 (1997) 477–486.

[279] Q. Wang, H. Li, A.F. Post, Nitrate assimilation genes of the marine diazotrophic, filamentous cyanobacterium *Trichodesmium* sp. strain WH9601, J. Bacteriol. 182 (2000) 1764–1767.

[280] A.C. Martiny, S. Kathuria, P.M. Berube, Widespread metabolic potential for nitrite and nitrate assimilation among *Prochlorococcus* ecotypes, Proc. Natl. Acad. Sci. U. S. A. 106 (2009) 10787–10792.

[281] J.E. Frias, E. Flores, Negative regulation of expression of the nitrate assimilation nirA operon in the heterocyst-forming cyanobacterium *Anabaena* sp. strain PCC 7120, J. Bacteriol. 192 (2010) 2769–2778.

[282] M. Wyman, C. Bird, Lack of control of nitrite assimilation by ammonium in an oceanic picocyanobacterium, *Synechococcus* sp. strain WH 8103, Appl. Environ. Microbiol. 73 (2007) 3028–3033.

[283] Q. Wu, V. Stewart, NasFED proteins mediate assimilatory nitrate and nitrite transport in *Klebsiella oxytoca* (*pneumoniae*) M5al, J. Bacteriol. 180 (1998) 1311–1322.

[284] J.C. Gutierrez, F. Ramos, L. Ortner, M. Tortolero, nasST, two genes involved in the induction of the assimilatory nitrite–nitrate reductase operon (nasAB) of *Azotobacter vinelandii*, Mol. Microbiol. 18 (1995) 579–591.

[285] C. Pino, F. Olmo-Mira, P. Cabello, M. Martinez-Luque, F. Castillo, M.D. Roldan, C. Moreno-Vivian, The assimilatory nitrate reduction system of the phototrophic bacterium *Rhodobacter capsulatus* E1F1, Biochem. Soc. Trans. 34 (2006) 127–129.

[286] J. Wang, G.P. Zhao, GlnR positively regulates nasA transcription in *Streptomyces coelicolor*, Biochem. Biophys. Res. Commun. 386 (2009) 77–81.

[287] Z. Shao, J. Gao, X. Ding, J. Wang, J. Chiao, G. Zhao, Identification and functional analysis of a nitrate assimilation operon nasACKBDEF from *Amycolatopsis mediterranei* U32, Arch. Microbiol. 193 (2011) 463–477.

[288] P. Cabello, M.D. Roldan, C. Moreno-Vivian, Nitrate reduction and the nitrogen cycle in archaea, Microbiology 150 (2004) 3527–3546.

[289] R.M. Martinez-Espinosa, F.C. Marhuenda-Egea, M.J. Bonete, Assimilatory nitrate reductase from the haloarchaeon *Haloferax mediterranei*: purification and characterisation, FEMS Microbiol. Lett. 204 (2001) 381–385.

[290] R.M. Martinez-Espinosa, F.C. Marhuenda-Egea, M.J. Bonete, Purification and characterisation of a possible assimilatory nitrite reductase from the halophile archaeon *Haloferax mediterranei*, FEMS Microbiol. Lett. 196 (2001) 113–118.

[291] B. Lledo, F.C. Marhuenda-Egea, R.M. Martinez-Espinosa, M.J. Bonete, Identification and transcriptional analysis of nitrate assimilation genes in the halophilic archaeon *Haloferax mediterranei*, Gene 361 (2005) 80–88.
[292] R.M. Martinez-Espinosa, B. Lledo, F.C. Marhuenda-Egea, S. Diaz, M.J. Bonete, NO_3^-/NO_2^- assimilation in halophilic archaea: physiological analysis, nasA and nasD expressions, Extremophiles 13 (2009) 785–792.
[293] S.H. Baek, G. Rajashekara, G.A. Splitter, J.P. Shapleigh, Denitrification genes regulate *Brucella virulence* in mice, J. Bacteriol. 186 (2004) 6025–6031.
[294] N.E. Van Alst, K.F. Picardo, B.H. Iglewski, C.G. Haidaris, Nitrate sensing and metabolism modulate motility, biofilm formation, and virulence in *Pseudomonas aeruginosa*, Infect. Immun. 75 (2007) 3780–3790.
[295] K.R. Barth, V.M. Isabella, V.L. Clark, Biochemical and genomic analysis of the denitrification pathway within the genus *Neisseria*, Microbiology 155 (2009) 4093–4103.
[296] D. Richardson, G. Sawers, Structural biology. PMF through the redox loop, Science 295 (2002) 1842–1843.
[297] H.D. Williams, J.E. Zlosnik, B. Ryall, Oxygen, cyanide and energy generation in the cystic fibrosis pathogen *Pseudomonas aeruginosa*, Adv. Microb. Physiol. 52 (2007) 1–71.
[298] M. Aminuddin, D.J. Nicholas, Sulphide oxidation linked to the reduction of nitrate and nitrite in *Thiobacillus denitrificans*, Biochim. Biophys. Acta 325 (1973) 81–93.
[299] H.R. Beller, P.S. Chain, T.E. Letain, A. Chakicherla, F.W. Larimer, P.M. Richardson, M.A. Coleman, A.P. Wood, D.P. Kelly, The genome sequence of the obligately chemolithoautotrophic, facultatively anaerobic bacterium *Thiobacillus denitrificans*, J. Bacteriol. 188 (2006) 1473–1488.
[300] H.R. Beller, T.E. Letain, A. Chakicherla, S.R. Kane, T.C. Legler, M.A. Coleman, Whole-genome transcriptional analysis of chemolithoautotrophic thiosulfate oxidation by *Thiobacillus denitrificans* under aerobic versus denitrifying conditions, J. Bacteriol. 188 (2006) 7005–7015.
[301] H.R. Beller, Anaerobic, nitrate-dependent oxidation of U(IV) oxide minerals by the chemolithoautotrophic bacterium *Thiobacillus denitrificans*, Appl. Environ. Microbiol. 71 (2005) 2170–2174.
[302] H.R. Beller, T.C. Legler, F. Bourguet, T.E. Letain, S.R. Kane, M.A. Coleman, Identification of c-type cytochromes involved in anaerobic, bacterial U(IV) oxidation, Biodegradation 20 (2009) 45–53.
[303] K.L. Straub, M. Benz, B. Schink, F. Widdel, Anaerobic, nitrate-dependent microbial oxidation of ferrous iron, Appl. Environ. Microbiol. 62 (1996) 1458–1460.
[304] J. Bosch, K.Y. Lee, G. Jordan, K.W. Kim, R.U. Meckenstock, Anaerobic, nitrate-dependent oxidation of pyrite nanoparticles by *Thiobacillus denitrificans*, Environ. Sci. Technol. 46 (2012) 2095–2101.
[305] S.E. Hoeft, J.S. Blum, J.F. Stolz, F.R. Tabita, B. Witte, G.M. King, J.M. Santini, R.S. Oremland, *Alkalilimnicola ehrlichii* sp. nov., a novel, arsenite-oxidizing haloalkaliphilic gammaproteobacterium capable of chemoautotrophic or heterotrophic growth with nitrate or oxygen as the electron acceptor, Int. J. Syst. Evol. Microbiol. 57 (2007) 504–512.
[306] K.A. Weber, J. Pollock, K.A. Cole, S.M. O'Connor, L.A. Achenbach, J.D. Coates, Anaerobic nitrate-dependent iron(II) bio-oxidation by a novel lithoautotrophic betaproteobacterium, strain 2002, Appl. Environ. Microbiol. 72 (2006) 686–694.
[307] L.J. Bird, V. Bonnefoy, D.K. Newman, Bioenergetic challenges of microbial iron metabolisms, Trends Microbiol. 19 (2011) 330–340.
[308] M. Ilbert, V. Bonnefoy, Insight into the evolution of the iron oxidation pathways, Biochim. Biophys. Acta 1827 (2013) 161–175.
[309] A. Chakraborty, E.E. Roden, J. Schieber, F. Picardal, Enhanced growth of *Acidovorax* sp. strain 2AN during nitrate-dependent Fe(II) oxidation in batch and continuous-flow systems, Appl. Environ. Microbiol. 77 (2011) 8548–8556.
[310] H.K. Carlson, I.C. Clark, R.A. Melnyk, J.D. Coates, Toward a mechanistic understanding of anaerobic nitrate-dependent iron oxidation: balancing electron uptake and detoxification, Front. Microbiol. 3 (2012) 57.
[311] T. Hoffmann, B. Troup, A. Szabo, C. Hungerer, D. Jahn, The anaerobic life of *Bacillus subtilis*: cloning of the genes encoding the respiratory nitrate reductase system, FEMS Microbiol. Lett. 131 (1995) 219–225.
[312] M.M. Nakano, P. Zuber, Anaerobic growth of a "strict aerobe" (*Bacillus subtilis*), Annu. Rev. Microbiol. 52 (1998) 165–190.
[313] H.I. Boshoff, C.E. Barry III, Tuberculosis — metabolism and respiration in the absence of growth, Nat. Rev. Microbiol. 3 (2005) 70–80.
[314] M.M. Nakano, Y.P. Dailly, P. Zuber, D.P. Clark, Characterization of anaerobic fermentative growth of *Bacillus subtilis*: identification of fermentation end products and genes required for growth, J. Bacteriol. 179 (1997) 6749–6755.
[315] E. Härtig, D. Jahn, Regulation of the anaerobic metabolism in *Bacillus subtilis*, Adv. Microb. Physiol. 61 (2012) 195–216.
[316] M.P. Tan, P. Sequeira, W.W. Lin, W.Y. Phong, P. Cliff, S.H. Ng, B.H. Lee, L. Camacho, D. Schnappinger, S. Ehrt, T. Dick, K. Pethe, S. Alonso, Nitrate respiration protects hypoxic *Mycobacterium tuberculosis* against acid- and reactive nitrogen species stresses, PLoS One 5 (2010) e13356.
[317] I. Weber, C. Fritz, S. Ruttkowski, A. Kreft, F.C. Bange, Anaerobic nitrate reductase (narGHJI) activity of *Mycobacterium bovis* BCG in vitro and its contribution to virulence in immunodeficient mice, Mol. Microbiol. 35 (2000) 1017–1025.
[318] C.D. Sohaskey, Nitrate enhances the survival of *Mycobacterium tuberculosis* during inhibition of respiration, J. Bacteriol. 190 (2008) 2981–2986.
[319] L.I. Hochstein, F. Lang, Purification and properties of a dissimilatory nitrate reductase from *Haloferax denitrificans*, Arch. Biochem. Biophys. 288 (1991) 380–385.
[320] S. Bickelsandkötter, M. Ufer, Properties of a dissimilatory nitrate reductase from the halophilic archaeon *Haloferax volcanii*, Z. Naturforsch. C Biosci. 50 (1995) 365–372.
[321] B. Lledo, R.M. Martinez-Espinosa, F.C. Marhuenda-Egea, M.J. Bonete, Respiratory nitrate reductase from haloarchaeon *Haloferax mediterranei*: biochemical and genetic analysis, Biochim. Biophys. Acta 1674 (2004) 50–59.
[322] K. Yoshimatsu, T. Sakurai, T. Fujiwara, Purification and characterization of dissimilatory nitrate reductase from a denitrifying halophilic archaeon, *Haloarcula marismortui*, FEBS Lett. 470 (2000) 216–220.
[323] K. Yoshimatsu, O. Araya, T. Fujiwara, *Haloarcula marismortui* cytochrome b-561 is encoded by the narC gene in the dissimilatory nitrate reductase operon, Extremophiles 11 (2007) 41–47.
[324] M. Schutz, M. Brugna, E. Lebrun, F. Baymann, R. Huber, K.O. Stetter, G. Hauska, R. Toci, D. Lemesle-Meunier, P. Tron, C. Schmidt, W. Nitschke, Early evolution of cytochrome bc complexes, J. Mol. Biol. 300 (2000) 663–675.
[325] P. Volkl, R. Huber, E. Drobner, R. Rachel, S. Burggraf, A. Trincone, K.O. Stetter, *Pyrobaculum aerophilum* sp. nov., a novel nitrate-reducing hyperthermophilic archaeum, Appl. Environ. Microbiol. 59 (1993) 2918–2926.
[326] L.F. Feinberg, J.F. Holden, Characterization of dissimilatory Fe(III) versus NO_3^- reduction in the hyperthermophilic archaeon *Pyrobaculum aerophilum*, J. Bacteriol. 188 (2006) 525–531.
[327] A.E. Cozen, M.T. Weirauch, K.S. Pollard, D.L. Bernick, J.M. Stuart, T.M. Lowe, Transcriptional map of respiratory versatility in the hyperthermophilic crenarchaeon *Pyrobaculum aerophilum*, J. Bacteriol. 191 (2009) 782–794.
[328] S. Ramirez-Arcos, L.A. Fernandez-Herrero, J. Berenguer, A thermophilic nitrate reductase is responsible for the strain specific anaerobic growth of *Thermus thermophilus* HB8, Biochim. Biophys. Acta 1396 (1998) 215–227.
[329] F. Cava, O. Zafra, A. Magalon, F. Blasco, J. Berenguer, A new type of NADH dehydrogenase specific for nitrate respiration in the extreme thermophile *Thermus thermophilus*, J. Biol. Chem. 279 (2004) 45369–45378.
[330] F. Cava, O. Zafra, M.S. da Costa, J. Berenguer, The role of the nitrate respiration element of *Thermus thermophilus* in the control and activity of the denitrification apparatus, Environ. Microbiol. 10 (2008) 522–533.
[331] D. Heintz, S. Gallien, S. Wischgoll, A.K. Ullmann, C. Schaeffer, A.K. Kretzschmar, A. van Dorsselaer, M. Boll, Differential membrane proteome analysis reveals novel proteins involved in the degradation of aromatic compounds in *Geobacter metallireducens*, Mol. Cell. Proteomics 8 (2009) 2159–2169.
[332] K.T. Finneran, M.E. Housewright, D.R. Lovley, Multiple influences of nitrate on uranium solubility during bioremediation of uranium-contaminated subsurface sediments, Environ. Microbiol. 4 (2002) 510–516.
[333] J.O. Lundberg, E. Weitzberg, J.A. Cole, N. Benjamin, Nitrate, bacteria and human health, Nat. Rev. Microbiol. 2 (2004) 593–602.
[334] C.E. Vine, J.A. Cole, Unresolved sources, sinks, and pathways for the recovery of enteric bacteria from nitrosative stress, FEMS Microbiol. Lett. 325 (2011) 99–107.
[335] D. Seth, A. Hausladen, Y.J. Wang, J.S. Stamler, Endogenous protein S-nitrosylation in *E. coli*: regulation by OxyR, Science 336 (2012) 470–473.
[336] A. Arkenberg, S. Runkel, D.J. Richardson, G. Rowley, The production and detoxification of a potent cytotoxin, nitric oxide, by pathogenic enteric bacteria, Biochem. Soc. Trans. 39 (2011) 1876–1879.
[337] A. Trivedi, N. Singh, S.A. Bhat, P. Gupta, A. Kumar, Redox biology of tuberculosis pathogenesis, Adv. Microb. Physiol. 60 (2012) 263–324.
[338] C.A. Lopez, S.E. Winter, F. Rivera-Chavez, M.N. Xavier, V. Poon, S.P. Nuccio, R.M. Tsolis, A.J. Baumler, Phage-mediated acquisition of a type III secreted effector protein boosts growth of *Salmonella* by nitrate respiration, MBio 3 (2012).
[339] W.G. Zumft, Cell biology and molecular basis of denitrification, Microbiol. Mol. Biol. Rev. 61 (1997) 533–616.
[340] D.J. Richardson, B.C. Berks, D.A. Russell, S. Spiro, C.J. Taylor, Functional, biochemical and genetic diversity of prokaryotic nitrate reductases, Cell. Mol. Life Sci. 58 (2001) 165–178.
[341] L. Potter, H. Angove, D. Richardson, J. Cole, Nitrate reduction in the periplasm of Gram-negative bacteria, Adv. Microb. Physiol. 45 (2001) 51–112.
[342] H.P. Liu, S. Takio, T. Satoh, I. Yamamoto, Involvement in denitrification of the napKEFDABC genes encoding the periplasmic nitrate reductase system in the denitrifying phototrophic bacterium *Rhodobacter sphaeroides* f. sp. *denitrificans*, Biosci. Biotechnol. Biochem. 63 (1999) 530–536.
[343] L. Bedzyk, T. Wang, R.W. Ye, The periplasmic nitrate reductase in *Pseudomonas* sp. strain G-179 catalyzes the first step of denitrification, J. Bacteriol. 181 (1999) 2802–2806.
[344] D.J. Richardson, G.F. King, D.J. Kelly, A.G. McEwan, S.J. Ferguson, J.B. Jackson, The role of auxiliary oxidants in maintaining redox balance during phototrophic growth of *Rhodobacter capsulatus* on proprionate or butyrate, Arch. Microbiol. 150 (1988) 131–137.
[345] D.J. Richardson, S.J. Ferguson, The influence of carbon substrate on the activity of the periplasmic nitrate reductase in aerobically grown *Thiosphaera pantotropha*, Arch. Microbiol. 157 (1992) 535–537.
[346] M.D. Roldan, F. Reyes, C. Morenovivian, F. Castillo, Chlorate and nitrate reduction in the phototrophic bacteria *Rhodobacter capsulatus* and *Rhodobacter sphaeroides*, Curr. Microbiol. 29 (1994) 241–245.
[347] H.J. Sears, S. Spiro, D.J. Richardson, Effect of carbon substrate and aeration on nitrate reduction and expression of the periplasmic and membrane-bound nitrate reductases in carbon-limited continuous cultures of *Paracoccus denitrificans* Pd1222, Microbiology-(UK) 143 (1997) 3767–3774.
[348] H.J. Sears, G. Sawers, B.C. Berks, S.J. Ferguson, D.J. Richardson, Control of periplasmic nitrate reductase gene expression (napEDABC) from *Paracoccus pantotrophus* in response to oxygen and carbon substrates, Microbiology 146 (Pt 11) (2000) 2977–2985.
[349] M. Gavira, M.D. Roldan, F. Castillo, C. Moreno-Vivian, Regulation of nap gene expression and periplasmic nitrate reductase activity in the phototrophic bacterium *Rhodobacter sphaeroides* DSM158, J. Bacteriol. 184 (2002) 1693–1702.
[350] L.C. Potter, P. Millington, L. Griffiths, G.H. Thomas, J.A. Cole, Competition between *Escherichia coli* strains expressing either a periplasmic or a membrane-bound nitrate

reductase: does Nap confer a selective advantage during nitrate-limited growth? Biochem. J. 344 (Pt 1) (1999) 77–84.
[351] V. Stewart, Y. Lu, A.J. Darwin, Periplasmic nitrate reductase (NapABC enzyme) supports anaerobic respiration by *Escherichia coli* K-12, J. Bacteriol. 184 (2002) 1314–1323.
[352] M.S. Pittman, D.J. Kelly, Electron transport through nitrate and nitrite reductases in *Campylobacter jejuni*, Biochem. Soc. Trans. 33 (2005) 190–192.
[353] M. Kern, J. Simon, Electron transport chains and bioenergetics of respiratory nitrogen metabolism in *Wolinella succinogenes* and other Epsilonproteobacteria, Biochim. Biophys. Acta 1787 (2009) 646–656.
[354] J.J. Rowe, T. Ubbink-Kok, D. Molenaar, W.N. Konings, A.J. Driessen, NarK is a nitrite-extrusion system involved in anaerobic nitrate respiration by *Escherichia coli*, Mol. Microbiol. 12 (1994) 579–586.
[355] N.J. Wood, T. Alizadeh, D.J. Richardson, S.J. Ferguson, J.W. Moir, Two domains of a dual-function NarK protein are required for nitrate uptake, the first step of denitrification in *Paracoccus pantotrophus*, Mol. Microbiol. 44 (2002) 157–170.
[356] W. Jia, N. Tovell, S. Clegg, M. Trimmer, J. Cole, A single channel for nitrate uptake, nitrite export and nitrite uptake by *Escherichia coli* NarU and a role for NirC in nitrite export and uptake, Biochem. J. 417 (2009) 297–304.
[357] J. Simon, Enzymology and bioenergetics of respiratory nitrite ammonification, FEMS Microbiol. Rev. 26 (2002) 285–309.
[358] M.J. Sellars, S.J. Hall, D.J. Kelly, Growth of *Campylobacter jejuni* supported by respiration of fumarate, nitrate, nitrite, trimethylamine-N-oxide, or dimethyl sulfoxide requires oxygen, J. Bacteriol. 184 (2002) 4187–4196.
[359] R.A. Weingarten, J.L. Grimes, J.W. Olson, Role of *Campylobacter jejuni* respiratory oxidases and reductases in host colonization, Appl. Environ. Microbiol. 74 (2008) 1367–1375.
[360] C. Cruz-Garcia, A.E. Murray, J.A. Klappenbach, V. Stewart, J.M. Tiedje, Respiratory nitrate ammonification by *Shewanella oneidensis* MR-1, J. Bacteriol. 189 (2007) 656–662.
[361] H. Gao, Z.K. Yang, S. Barua, S.B. Reed, M.F. Romine, K.H. Nealson, J.K. Fredrickson, J.M. Tiedje, J. Zhou, Reduction of nitrate in *Shewanella oneidensis* depends on atypical NAP and NRF systems with NapB as a preferred electron transport protein from CymA to NapA, ISME J. 3 (2009) 966–976.
[362] A. Marietou, D. Richardson, J. Cole, S. Mohan, Nitrate reduction by *Desulfovibrio desulfuricans*: a periplasmic nitrate reductase system that lacks NapB, but includes a unique tetraheme c-type cytochrome, NapM, FEMS Microbiol. Lett. 248 (2005) 217–225.
[363] R.A. Siddiqui, U. Warnecke-Eberz, A. Hengsberger, B. Schneider, S. Kostka, B. Friedrich, Structure and function of a periplasmic nitrate reductase in *Alcaligenes eutrophus* H16, J. Bacteriol. 175 (1993) 5867–5876.
[364] Y. Li, E. Katzmann, S. Borg, D. Schuler, The periplasmic nitrate reductase nap is required for anaerobic growth and involved in redox control of magnetite biomineralization in *Magnetospirillum gryphiswaldense*, J. Bacteriol. 194 (2012) 4847–4856.
[365] F. Reyes, M. Gavira, F. Castillo, C. Moreno-Vivian, Periplasmic nitrate-reducing system of the phototrophic bacterium *Rhodobacter sphaeroides* DSM 158: transcriptional and mutational analysis of the napKEFDABC gene cluster, Biochem. J. 331 (Pt 3) (1998) 897–904.
[366] H.P. Koops, A. Pommerening-Roser, Distribution and ecophysiology of the nitrifying bacteria emphasizing cultured species, FEMS Microbiol. Ecol. 37 (2001) 1–9.
[367] S.E. Vlaeminck, A.G. Hay, L. Maignien, W. Verstraete, In quest of the nitrogen oxidizing prokaryotes of the early Earth, Environ. Microbiol. 13 (2011) 283–295.
[368] K. Kirstein, E. Bock, Close genetic relationship between *Nitrobacter hamburgensis* nitrite oxidoreductase and *Escherichia coli* nitrate reductases, Arch. Microbiol. 160 (1993) 447–453.
[369] H. Sundermeyer-klinger, W. Meyer, B. Warninghoff, E. Bock, Membrane-bound nitrite oxidoreductase of nitrobacter — evidence for a nitrate reductase system, Arch. Microbiol. 140 (1984) 153–158.
[370] A. Freitag, M. Rudert, E. Bock, Growth of *Nitrobacter* by dissimilatoric nitrate reduction, FEMS Microbiol. Lett. 48 (1987) 105–109.
[371] E. Bock, P.A. Wilderer, A. Freitag, Growth of *Nitrobacter* in the absence of dissolved oxygen, Water Res. 22 (1988) 245–250.
[372] A. Teske, E. Alm, J.M. Regan, S. Toze, B.E. Rittmann, D.A. Stahl, Evolutionary relationships among ammonia- and nitrite-oxidizing bacteria, J. Bacteriol. 176 (1994) 6623–6630.
[373] T. Yamanaka, Y. Fukumori, The nitrite oxidizing system of *Nitrobacter winogradskyi*, FEMS Microbiol. Rev. 4 (1988) 259–270.
[374] L. van Niftrik, M.S. Jetten, Anaerobic ammonium-oxidizing bacteria: unique microorganisms with exceptional properties, Microbiol. Mol. Biol. Rev. 76 (2012) 585–596.
[375] M. Strous, E. Pelletier, S. Mangenot, T. Rattei, A. Lehner, M.W. Taylor, M. Horn, H. Daims, D. Bartol-Mavel, P. Wincker, V. Barbe, N. Fonknechten, D. Vallenet, B. Segurens, C. Schenowitz-Truong, C. Medigue, A. Collingro, B. Snel, B.E. Dutilh, H.J. Op den Camp, C. van der Drift, I. Cirpus, K.T. van de Pas-Schoonen, H.R. Harhangi, L. van Niftrik, M. Schmid, J. Keltjens, J. van de Vossenberg, B. Kartal, H. Meier, D. Frishman, M.A. Huynen, H.W. Mewes, J. Weissenbach, M.S. Jetten, M. Wagner, D. Le Paslier, Deciphering the evolution and metabolism of an *Anammox bacterium* from a community genome, Nature 440 (2006) 790–794.
[376] B. Kartal, W.J. Maalcke, N.M. de Almeida, I. Cirpus, J. Gloerich, W. Geerts, H.J. Op den Camp, H.R. Harhangi, E.M. Janssen-Megens, K.J. Francoijs, H.G. Stunnenberg, J.T. Keltjens, M.S. Jetten, M. Strous, Molecular mechanism of anaerobic ammonium oxidation, Nature 479 (2011) 127–130.
[377] B. Kartal, M.M. Kuypers, G. Lavik, J. Schalk, H.J. Op den Camp, M.S. Jetten, M. Strous, *Anammox* bacteria disguised as denitrifiers: nitrate reduction to dinitrogen gas via nitrite and ammonium, Environ. Microbiol. 9 (2007) 635–642.
[378] J. van de Vossenberg, J.E. Rattray, W. Geerts, B. Kartal, L. van Niftrik, E.G. van Donselaar, J.S. Sinninghe Damste, M. Strous, M.S. Jetten, Enrichment and characterization of marine anammox bacteria associated with global nitrogen gas production, Environ. Microbiol. 10 (2008) 3120–3129.
[379] N.M. de Almeida, W.J. Maalcke, J.T. Keltjens, M.S. Jetten, B. Kartal, Proteins and protein complexes involved in the biochemical reactions of anaerobic ammonium-oxidizing bacteria, Biochem. Soc. Trans. 39 (2011) 303–308.
[380] J.F. Heidelberg, I.T. Paulsen, K.E. Nelson, E.J. Gaidos, W.C. Nelson, T.D. Read, J.A. Eisen, R. Seshadri, N. Ward, B. Methe, R.A. Clayton, T. Meyer, A. Tsapin, J. Scott, M. Beanan, L. Brinkac, S. Daugherty, R.T. DeBoy, R.J. Dodson, A.S. Durkin, D.H. Haft, J.F. Kolonay, R. Madupu, J.D. Peterson, L.A. Umayam, O. White, A.M. Wolf, J. Vamathevan, J. Weidman, M. Impraim, K. Lee, K. Berry, C. Lee, J. Mueller, H. Khouri, J. Gill, T.R. Utterback, L.A. McDonald, T.V. Feldblyum, H.O. Smith, J.C. Venter, K.H. Nealson, C.M. Fraser, Genome sequence of the dissimilatory metal ion-reducing bacterium *Shewanella oneidensis*, Nat. Biotechnol. 20 (2002) 1118–1123.
[381] I. Yamamoto, M. Ishimoto, Anaerobic growth of *Escherichia coli* on formate by reduction of nitrate, fumarate, and trimethylamine N-oxide, Z. Allg. Mikrobiol. 17 (1977) 235–242.
[382] A.G. McEwan, S.J. Ferguson, J.B. Jackson, Electron flow to dimethylsulphoxide or trimethylamine-N-oxide generates a membrane potential in *Rhodopseudomonas capsulata*, Arch. Microbiol. 136 (1983) 300–305.
[383] R. Hedderich, O. Klimmek, A. Kröger, R. Dirmeier, M. Keller, K.O. Stetter, Anaerobic respiration with elemental sulfur and with disulfides, FEMS Microbiol. Rev. 22 (1999) 353–381.
[384] A. Kletzin, T. Urich, F. Muller, T.M. Bandeiras, C.M. Gomes, Dissimilatory oxidation and reduction of elemental sulfur in thermophilic archaea, J. Bioenerg. Biomembr. 36 (2004) 77–91.
[385] G.D. Fauque, L.L. Barton, Hemoproteins in dissimilatory sulfate- and sulfur-reducing prokaryotes, Adv. Microb. Physiol. 60 (2012) 1–90.
[386] M. Guiral, L. Prunetti, C. Aussignargues, A. Ciaccafava, P. Infossi, M. Ilbert, E. Lojou, M.T. Giudici-Orticoni, The hyperthermophilic bacterium *Aquifex aeolicus*: from respiratory pathways to extremely resistant enzymes and biotechnological applications, Adv. Microb. Physiol. 61 (2012) 125–194.
[387] I. Schroder, A. Kroger, J.M. Macy, Isolation of the sulfur reductase and reconstitution of the sulfur respiration of *Wolinella succinogenes*, Arch. Microbiol. 149 (1988) 572–579.
[388] T. Krafft, M. Bokranz, O. Klimmek, I. Schroder, F. Fahrenholz, E. Kojro, A. Kroger, Cloning and nucleotide sequence of the psrA gene of *Wolinella succinogenes* polysulphide reductase, Eur. J. Biochem. 206 (1992) 503–510.
[389] T. Krafft, R. Gross, A. Kroger, The function of *Wolinella succinogenes* psr genes in electron transport with polysulphide as the terminal electron acceptor, Eur. J. Biochem. 230 (1995) 601–606.
[390] J.M. Macy, I. Schroder, R.K. Thauer, A. Kroger, Growth of *Wolinella succinogenes* on H_2S plus fumarate and on formate plus sulfur as energy sources, Arch. Microbiol. 144 (1986) 147–150.
[391] O. Klimmek, A. Kroger, R. Steudel, G. Holdt, Growth of *Wolinella succinogenes* with polysulfide as terminal acceptor of phosphorylative electron transport, Arch. Microbiol. 155 (1991) 177–182.
[392] M. Yamamoto, S. Nakagawa, S. Shimamura, K. Takai, K. Horikoshi, Molecular characterization of inorganic sulfur-compound metabolism in the deep-sea epsilonproteobacterium *Sulfurovum* sp. NBC37-1, Environ. Microbiol. 12 (2010) 1144–1153.
[393] S. Laska, F. Lottspeich, A. Kletzin, Membrane-bound hydrogenase and sulfur reductase of the hyperthermophilic and acidophilic archaeon *Acidianus ambivalens*, Microbiology 149 (2003) 2357–2371.
[394] A. Magalon, R. Arias-Cartin, A. Walburger, Supramolecular organization in prokaryotic respiratory systems, in: R.K. Poole (Ed.), Adv Microb Physiol, Academic press, 2012, pp. 217–266.
[395] A. Jankielewicz, O. Klimmek, A. Kröger, The electron transfer from hydrogenase and formate dehydrogenase to polysulfide reductase in the membrane of *Wolinella succinogenes*, Biochim. Biophys. Acta 1231 (1995) 157–162.
[396] G. Lenaz, M.L. Genova, Structure and organization of mitochondrial respiratory complexes: a new understanding of an old subject, Antioxid. Redox Signal. 12 (2010) 961–1008.
[397] K. Yokoyama, T. Oshima, M. Yoshida, Thermus thermophilus membrane-associate ATPase: indication of a eubacterial V-type ATPase, J. Biol. Chem. 265 (1990) 21946–21950.
[398] D.P. Moser, K.H. Nealson, Growth of the facultative anaerobe *Shewanella putrefaciens* by elemental sulfur reduction, Appl. Environ. Microbiol. 62 (1996) 2100–2105.
[399] J.L. Burns, T.J. DiChristina, Anaerobic respiration of elemental sulfur and thiosulfate by *Shewanella oneidensis* MR-1 requires psrA, a homolog of the phsA gene of *Salmonella enterica* serovar typhimurium LT2, Appl. Environ. Microbiol. 75 (2009) 5209–5217.
[400] A.P. Hinsley, B.C. Berks, Specificity of respiratory pathways involved in the reduction of sulfur compounds by *Salmonella enterica*, Microbiology 148 (2002) 3631–3638.
[401] F. Fischer, W. Zillig, K.O. Stetter, G. Schreiber, Chemolithoautotrophic metabolism of anaerobic extremely thermophilic archaebacteria, Nature 301 (1983) 511–513.
[402] L.F. Feinberg, R. Srikanth, R.W. Vachet, J.F. Holden, Constraints on anaerobic respiration in the hyperthermophilic Archaea *Pyrobaculum islandicum* and *Pyrobaculum aerophilum*, Appl. Environ. Microbiol. 74 (2008) 396–402.
[403] S.T. Fitz-Gibbon, H. Ladner, U.J. Kim, K.O. Stetter, M.I. Simon, J.H. Miller, Genome sequence of the hyperthermophilic crenarchaeon *Pyrobaculum aerophilum*, Proc. Natl. Acad. Sci. U. S. A. 99 (2002) 984–989.
[404] P.P. Chan, A.D. Holmes, A.M. Smith, D. Tran, T.M. Lowe, The UCSC Archaeal genome browser: 2012 update, Nucleic Acids Res. 40 (2012) D646–D652.

[405] S.E. Winter, P. Thiennimitr, M.G. Winter, B.P. Butler, D.L. Huseby, R.W. Crawford, J.M. Russell, C.L. Bevins, L.G. Adams, R.M. Tsolis, J.R. Roth, A.J. Baumler, Gut inflammation provides a respiratory electron acceptor for *Salmonella*, Nature 467 (2010) 426–429.
[406] S.P. Hanlon, R.A. Holt, G.R. Moore, A.G. McEwan, Isolation and characterization of a strain of *Rhodobacter sulfidophilus*: a bacterium which grows autotrophically with dimethylsulfide as electron donor, Microbiology 140 (1994) 6.
[407] J.H. Weiner, R.A. Rothery, D. Sambasivarao, C.A. Trieber, Molecular analysis of dimethylsulfoxide reductase: a complex iron–sulfur molybdoenzyme of *Escherichia coli*, Biochim. Biophys. Acta 1102 (1992) 1–18.
[408] D.A. Saffarini, S.L. Blumerman, K.J. Mansoorabadi, Role of menaquinones in Fe(III) reduction by membrane fractions of *Shewanella putrefaciens*, J. Bacteriol. 184 (2002) 846–848.
[409] C. Gruber, A. Legat, M. Pfaffenhuemer, C. Radax, G. Weidler, H.J. Busse, H. Stan-Lotter, *Halobacterium noricense* sp. nov., an archaeal isolate from a bore core of an alpine Permian salt deposit, classification of *Halobacterium* sp. NRC-1 as a strain of *H. salinarum* and emended description of *H. salinarum*, Extremophiles 8 (2004) 431–439.
[410] A. Oren, H.G. Trüper, Anaerobic growth of halophilic archaebacteria by reduction of dimethylsulfoxide and trimethylamine N-oxide, FEMS Microbiol. Lett. 70 (1990) 33–36.
[411] S.L. McCrindle, U. Kappler, A.G. McEwan, Microbial dimethylsulfoxide and trimethylamine-N-oxide respiration, Adv. Microb. Physiol. 50 (2005) 147–198.
[412] G. Sawers, The hydrogenases and formate dehydrogenases of *Escherichia coli*, Antonie Van Leeuwenhoek 66 (1994) 57–88.
[413] S.M. da Silva, I. Pacheco, I.A. Pereira, Electron transfer between periplasmic formate dehydrogenase and cytochromes c in *Desulfovibrio desulfuricans* ATCC 27774, J. Biol. Inorg. Chem. 17 (2012) 831–838.
[414] D.J. Steenkamp, H.D. Peck Jr., Proton translocation associated with nitrite respiration in *Desulfovibrio desulfuricans*, J. Biol. Chem. 256 (1981) 5450–5458.
[415] L.L. Barton, J. LeGall, J.M. Odom, H.D. Peck Jr., Energy coupling to nitrite respiration in the sulfate-reducing bacterium *Desulfovibrio gigas*, J. Bacteriol. 153 (1983) 867–871.
[416] D.R. Lovley, D.E. Holmes, K.P. Nevin, Dissimilatory Fe(III) and Mn(IV) reduction, Adv. Microb. Physiol. 49 (2004) 219–286.
[417] D.R. Lovley, T. Ueki, T. Zhang, N.S. Malvankar, P.M. Shrestha, K.A. Flanagan, M. Aklujkar, J.E. Butler, L. Giloteaux, A.E. Rotaru, D.E. Holmes, A.E. Franks, R. Orellana, C. Risso, K.P. Nevin, Geobacter: the microbe electric's physiology, ecology, and practical applications, Adv. Microb. Physiol. 59 (2011) 1–100.
[418] C.R. Myers, J.M. Myers, Cloning and sequence of cymA, a gene encoding a tetraheme cytochrome c required for reduction of iron(III), fumarate, and nitrate by *Shewanella putrefaciens* MR-1, J. Bacteriol. 179 (1997) 1143–1152.
[419] L. Shi, T.C. Squier, J.M. Zachara, J.K. Fredrickson, Respiration of metal (hydr)oxides by *Shewanella* and *Geobacter*: a key role for multihaem c-type cytochromes, Mol. Microbiol. 65 (2007) 12–20.
[420] A. Niggemyer, S. Spring, E. Stackebrandt, R.F. Rosenzweig, Isolation and characterization of a novel As(V)-reducing bacterium: implications for arsenic mobilization and the genus *Desulfitobacterium*, Appl. Environ. Microbiol. 67 (2001) 5568–5580.
[421] K.C. Costa, P.M. Wong, T. Wang, T.J. Lie, J.A. Dodsworth, I. Swanson, J.A. Burn, M. Hackett, J.A. Leigh, Protein complexing in a methanogen suggests electron bifurcation and electron delivery from formate to heterodisulfide reductase, Proc. Natl. Acad. Sci. U. S. A. 107 (2010) 11050–11055.
[422] M. Karrasch, G. Borner, M. Enssle, R.K. Thauer, Formylmethanofuran dehydrogenase from methanogenic bacteria, a molybdoenzyme, FEBS Lett. 253 (1989) 226–230.
[423] M. Karrasch, G. Borner, M. Enssle, R.K. Thauer, The molybdoenzyme formylmethanofuran dehydrogenase from *Methanosarcina barkeri* contains a pterin cofactor, Eur. J. Biochem. 194 (1990) 367–372.
[424] M. Karrasch, G. Borner, R.K. Thauer, The molybdenum cofactor of formylmethanofuran dehydrogenase from *Methanosarcina barkeri* is a molybdopterin guanine dinucleotide, FEBS Lett. 274 (1990) 48–52.
[425] P.A. Bertram, R.K. Thauer, Thermodynamics of the formylmethanofuran dehydrogenase reaction in *Methanobacterium thermoautotrophicum*, Eur. J. Biochem. 226 (1994) 811–818.
[426] A. Hochheimer, R.A. Schmitz, R.K. Thauer, R. Hedderich, The tungsten formylmethanofuran dehydrogenase from *Methanobacterium thermoautotrophicum* contains sequence motifs characteristic for enzymes containing molybdopterin dinucleotide, Eur. J. Biochem. 234 (1995) 910–920.
[427] A. Hochheimer, D. Linder, R.K. Thauer, R. Hedderich, The molybdenum formylmethanofuran dehydrogenase operon and the tungsten formylmethanofuran dehydrogenase operon from *Methanobacterium thermoautotrophicum*. Structures and transcriptional regulation, Eur. J. Biochem. 242 (1996) 156–162.
[428] B. Ezraty, J. Bos, F. Barras, L. Aussel, Methionine sulfoxide reduction and assimilation in *Escherichia coli*: new role for the biotin sulfoxide reductase BisC, J. Bacteriol. 187 (2005) 231–237.
[429] V.V. Pollock, M.J. Barber, Kinetic and mechanistic properties of biotin sulfoxide reductase, Biochemistry 40 (2001) 1430–1440.
[430] D.E. Pierson, A. Campbell, Cloning and nucleotide sequence of bisC, the structural gene for biotin sulfoxide reductase in *Escherichia coli*, J. Bacteriol. 172 (1990) 2194–2198.
[431] A. Brune, B. Schink, Pyrogallol-to-phloroglucinol conversion and other hydroxyltransfer reactions catalyzed by cell extracts of *Pelobacter acidigallici*, J. Bacteriol. 172 (1990) 1070–1076.
[432] P.I. Darley, J.A. Hellstern, J.I. Medina-Bellver, S. Marques, B. Schink, B. Philipp, Heterologous expression and identification of the genes involved in anaerobic degradation of 1,3-dihydroxybenzene (resorcinol) in *Azoarcus anaerobius*, J. Bacteriol. 189 (2007) 3824–3833.
[433] S. Schnell, F. Bak, N. Pfennig, Anaerobic degradation of aniline and dihydroxybenzenes by newly isolated sulfate-reducing bacteria and description of *Desulfobacterium anilini*, Arch. Microbiol. 152 (1989) 556–563.
[434] A. Tschech, B. Schink, Fermentative degradation of resorcinol and resorcylic acids, Arch. Microbiol. 143 (1985) 8.
[435] C. Kluge, A. Tschech, G. Fuchs, Anaerobic metabolism of resorcyclic acids (m-dihydroxybenzoic acids) and resorcinol (1,3-benzenediol) in a fermenting and in a denitrifying bacterium, Arch. Microbiol. 155 (1990) 7.
[436] N. Springer, W. Ludwig, B. Philipp, B. Schink, *Azoarcus anaerobius* sp. nov., a resorcinol-degrading, strictly anaerobic, denitrifying bacterium, Int. J. Syst. Bacteriol. 48 (Pt 3) (1998) 953–956.
[437] B. Philipp, B. Schink, Evidence of two oxidative reaction steps initiating anaerobic degradation of resorcinol (1,3-dihydroxybenzene) by the denitrifying bacterium *Azoarcus anaerobius*, J. Bacteriol. 180 (1998) 3644–3649.
[438] H.A. Ball, H.A. Johnson, M. Reinhard, A.M. Spormann, Initial reactions in anaerobic ethylbenzene oxidation by a denitrifying bacterium, strain EB1, J. Bacteriol. 178 (1996) 5755–5761.
[439] O. Kniemeyer, J. Heider, (S)-1-phenylethanol dehydrogenase of *Azoarcus* sp. strain EbN1, an enzyme of anaerobic ethylbenzene catabolism, Arch. Microbiol. 176 (2001) 129–135.
[440] O. Kniemeyer, J. Heider, Ethylbenzene dehydrogenase, a novel hydrocarbon-oxidizing molybdenum/iron–sulfur/heme enzyme, J. Biol. Chem. 276 (2001) 21381–21386.
[441] A.S. Backlund, J. Bohlin, N. Gustavsson, T. Nilsson, Periplasmic c cytochromes and chlorate reduction in *Ideonella dechloratans*, Appl. Environ. Microbiol. 75 (2009) 2439–2445.
[442] M.K. Saiki, T.P. Lowe, Selenium in aquatic organisms from subsurface agricultural drainage water, San Joaquin Valley, California, Arch. Environ. Contam. Toxicol. 16 (1987) 657–670.
[443] M. Bebien, J. Kirsch, V. Mejean, A. Vermeglio, Involvement of a putative molybdenum enzyme in the reduction of selenate by *Escherichia coli*, Microbiology 148 (2002) 3865–3872.
[444] H. Ridley, C.A. Watts, D.J. Richardson, C.S. Butler, Resolution of distinct membrane-bound enzymes from *Enterobacter cloacae* SLD1a-1 that are responsible for selective reduction of nitrate and selenate oxyanions, Appl. Environ. Microbiol. 72 (2006) 5173–5180.
[445] D. Ahmann, A.L. Roberts, L.R. Krumholz, F.M. Morel, Microbe grows by reducing arsenic, Nature 371 (1994) 750.
[446] W. Sun, R. Sierra-Alvarez, L. Milner, J.A. Field, Anaerobic oxidation of arsenite linked to chlorate reduction, Appl. Environ. Microbiol. 76 (2010) 6804–6811.
[447] T.R. Kulp, S.E. Hoeft, M. Asao, M.T. Madigan, J.T. Hollibaugh, J.C. Fisher, J.F. Stolz, C.W. Culbertson, L.G. Miller, R.S. Oremland, Arsenic(III) fuels anoxygenic photosynthesis in hot spring biofilms from Mono Lake, California, Science 321 (2008) 967–970.
[448] C. Richey, P. Chovanec, S.E. Hoeft, R.S. Oremland, P. Basu, J.F. Stolz, Respiratory arsenate reductase as a bidirectional enzyme, Biochem. Biophys. Res. Commun. 382 (2009) 298–302.
[449] E.D. Rhine, S.M. Ni Chadhain, G.J. Zylstra, L.Y. Young, The arsenite oxidase genes (aroAB) in novel chemoautotrophic arsenite oxidizers, Biochem. Biophys. Res. Commun. 354 (2007) 662–667.
[450] W. Sun, R. Sierra-Alvarez, L. Milner, R. Oremland, J.A. Field, Arsenite and ferrous iron oxidation linked to chemolithotrophic denitrification for the immobilization of arsenic in anoxic environments, Environ. Sci. Technol. 43 (2009) 6585–6591.
[451] J.C. Fisher, J.T. Hollibaugh, Selenate-dependent anaerobic arsenite oxidation by a bacterium from Mono Lake, California, Appl. Environ. Microbiol. 74 (2008) 2588–2594.
[452] P. Mitchell, Chemiosmotic coupling in oxidative and photosynthetic phosphorylation, Biol. Rev. Camb. Philos. Soc. 41 (1966) 445–502.
[453] B. Frangioni, B. Guigliarelli, C. Iobbi-Nivol, Unpublished results.
[454] P.J. Simpson, A.A. McKinzie, R. Codd, Resolution of two native monomeric 90 kDa nitrate reductase active proteins from *Shewanella gelidimarina* and the sequence of two napA genes, Biochem. Biophys. Res. Commun. 398 (2010) 13–18.
[455] M.J. Barber, H.D. May, J.G. Ferry, Inactivation of formate dehydrogenase from *Methanobacterium-formicicum* by cyanide, Biochemistry 25 (1986) 8150–8155.
[456] R. Gangeswaran, D.J. Lowe, R.R. Eady, Purification and characterization of the assimilatory nitrate reductase of *Azotobacter vinelandii*, Biochem. J. 289 (Pt 2) (1993) 335–342.
[457] K.R. Hoke, N. Cobb, F.A. Armstrong, R. Hille, Electrochemical studies of arsenite oxidase: an unusual example of a highly cooperative two-electron molybdenum center, Biochemistry 43 (2004) 1667–1674.
[458] C.A. Libeu, M. Kukimoto, M. Nishiyama, S. Horinouchi, E.T. Adman, Site-directed mutants of pseudoazurin: explanation of increased redox potentials from X-ray structures and from calculation of redox potential differences, Biochemistry 36 (1997) 13160–13179.
[459] N.L. Creevey, A.G. McEwan, P.V. Bernhardt, A mechanistic and electrochemical study of the interaction between dimethyl sulfide dehydrogenase and its electron transfer partner cytochrome c2, J. Biol. Inorg. Chem. 13 (2008) 1231–1238.
[460] R.A. Rothery, C.A. Trieber, J.H. Weiner, Interactions between the molybdenum cofactor and iron–sulfur clusters of *Escherichia coli* dimethylsulfoxide reductase, J. Biol. Chem. 274 (1999) 13002–13009.
[461] C. Hagel, Struktur und Funktion der Ethylbenzol Dehydrogenase, einer anaeroben Kohlenwasserstoff-Hydroxylase (Dissertation), Technical University of Darmstadt, Darmstadt, 2006.
[462] M.A. Picarra-Pereira, D.L. Turner, J. LeGall, A.V. Xavier, Structural studies on *Desulfovibrio gigas* cytochrome c3 by two-dimensional ^{1}H-nuclear-magnetic-resonance spectroscopy, Biochem. J. 294 (Pt 3) (1993) 909–915.

[463] R.K. Thauer, K. Jungermann, K. Decker, Energy conservation in anaerobic chemotrophic bacteria, Bacteriol. Rev. 41 (1977) 80.
[464] A. Kröger, G. Unden, The function of menaquinone in bacterial electron transport, in: G. Lenaz (Ed.), Coenzyme Q: Biochemistry, Bioenergetics, and Clinical Applications of Ubiquinone, John Wiley and Sons Ltd., Chichester [West Sussex]; New York, 1985, pp. 285–300.
[465] P. Infossi, E. Lojou, J.-P. Chauvin, G. Herbette, M. Brugna, M.-T. Giudici-Orticoni, *Aquifex aeolicus* membrane hydrogenase for hydrogen biooxidation: role of lipids and physiological partners in enzyme stability and activity, Int. J. Hydrog. Energy 35 (2010) 10778–10789.
[466] R.K. Thauer, K. Jungermann, K. Decker, Energy conservation in chemotrophic anaerobic bacteria, Bacteriol. Rev. 41 (1977) 100–180.
[467] F. Kapralek, The physiological role of tetrathionate respiration in growing citrobacter, J. Gen. Microbiol. 71 (1972) 133–139.
[468] B.W. Vink, Stability relations of antimony and arsenic compounds in the light of revised and extended Eh–pH diagrams, Chem. Geol. 130 (1996) 9.
[469] F. Maixner, M. Wagner, S. Lucker, E. Pelletier, S. Schmitz-Esser, K. Hace, E. Spieck, R. Konrat, D. Le Paslier, H. Daims, Environmental genomics reveals a functional chlorite dismutase in the nitrite-oxidizing bacterium '*Candidatus Nitrospira defluvii*', Environ. Microbiol. 10 (2008) 3043–3056.